INTEGRATION OF GEOPHYSICAL, GEOCHEMICAL AND GEOLOGICAL DATA TO DERIVE A METALLOGENIC MODEL FOR THE DEER LAKE BASIN, WESTERN NEWFOUNDLAND

JODY HODDER

INFORMATION TO USERS

This manuscript has been reproduced from the microfilm master. UMI films the text directly from the original or copy submitted. Thus, some thesis and dissertation copies are in typewriter face, while others may be from any type of computer printer.

The quality of this reproduction is dependent upon the quality of the copy submitted. Broken or indistinct print, colored or poor quality illustrations and photographs, print bleedthrough, substandard margins, and improper alignment can adversely affect reproduction.

In the unlikely event that the author did not send UMI a complete manuscript and there are missing pages, these will be noted. Also, if unauthorized copyright material had to be removed, a note will indicate the deletion.

Oversize materials (e.g., maps, drawings, charts) are reproduced by sectioning the original, beginning at the upper left-hand corner and continuing from left to right in equal sections with small overlaps. Each original is also photographed in one exposure and is included in reduced form at the back of the book.

Photographs included in the original manuscript have been reproduced xerographically in this copy. Higher quality 6" x 9" black and white photographic prints are available for any photographs or illustrations appearing in this copy for an additional charge. Contact UMI directly to order.

UMI

A Bell & Howell Information Company
300 North Zeeb Road, Ann Arbor MI 48106-1346 USA
313/761-4700 800/521-0600

INTEGRATION OF GEOPHYSICAL, GEOCHEMICAL AND GEOLOGICAL DATA TO DERIVE A METALLOGENIC MODEL FOR THE DEER LAKE BASIN, WESTERN NEWFOUNDLAND

BY

JODY HODDER

A Thesis submitted to the
School of Graduate Studies
in partial fulfilment of the
requirements for the degree of
Master of Science

Department of Earth Science
Memorial University of Newfoundland

1997

St. John's Newfoundland

National Library of Canada
Acquisitions and Bibliographic Services
395 Wellington Street
Ottawa ON K1A 0N4
Canada

Bibliothèque nationale du Canada
Acquisitions et services bibliographiques
395, rue Wellington
Ottawa ON K1A 0N4
Canada

Your file Votre référence

Our file Notre référence

0-612-34186-0

Canada

ABSTRACT

This study examines fluid flow from and within the Carboniferous Deer Lake lacustrine Basin and adjacent Paleozoic basement, using potential field, geological and geophysical data. Whole rock samples were collected throughout the basin and were subjected to a number of analytical techniques to determine isotopic major and trace element geochemistry. A fluid inclusion study was also undertaken to determine temperatures and salinities of fluids.

Gravity and magnetic residuals suggest that the basement within the basin is block faulted. The basin can be divided up into eight distinct sections of fault bounded blocks based on the character of the potential field anomaly maps. The combined potential field and geochemical data show that some forms of mineralization in the basin occur near residual gravity and magnetic highs while other forms are correlated with high magnetic gradients. The trends indicate the association of mineralization and hydrocarbon deposits with the underlying basement topography and the faults that formed structural conduits along which these fluids migrated. The association of bitumen samples with mineralizing fluids appears to be the result of their utilization of the same regional fault system for migration. Formation of mineral deposits is a secondary feature related to structural and stratigraphic features and are controlled by the major basement faults.

ACKNOWLEDGMENTS

The Author wishes to thank Drs Derek Wilton and Hugh Miller for all their guidance and support. Appreciation is expressed to R. Churchill and J. Fowler of Black Pine. G. Kilfoil of the Mines and Energy Branch. B. Hoffe, R. Patzold, E. Hatfield, P. King, P. Horan, M. Tubertt, D. Clarke, B. Stanley, and A. Pye of Memorial University for their technical assistance. Last, but certainly not least, the author wishes to thank her family and friends for all their love and support.

TABLE OF CONTENTS **PAGE**

Table Of Contents cont'd **Page**

List Of Figures **Page**

List of Figures cont'd **Page**

List of Tables **Page**

List Of Abbreviations And Symbols

DLB - Deer Lake Basin

ICP-MS - Inductively Coupled Plasma Mass Spectrometer

LAM-ICP-MS - Laser Ablation Microprobe Inductively Coupled Plasma Mass Spectrometer

XRF - X-Ray Fluorescence

CHN - Carbon-Hydrogen-Nitrogen Analysis

NDME - Newfoundland Department of Mines And Energy

MVT - Mississippi Valley Type Deposit

UQAM - Université du Quebéc á Montréal

List of Maps In Map Folder

Map 1 - Base Map of the Deer Lake Basin

Map 2 - Bouguer Gravity Residual 3A Anomaly Map

Map 3 - Total Field Aeromagnetic Residual 3A Anomaly Map

Map 4 - Total Field Aeromagnetic Horizontal Gradient Map

Map 5 - Geochemistry Anomaly Map -Ag

Map 6 - Geochemistry Anomaly Map -As

Map 7 - Geochemistry Anomaly Map -Au

Map 8 - Geochemistry Anomaly Map -Ba

Map 9 - Geochemistry Anomaly Map -Ce

Map 10 - Geochemistry Anomaly Map -Co

Map 11 - Geochemistry Anomaly Map -Cr

Map 12 - Geochemistry Anomaly Map -Cu

Map 13 - Geochemistry Anomaly Map -Eu

Map 14 - Geochemistry Anomaly Map -F

Map 15 - Geochemistry Anomaly Map -Fe

Map 16 - Geochemistry Anomaly Map -La

List of Maps cont'd

CHAPTER 1: - Introduction

1.1 - Introduction and Objective

The Carboniferous Deer Lake Basin, located in Western Newfoundland, lies entirely in the Humber Zone of the Appalachian Orogen (Grenvillian basement overlain by shallow platformal and deeper water successions) between latitudes 48°45' and 49°45' and longitudes 56°45' and 57°45' (Figure1, Map1) (Williams, 1979).

Lithological exposures within the basin are poorly developed and are located within waterways for the most part. Due to the relatively flat topography, even those exposures in waterways are accessible only at times of low water. Most of the basin can be accessed from the Trans Canada Highway and various logging roads. Helicopter use is necessary in the northern part of the basin as roads and outcrop are scarce due to the tree cover and the many lakes and rivers.

The aim of this thesis is to examine the type(s) and nature(s) of hydrothermal fluids that coursed through the basin by examining geophysical, geological, and geochemical data from the basin. Economic interest in the basin has risen since the increase of exploration activity in Western Newfoundland, specifically in the Bay St. George region (Telegram press release, 1997).

Potentially economic mineral and hydrocarbon occurrences have been noted throughout the basin, and the migration of both hydrocarbons and hydrothermal solutions presumably involved fluid flow through similar porous-permeable pathways.

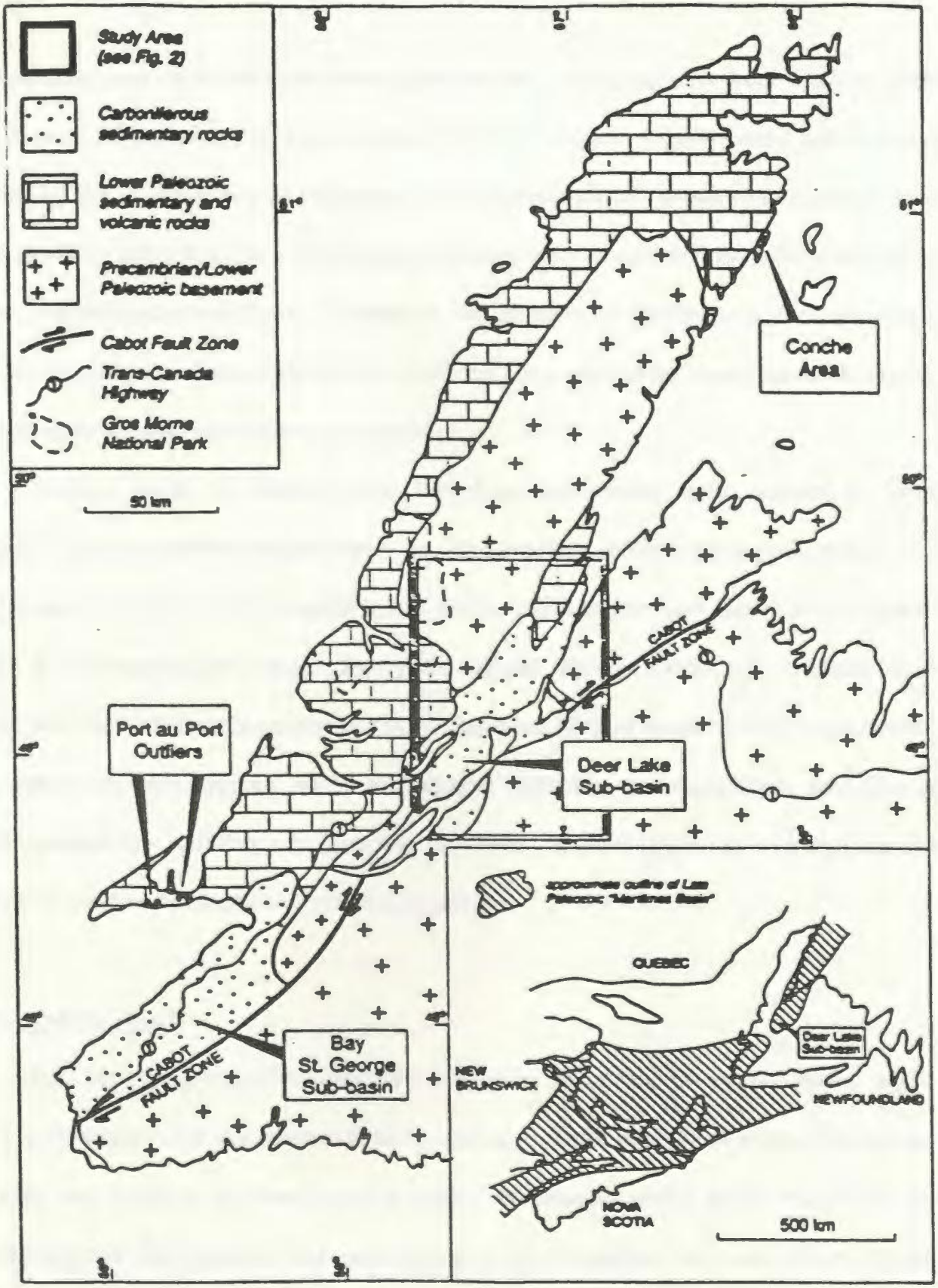

Figure 1: Location Map For The Deer Lake Sub-Basin (From Hamblin et al., (in prep)).

The potential also exists that the same migration pathways may have been used by both fluid types. If the two fluids co-migrate, then the organic matter could affect metal activity in the fluids either by reduction or by formation of metal-organic complexes. Since the Deer Lake Basin is a fault-bounded basin, faults could obviously have served as feeders for hydrothermal fluids. Based on the number of occurrences, their potential inter-relationships, and probable fault control, the basin should be looked upon favorably for both mineral and hydrocarbon prospects.

Similar work on other basins has been completed with respect to both hydrocarbons and metallic mineral deposits. The association between organic matter and ore minerals has also lead to speculation about co-migration and the role of organic matter in ore-forming processes. Examples include Disnar (1996) and Ewbank et al (1995) who studied organic matter and MVT deposits. Ho and Mauk (1996) looked at the relationship between organic matter and copper deposits, and Rasmussen and Glover (1994) studied low mobility elements and bitumens. Parnell (1994) published a special volume on studies of bitumens and ore deposits.

1.2 - Previous Work

Baird (1950) produced a simplified geological map of the Deer Lake Basin. Hyde et al., (1994) provided the most extensive, and up to date, geological map of the basin; this map was used as the base for this study. Sediments which define the basin fill include alluvial fan, braided and meandering river, lacustrine and coal swamp facies

(Hyde, 1994). Hyde (1989) stated that the sedimentary lithofacies suggest a shallow perennial lake with moderately saline, alkaline water high in magnesium and sodium. He further suggested that cyclic sedimentation of the units was characterized by carbonate deposition during highstands and mudflat deposition as a result of lowstands. Formations representing basin-fill from oldest to youngest are the Anguille Group, Wetstone Point and Wigwam Brook Formations, Deer Lake Group, and Howley Formation (Figure 2). The Anguille Group occurs within two elongate structural blocks (known as the Fisher Hills and Birchy Ridge) classified as flower structures (Hyde, 1988). The younger units are found on both sides of the flower structures resting on PreCarboniferous basement.

The Deer Lake Basin has been described as a frontier basin in terms of mineral and hydrocarbon potential (Hyde et al., 1994) as it has only been lightly explored. Since the early 1900's, however, the Deer Lake Basin has been the focus of geological investigations. Jukes (1843) first documented and described the coal beds in the Howley area (Hayes, 1949). Coal beds were explored and diamond drilling was undertaken in the early 1900's by the Reid Newfoundland Company and the Newfoundland Government (Hayes, 1949). Additional coal occurrences on Coal, Adler, Kelvin, and Goose Brook areas were referenced by Howley (1917), but he was ultimately unsuccessful in locating a coal field. Coal seams were exploited by the Reid-Nfld Development Company in 1914 and later by the Anglo-Nfld Development Company in 1947 (Hayes, 1949). Hatch (1919) examined and sampled oil shales in the Deer Lake Basin (Hayes, 1949). Research by Baird (1950), Hyde (1984), Macauley (1987),

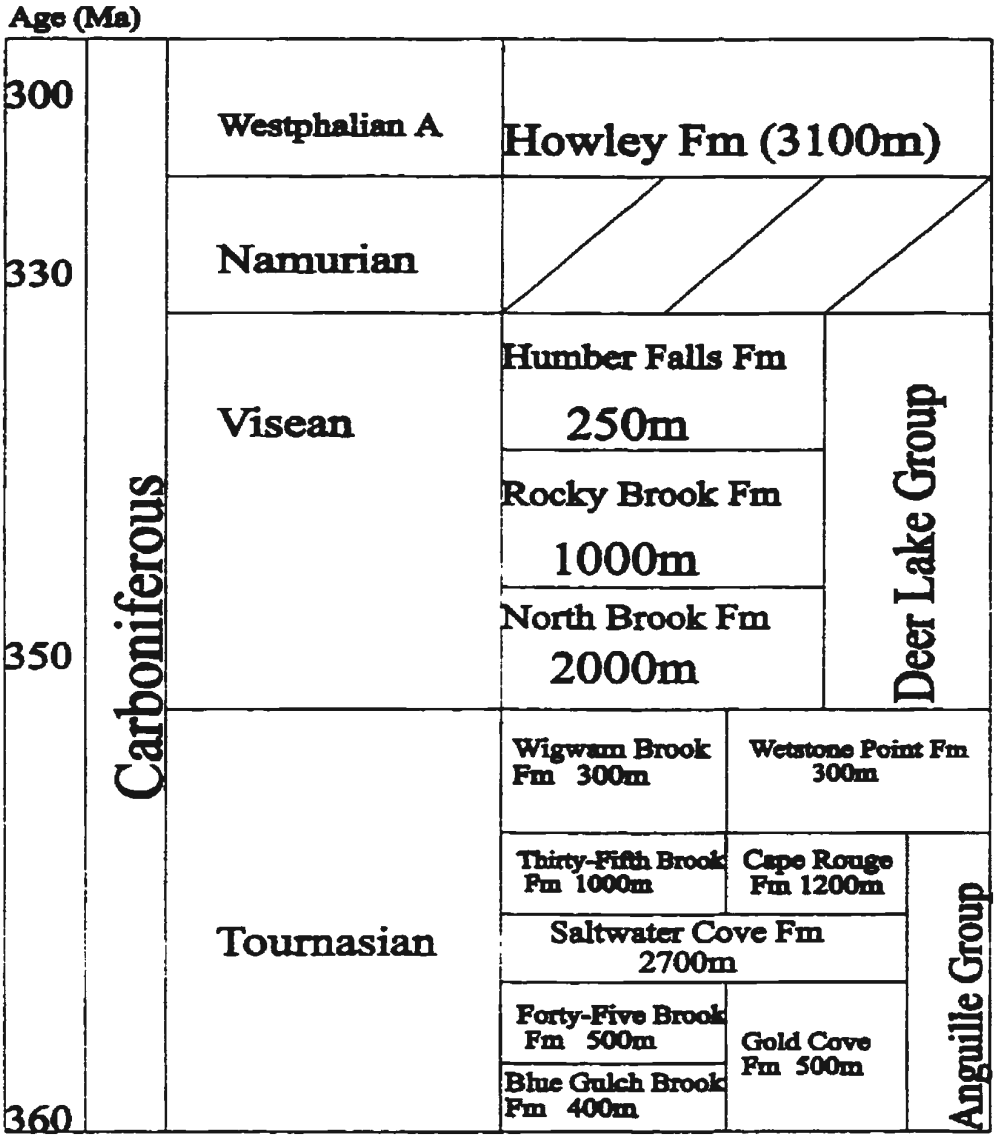

Figure 2 Stratigraphy, age, and thickness of the Carboniferous Deer Lake Basin (modified from Gall, 1984).

and Kalkreuth and Macauley (1989) focused on the oil shales of the Deer Lake Basin Area. Landell-Mills and Claybar Uranium Ltd (1955-56) conducted exploration programs that included drilling in search for oil shales and uranium. Fleming (1970) summarized oil and gas exploration and noted that most of the activity was focused on the North-West portion of the basin.

Various geophysical studies have been made in the Deer Lake Basin. Weaver (1969) undertook a gravity survey. Miller and Wright (1984), completed gravity and magnetic surveys, and using a crude experimental seismic survey, they commented on the basin architecture. In a joint project between the Center for Earth Resources Research at Memorial University and Vinland Petroleum, a seismic survey was completed in 1994 to constrain the basement structure. This seismic study showed that the Deer Lake Group sediments are up to 2.5 km thick.

Hyde (1979) outlined the various mineral occurrences in the Deer Lake Basin observed during his mapping program in the area. Tuach (1987) studied mineralizing environments and metallogenesis in the Doucers Valley complex, western White Bay, which includes a small portion of the Deer Lake Basin area; most importantly the Turners Ridge and Side Pond lead occurrences. Saunders et al. (1992) analyzed carbonate-hosted lead zinc deposits of western Newfoundland, including Turners Ridge and Side Pond. Dalley (1981) examined the relationship between magnetic minerals and uranium mineralization, and the aeromagnetic signatures.

Gall (1984) studied the petrography and diagenesis of the Carboniferous Deer Lake Group and Howley Formation in the Deer Lake Basin. His results indicated that the petrographic and diagenetic characteristics were essentially the same in each formation. The paragenetic sequence for the North Brook and Howley Formations reflect an acidic to alkaline geochemical environment, whereas the Rocky Brook developed within a more stable alkaline geochemical environment. Gall and Hyde (1989) examined analcime in lake and lake-margin sediments of the Rocky Brook Formation. Results of the study suggest that the analcime formed either by direct lakewater/porewater precipitation or by reaction of these waters with one or more clay mineral types or plagioclase.

1.3 - Present Study Techniques

This study presents the results of an integrated geological, geochemical, and geophysical approach to the examination of the structural controls on the type(s) and nature(s) of hydrothermal fluids that coursed through the Deer Lake Basin. Few studies integrate all of these aspects, in particular, the association between organic matter and ore mineralization in vein systems. Whole-rock samples were collected throughout the Deer Lake Basin area and were subjected to a number of analytical techniques to determine isotopic major and trace element geochemistry. The techniques include X-Ray Fluorescence (XRF) and Inductively Coupled Plasma-Mass Spectrometry (ICP-MS). Sulphur, carbon, oxygen, and lead isotope analyses were performed on a smaller number of samples (mineral separates) in an attempt to determine the source of ore-forming

fluids. Micro-thermometric analyses were performed on primary fluid inclusions using a Fluid Inc. U.S.G.S. gas-flow heating-freezing system attached to a Leitz Ortholux microscope to determine trapping temperatures and salinities. Other petrographic descriptions of the samples and veins were completed using standard transmitted-light and reflected-light microscopy.

Carbon isotope, Carbon-Hydrogen-Nitrogen (CHN), Inductively Coupled Plasma Mass Spectrometer (ICP-MS) and Laser Ablation Microprobe ICP-MS (LAM-ICP-MS) analyses were undertaken to examine bitumen and coal samples from various parts of the basin. Since coal and bitumen had not been previously analyzed by the ICP-MS group at Memorial, new procedures were developed and employed, producing encouraging results.

In a further attempt to understand the geology in the Deer Lake Basin, the Geosoft computer software package was used to produce various geophysical and geochemical maps (Bouguer gravity, total field aeromagnetic and geochemical anomaly maps). The potential field dataset used was the gravity data from Miller and Wright (1984) along with the GSC gridded aeromagnetic data (Kilfoil and Bruce, 1989), while the geochemical dataset was extracted from the digital geochemical atlas of Newfoundland (Davenport et al., 1996). The results of each method will be discussed in subsequent chapters.

CHAPTER 2: - Geological Constraints of The Deer Lake Basin

2.1 - General Geology

Middle Devonian-Carboniferous rocks are widespread in Atlantic Canada and constitute the Maritimes Basin (Langdon and Hall, 1994). Covering 150,000 km^2, the basin extends from Newfoundland to Quebec (Figure 1). The Cabot Strait separates southwestern Newfoundland from Cape Breton Island in the eastern Gulf of St Lawrence (Figure 1). The Strait is underlain in part by the Maritimes Basin, the boundary between constituent subbasins, the Magdelen Basin to the west and the Sydney Basin to the east. Langdon and Hall (1994) report that up to 6 km of Devonian-Carboniferous sedimentary rocks (predominantly siliciclastics deposited in alluvial, fluvial, and lacustrine environments) are preserved under the Cabot Strait, concentrated in two linear grabens that parallel and are defined by the major fault trends.

The geology in western Newfoundland and the Maritimes area is largely controlled by the regional strike-slip fault system, comprising the Cape Ray Fault, the Cabot Fault, and the Hollow-St George's Bay Fault. The Cabot Fault was the master fault along which most of the strike-slip deformation occurred. Since the Paleozoic, the Maritimes Basin has experienced uplift and erosion associated with the Tertiary opening of the Atlantic Ocean during which time 1-3 km of Carboniferous sediment was removed (Langdon and Hall, 1994). Carboniferous rock exposures now straddle and outline the fault traces often in the form of small, individual, linear, inverted or partially inverted

basins; examples include the St. Georges Basin and the Deer Lake Basin (Langdon and Hall, 1994) (Figure 1).

Based on structural and stratigraphic criteria, Williams (1979) divided the Appalachian Orogen into five broad zones, which comprise from west to east, the Humber, Dunnage, Gander, Avalon and Meguma zones. The Appalachian Orogen was affected by three major orogenic events, the Taconic orogeny (Ordovician), Acadian Orogeny (Devonian) and the Alleghanian orogeny (Permian to Carboniferous) (Williams, 1979). The Doucers Valley fault complex in the northern part of the study area separates the Humber and Dunnage zones and marks a major tectonostratigraphic break in the Appalachian Orogen (Tuach, 1987). The Deer Lake Basin, a Carboniferous successor basin to the Appalachian Orogen, lies entirely within the Humber zone, the eastern margin of which is defined by the Baie Verte-Brompton line. The Cabot Fault has reactivated and overprinted parts of the Baie Verte-Brompton line (Hyde et al., 1994). In detail, early Carboniferous (Visean to earliest Namurian) sedimentary rocks of the Deer Lake Group rest unconformably on Grenvillian basement rocks of the Humber Zone, the western cratonic border to the early Palaeozoic Appalachian Orogen (Irving and Strong, 1984).

2.2 - Stratigraphy

The distribution of calcretes and organic accumulations in the Deer Lake Basin suggests that there were large periodic fluctuations in paleoclimate during the

Carboniferous (Hyde et al., 1994). The Deer Lake Basin was entirely non-marine, being either topographically high enough above Carboniferous sea level, or land-locked by mountain ranges, to remain non-marine even during times of marine transgression (Hyde, 1994). Irving and Strong (1984) have determined that the paleolatitude for the basin during deposition was 20° +/- 6°S of the equator indicating a warm semi-arid environment.

The Deer Lake Basin is surrounded by Pre-Carboniferous rocks of various types, ranging from granites, gabbros, and volcanics to metasediments, clastics and carbonates and is interpreted to contain approximately 1700m of predominantly non-marine sediments (Figure 2) (Hyde and Ware, 1981). Sediments of the Deer Lake Basin include alluvial fan, braided and meandering river, lacustrine, and coal swamp facies. Formations representing basin-fill from oldest to youngest are the Anguille Group, Wetstone Point and Wigwam Brook Formations, Deer Lake Group, and Howley Formation (Figure 2).

The Anguille Group, resting on PreCarboniferous basement is a fining upwards megasequence that consists predominantly of well-cemented grey sandstones, siltstones and mudstones, and represents the infill of a pull-apart basin. Plant and spore evidence suggest a Tournaisian age for the Anguille Group (Hyde, 1984). The Tournaisian Wetstone Point and Wigwam Brook Formation consist of fluvial conglomerates, sandstones, and limestones. Unconformably overlying the Anguille Group and Pre-Carboniferous basement is the Deer Lake Group which consists of conglomerates, sandstones, siltstones, siliciclastics, limestones, and oil shales. The Deer Lake Group has

been subdivided into the North Brook Formation (no definite age), the Rocky Brook Formation (late Visean-early Namurian) and the Humber Falls Formation (perhaps of late Namurian age). Both the Rocky Brook and North Brook Formations formed in a lacustrine / fluvial type depositional environment. The Howley Formation (the youngest) consists of Carboniferous siliciclastic rocks ranging from mudstone to conglomerate and includes coals. The Howley beds were deposited in a fluvial/swampy type depositional environment and spore evidence defines a Westphalian age (Hyde et al.. 1994).

2.3 - Tectonic Development

The Deer Lake Basin is situated at the NE margin of the regional Maritimes Basin, a successor basin covering the area between Newfoundland and Quebec which was generated by post-orogenic extensional processes (mid-late Devonian) after the main Acadian orogeny (Langdon. 1993) (Figure 1). Strike-slip tectonics which enhanced and altered the physical form of the basin. were localized along the Cabot Fault system.

The Doucers Valley Fault complex, separates platformal sequences in Western Newfoundland (Humber Zone) from continental slope/rise and oceanic facies to the east (Dunnage Zone), and this complex relationship to the Deer Lake Basin marks a major tectonostratigraphic break in the Appalachian Orogeny (Tuach, 1987).

The Deer Lake area is underlain largely by Carboniferous rocks which were deposited on the downwarped surface of Lower Paleozoic and Precambrian rocks (Fleming, 1970). The area is a rolling lowland with sharply incised streams rimmed by

high hills underlain by older rocks. The lowland surface is interrupted by two higher areas, of lower Mississippian rocks, the Grand Lake-Deer Lake uplift and the Birchy Ridge (Fleming, 1970).

Structural and stratigraphic evidence suggests that there was dextral strike-slip movement along the Doucers Valley Fault complex during Tournaisian-Visean time. Two elongated end-on structural blocks (probable positive flower structures) contain fold axes and second-order faults oriented obliquely to fault traces bounding the blocks, in a manner implying dextral movements (Hyde et al., 1988). In one part of the basin, the stratigraphic thickness of a long homoclinal section of later basin-fill sediment (Deer Lake Group) greatly exceeds the suggested depth to basement based on gravity measurements, a situation common to strike-slip basins (Hyde et al., 1988). Deformation of the Deer Lake Group is displayed by occurrences of major NE-SW oriented strike-slip faults intimately associated with intense folding. Folding diminishes considerably away from the faults and this is considered as major evidence that folding was a result of faulting (Hyde, 1979)

Although most workers agree that major faults are strike slip in character there is little agreement as to the timing and movement history of the faults. Hyde et al., (1994) described the Deer Lake Basin in terms of two major tectonic elements, that of flower structures and 'lateral basins'. He suggested that development of Visean transpressive positive flower structures along a strand of the Cabot Fault created a topographic high

which subdivided the basin into two shallow lateral basins; the Deer Lake Sub-Basin and the Howley Sub-Basin approximately 1.2 km and 1.5 km deep respectively.

Langdon (Pers. Comm., 1996) presents an alternate viewpoint suggesting that a post-Visean transpressional event overprinted the lower Carboniferous event and is probably the same one as that responsible for Namurian-Westphalian inversion in the Cabot Strait. The Deer Lake Basin has had a complex history involving extensional collapse in late-Devonian-Tournaisian time resulting in deposition of the Anguille Group and then later pull-apart tectonics in late Visean-Namurian time along an irregular strike-slip fault system combined with the northward escape of the Baie Verte Peninsula.

Hyde and Ware (1981) mapped early deformation of features along the Humber River Strand of the Cabot Fault. Interpretation of seismic data by Hamblin et al. (in prep) suggest that this deformation was late Tournaisian-Visean age and that Anguille rocks were deformed in a narrow zone. The thickness of the Deer Lake Group and Howley Formation have also been controlled by movement on the Humber River strand of the Cabot Fault. Hamblin et al. (in prep.) note that the presence of pronounced anticlinal structures (likely en-echelon fold axes) further supports the concept of post-Visean deformation. Saunders et al. (1992) support post-Visean deformation by noting the westward thrust faulting of Silurian volcanic rocks over the North Brook Formation.

The presence of a half-graben likely controlled Westphalian subsidence of the Deer Lake Basin in the mid-late Carboniferous. Since the Carboniferous, the Deer Lake Basin has been partly exhumed so that rocks originally at the upper boundary of the oil

window (1 - 1.5 km depth) are now exposed at the surface. Exploration targets therefore should lie within 1-3 km of the surface.

CHAPTER 3: - Potential Fields

3.1 - Previous Geophysical Work

The first regional geophysical survey which included the Deer Lake Basin was the gravity survey of Newfoundland completed in 1967 by Weaver (1967). It defined a high positive gravity anomaly in the Adies Pond area which was ascribed to a gabbro and/or diorite intrusion previously mapped by Baird (1950). Weaver (1967) also concluded that there was a pronounced eastward-trending gravity low over the Howley Formation; using the amplitude of this anomaly, and a representative density, he interpreted the Howley Formation and underlying sediments to be approximately 5 km thick. Miller and Wright's (1984) gravity modeling results re-defined the thickness of the Deer Lake Group sediments as 1.5 km, significantly less than the 5 km estimated by Weaver (1967).

Ahmed (1983) completed a seismic survey along a line through Sir Richard Squires Park in the Humber syncline using a 6-fold CDP technique. One of the results of the survey was the velocity definition of the units in the subsurface which helped to constrain the geology in the area. The velocities of the units agreed with Hyde's (1984) interpretation of the geology in that the highest velocities were in the Precambrian strata consisting of compact high density metamorphic rocks such as quartzite, and mica schist, while the lower velocities were associated with the Carboniferous strata.

Miller and Wright (1984) undertook a gravity study of the Deer Lake Basin, the dataset of which is used in this present study. Their Bouguer anomaly gravity map showed strong positive anomalies in the NE and SE parts of the basin, which correlate

with the presence of the Wild Cove Pond and Topsails Igneous Suites respectively. Another positive anomaly in the North-West part of the basin correlates with Weaver's (1967) Adies Pond High and coincides with the location of the oldest crystalline rocks in the area. Miller and Wright (1984) also defined a NE regional trend with the presence of an E-W trend in the eastern part of the Deer Lake Basin. Features close to the surface were prominent on the residual anomaly map defining slightly negative gravity features in the Humber syncline and major magnetic anomalies in the north of the basin, with a N-S trend which may be attributed to uranium occurrences in the basin.

Dalley (1981) undertook a magnetic survey of the basin as part of a uranium exploration program by Westfield Minerals Ltd. High-grade uraniferous and highly magnetic till had been found in the Deer Lake Basin (Tuach, 1987). Dalley (1981) noted that magnetic minerals were concentrated in proximity to certain uranium deposits, but he also found that it was difficult to establish a relationship between magnetic signature and the occurrence of uranium mineralization, as detrital magnetic minerals are often destroyed by the same oxygenic processes that form uranium deposits. Dalley's (1981) magnetic survey outlined several magnetic high anomalies in the area shaped like a tongue and Dalley suggested two probable models for the origin of the anomalies: (1) that basement material was more highly magnetized over a paleoridge; or (2) they result from the movement of fluids in a channel in which ferromagnetic minerals were carried in solution or suspension. Hyde (1979) postulated that there was a paleoflow in the direction NE-SW which coincided with the magnetic model. The SE-trending magnetic

anomalies (associated with uranium mineralization) also coincided with the regional residual gravity high defined by Miller and Wright (1984).

The Center for Earth Resources Research, in conjunction with Vinland Petroleum, acquired and processed seismic data in mid 1994 along 2 test lines in the North-West section of the basin. The results of this study showed that the Deer Lake Group sediments are up to 2.5 km thick, and that there was considerable faulting in the basin associated with both the formation of a flower structure in Pre-Visean time and continued strike-slip transtensional tectonics throughout the Visean (Wright et al., (in prep)). This is important as it indicates that the Deer Lake Basin is deeper than in previous interpretations. The most recent geophysical work (1997) has been completed by Inglewood Resources, in association with Vinland Petroleum, who acquired seismic data along a number of test lines in the basin. This new seismic data will bring about a better understanding of the structural control in the basin.

3.2.1 - General Introduction

The Geosoft computer software package was used to produce geochemical and geophysical maps in order to provide a basis for interpreting the geological, geochemical, and geophysical data. The potential field dataset used was the gravity data from Miller and Wright (1984) along with the GSC gridded aeromagnetic data (Kilfoil and Bruce, 1989), while the geochemical dataset was extracted from the digital geochemical atlas of

Newfoundland (Davenport et al., 1996). Maps created for this study were overlain on a geological base map (Map 1) with a scale of 1:150,000.

The predominant trend of the geophysical anomalies in the Deer Lake Basin is northeasterly with a strong east-west trend developed in the center of the eastern portion of the map (coincident with the Howley Fm.) (Miller and Wright, 1984). The potential field data analysis in the Deer Lake Basin involved removing the regional trend by regional-residual separation to examine the effect of near-surface, smaller-scale features.

The geochemistry maps created for this study used a subset of the Newfoundland Department of Mines and Energy (NDME), Newfoundland geochemical dataset in Arcview (Davenport et al., 1996), extracted to include only those values within the Deer Lake Basin. The Geosoft computer program was then used to produce various geochemical maps (Maps 5 - 27).

Four hundred and twenty seven samples were collected by the NDME from lakes and streams in and around the Deer Lake Basin area. Map 28 shows the location of each geochemical sample site. Depending on the range of concentrations and distribution of samples, either the histogram normalization or linear normalization method in Geosoft was used for the colour zone distribution on the geochemical maps.

The distribution of sample sites indicates that the geochemical anomalies defined for the basin are real anomalies. This is further substantiated by the low concentrations of manganese. Manganese is a sponge element, (Hawkes and Webb, 1962) that acts locally

to concentrate other elements; the low values of manganese thus indicate that the geochemical anomalies are not manganese induced._

3.2.2 - Gravity Introduction

Detailed reconnaissance gravity surveys by Miller and Wright (1984) in the Deer Lake Basin were conducted using 230 stations (Map 29) with a station spacing along roads of 2.5km. In areas not accessible by roads, helicopter transportation was used. Data were collected using a Sharp CG2 Gravimeter with ancillary elevation data obtained using Wallace and Tiernan Barometric Altimeters and sling Psychrometers for temperature and humidity information (Miller and Wright, 1984). The elevations for the barometrically leveled stations were tied to the Geodetic Survey of Canada Bench Mark at the Deer Lake Airport, and all gravity readings were tied to the national network and the International Gravity Standardization Net (1971) (Miller and Wright, 1984). Using the IGSN71 system with the international gravity formula, a mean crustal density of $2.67 g/cm^{-3}$, the elevation and position of the station, Bouguer anomalies were calculated (Miller and Wright, 1984). These anomalies included standard corrections for instrumental drift, latitude, and elevation.

3.2.3 - Gravity Discussion

This study uses the data collected by Miller and Wright (1984) for further investigation into the Deer Lake Basin. The intention of this study was not to present a

detailed interpretation essentially completed by others, but to present an interpretation of the correlation between the geochemical signatures and the fault bounded blocks identified from the geophysical data. New maps created for this study extracted only those values within the basin from the original Bouguer gravity values; the Bouguer values were then subjected to a regional-residual separation process to study localized features (Map 2).

The predominant trend of the residual gravity and original Bouguer anomalies is northeasterly with a strong east-west trend developed in the center of the eastern portion of the map (coincident with the Howley Fm.) (Miller and Wright, 1984). Other prominent features are the closed positive anomaly patterns in the NE-SE sections of the map which correlate with the Wild Cove Pond (mainly granitic to gabbroic rocks) and the Topsails igneous suite (a mid-Paleozoic granitoid suite) respectively. The gravity high in the North-West portion of the map is a more detailed mapping of the Adies Pond high and coincides with the location of the oldest crystalline rocks (Grenvillian) in the area (Miller and Wright, 1984). The main Humber syncline, composed mainly of Deer Lake Group strata, is not easily visible on the regional Bouguer gravity map (Miller and Wright, 1984).

To examine the effect of near-surface, smaller-scale features, the Bouguer gravity anomaly map was subjected to a regional-residual separation process using a polynomial trend surface analysis via Geosoft. The regional anomalies were calculated from the 3rd order statistically best-fitted trend surface taking into consideration all the points inside

the basin. The resulting residuals were determined by the subtraction of the trend surface anomaly from the Bouguer anomaly at each grid location (Map 2). The color zoning of the potential field maps used a normal distribution of the values for gravity maps and a linear distribution for magnetic maps. The rationale for this is to achieve the best possible gridding distribution for the data by isolating and emphasizing trends. This process also allows the edges of anomalies to be sharpened and enhances the shallow features. which is important in the Deer Lake Basin since it is a relatively shallow basin.__

Contours on the Bouguer gravity residual anomaly map (Map 2) range from +11.2 mGal to -11.1 mGal; this map is localized and not contaminated by the Long Range Mountains to the North-West. Overall this map shows that the North-East trend arises mainly from the Adies Pond high.

Several features with near-surface sources are apparent on Map 2. With removal of the regional trend, the Humber syncline (latitudes 49°25' and 49°10' and longitudes 57°15' and 57°30') can be identified as a NW-SE trending feature with a slightly negative gravity value having a second smaller trough east of it, near Sandy Lake. Both of these low troughs coincide with areas underlain by the Humber Falls Formation (Map 1). The gravity highs in the NE, SW, and mid SE quadrant of the map are associated with PreCambrian crystalline rocks, and are also influenced by granite intrusions on the eastern edge of the basin. The low in the eastern middle section of the map is centered over the youngest formation, the Howley Formation (Map 1) and is an expression of relatively greater thickness of sediments in that part of the basin (Miller and Wright,

1984). Turners Ridge, a Mississippi Valley-type galena deposit near the Wigwam fault in the North-East part of the basin, shows a gravity low.

The positive residual anomalies correlate with up-thrown blocks such as the Birchy Ridge, and negative residuals indicate areas of syn- and post-transpressive sediment accumulation (Miller and Wright, 1984). The main NE-trending fault system is clearly identified and a second fault system perpendicular to this main system is also delineated. This suggests that the southern part of the basin is down-thrown with respect to the northern part. This second fault system was formed at a later date than the original NE-trending system since displacement of the main fault system is evident.

3.3.1 - Magnetic Introduction

Magnetic anomalies are caused by magnetic minerals (mainly magnetite and pyrrhotite) contained in the rocks. Magnetic anomalies are associated with the upper crust since temperatures below ~40 km depth should be above the Curie Point (T= 550°C) at which rocks lose their magnetic properties. Magnetic maps are more indicative of shallow features than gravity (Telford et al., 1990).

Total field aeromagnetic maps published by the Geological Survey of Canada at 1: 63,360 scale were based upon data collected along east-west flight lines separated horizontally by 812m, flown at an altitude of 300m from February 1966 - August 1967. An original total field aeromagnetic map was produced by Miller and Wright (1984). These data were re-digitized as part of a project to provide digital data for all of

Newfoundland in 1989 (Kilfoil and Bruce, 1989). To further investigate the Deer Lake Basin, the total field aeromagnetic data were extracted to include only those values that occur within the Deer Lake Basin, and a regional-residual separation process was employed using a polynomial trend-surface analysis in the Geosoft computer program producing various magnetic maps (Maps 3 and 4). The residual anomalies were calculated from the 3rd order statistically best-fitted surface using all the values in the basin.

3.3.2 - Magnetic Discussion

The features of the aeromagnetic maps are more dramatic than the residual gravity maps. Map 3 is the total field aeromagnetic residual map (in colour) which ranges from -253.8 nT to +253.8 nT, with a shaded relief map (grey tones) underlay. Magnetic (positive values) highs tend to coincide with faults (with the exception of the low on the fault on the east side of Grand lake) which have been previously mapped, and (negative values) lows occur on the north-west edge of the basin, suggesting that the eastern side of the basin is fault bounded. The Humber Falls Formation (Map 1) uranium occurrences coincide with magnetic highs. The positive anomalies along the northern part of the map suggest that the Anguille group of Birchy Ridge may be underlain at relatively shallow depth by more magnetic rocks (Miller and Wright, 1984).

NW-SE structures continue into the rocks on either side of the basin suggesting that they may be older features which controlled the size of the Humber syncline. The

Humber syncline (latitudes 49°25' and 49°10' and longitudes 57°15' and 57°30') is readily identifiable on Map 3 from the shaded relief of the residual map created with a declination of 135°, and an inclination of 25°. The west limb of the syncline is underlain by mafic-ultramafic rocks while the eastern limb is underlain by granitic rocks. The contact between the two different basement complexes, which coincides with the axis of the syncline is interpreted to represent the extension of the Taylors Brook fault beneath the basin. Miller and Wright (1984) interpret the extension of this fault to represent the edge of the Precambrian North American continent.

Map 4 is the total field magnetic horizontal gradient map which results from the difference between successive magnetic grid data points (high and low values). This is illustrated by the good correlation between the geologically mapped faults (Map 1) and the gradient maxima or minima. This technique is particularly effective at delineating subsurface blocks. Maxima in the horizontal gradient tend to occur over the edges of sources. This map indicates the major features in the basin, such as faults and also large blocks of subsurface material in the SW and NW.

A horizontal gradient maximum occurs on the eastern edge of the basin due to a large block of subsurface material along the Grand Lake fault (latitudes 49°20' and 49°00' and longitudes 57°15' and 56°50'). This is also seen on Maps 2 and 3 as positive gravity residuals and positive magnetic residuals respectively, with the shaded relief magnetic residual outlining the edge of the fault. A horizontal gradient maximum (Map 4) appears in the wedge between the Birchy Ridge and Wigwam faults (latitudes 49°20' and 49°45'

and longitudes 57°10' and 56°50'). This magnetic gradient maximum is shown as positive magnetic residuals (Map 3), and positive to slightly negative gravity residuals (Map 2). while the shaded relief magnetic residual outlines the faults bounding this wedge.

Between latitudes 49°15' and 49°35' and longitudes 57°10' and 56°50', a horizontal gradient maximum occurs, corresponding to negative gravity and magnetic residuals (Maps 2 and 3). The shaded relief magnetic residual outlines the edge of this subsurface block. Another maximum on the horizontal gradient map is indicative of the Adies Pond high, (latitudes 49°15' and 49°35' and longitudes 57°30' and 57°00') outlined by the shaded relief magnetic residual and seen as a positive gravity residual and positive to slightly negative magnetic residual.

The major magnetic anomalies in the center of the study area are dominated by an E-W trend. The trend of this anomaly pattern is perpendicular to that of the Humber syncline in the area, suggesting the presence of an E-W trending fault, a feature noted by Miller and Wright (1984). It appears that the southern portion of the basin is down-thrown with respect to the northern part.

3.4.1 - Geochemistry Introduction

The geochemistry maps created for this study used a subset of the NDME, Newfoundland geochemical dataset in Arcview (Davenport et al., 1996), extracted to include only those values within the Deer Lake Basin. The Geosoft computer program was then used to produce various geochemical maps (Maps 5 - 27). The histogram

normalization method in Geosoft was used for the colour zone distribution on most of the geochemical maps, with the exception of maps 5, 7, 13, 18, 22, 24, and 26 which used a linear distribution due to the low range in concentrations, to counteract any smearing effect.

3.4.2- Geochemistry Discussion

Geochemistry maps for the Deer Lake Basin were created with a two-fold purpose: 1) to study which elements are related to the presence of faults and / or to subsurface strata; and 2) to use potential field data to interpret the nature of the geochemical anomalies. Twenty-two maps were created for this purpose. The geochemical maps are compared with the magnetic horizontal gradient map (Map 4), magnetic residual map (Map 3) and Bouguer gravity residual map (Map 2). The distributions of several mobile elements were deemed to be fault related, and these include As, Au, Cu, Eu, Fe, Mo, Pb, Sb, U, and Zn (Maps 5, 6, 12, 13, 15, 18, 20, 22, 25, and 27 respectively). The distributions of the other elements are indicative of variations in the nature of the subsurface strata, which in some cases are fault bounded.

Map 17 is the manganese distribution map in which Mn ranges from 0-44175 ppm. Manganese is a sponge element (Hawkes and Webb, 1962), which is often responsible for concentrating other elements. The generally low concentrations of manganese indicate that the geochemical anomalies seen in the basin for other elements are true anomalies and not manganese induced. At latitude 49°10' longitude 57°10', an

elevated manganese anomaly is observed in a subsurface block coinciding with a magnetic gradient maximum (Map 4), positive magnetic residuals (Map 3) and negative gravity residuals (Map 2). At latitude 49°10' longitude 57°20', another manganese anomaly is observed coinciding with a magnetic gradient maximum (Map 4), negative gravity residual (Map 2) and positive magnetic residuals (Map 3). A third manganese anomaly is observed at latitude 49° 30' longitude 57° 10', with a magnetic gradient maximum (Map 4), and positive magnetic and gravity residuals (Maps 3 and 4).

The lead contents map ranges from 0-53 ppm (Map 20). This map indicates that lead is probably fault related as the high values occur over fault bounded blocks and coincide with faults mapped by Hyde (1982). A lead anomaly occurs at latitude 49°10' longitude 57°40' with a magnetic gradient maximum, positive gravity residuals and positive to slightly negative magnetic residuals (Maps 4, 2 and 3 respectively). This anomaly is probably reflecting lead contents in basement rocks. Another lead anomaly occurs at latitude 49°20' and longitude 57°00' coinciding with a magnetic gradient maximum, positive magnetic residuals and positive to slightly negative gravity residuals (Maps 4, 3, and 2 respectively); again possibly reflecting lead contents in basement rocks. Turners Ridge, a MVT galena deposit, shows low concentrations of lead (Map 20). This lead showing occurs on a ridge in the basin, thus basinal fluids would be expected to carry lead away from the ridge causing misplaced anomalies especially in the fault pathways . The topography of the surrounding area outside the basin shows drainage into the basin presumably through faults, suggesting that the lead (for Turners Ridge) was

sourced from outside the basin, possibly from felsic rocks. and came in through porous-permeable pathways such as the Wigwam Fault.

Concentrations in the zinc anomaly map ranges from 0-313 ppm (Map 27). High zinc values occur on mapped faults (Hyde, 1982) and appear to be fault related. Zinc values are high on the western side of the basin in Humber Zone carbonates mapped by Hyde (1982), showing a magnetic gradient minimum (Map 4), negative magnetic residuals (Map 3) and positive gravity residuals (Map 2). Zinc is a mobile element and thus migrated through porous-permeable pathways provided by fault structures in the basin as seen by the shaded relief magnetic residual map (Map 3).

The shaded relief magnetic residual map (Map 3) illuminates the fault structures in the Deer Lake Basin. In comparison with this map, several other geochemical anomalies coincide with the fault structures. These include silver (Map 5) ranging from 0.1 - 0.3 ppm, antimony (Map 22) ranging from 0 - 1 ppm, europium ranging from 0 - 4 ppm (Map 13) and iron (Map 15) ranging from 0 - 35%, all with magnetic gradient maximum (Map 4), and low magnetic and gravity residuals (Maps 3 and 2 respectively).

Arsenic can serve as a pathfinder element for gold (Hawkes and Webb, 1962). This means that arsenic anomalies are used to help find gold since the anomalies are coincident with gold showings. Arsenic ranges from 0 - 73 ppm (Map 6). Some of the anomalous highs on Map 6 coincide with mapped faults (Hyde, 1982). Other arsenic anomaly highs coincide with bitumen and coal deposits (sample 24, 19) at latitude 49°10' and longitude 57°10' with a magnetic gradient maximum (Map 4), low magnetic and

gravity residuals (Maps 3 and 2). Another arsenic anomaly at latitude 49°10' and longitude 57°40 coincides with a magnetic gradient minimum (Map 4), low positive magnetic residuals (Map 3) and high positive gravity residuals (Map 2); it is possibly due to arsenic contents in basement rocks.

Map 7 is of gold which ranges from 0 - 10 ppb. The anomalous highs are controlled by faults in the basin, as supported by the shaded relief magnetic residual map (Map 3) and also coincide with the bitumen and coal deposits at latitude 49°10' and longitude 57°10' with a magnetic gradient maximum (Map 4), and low magnetic and gravity residuals (Maps 3 and 2). The extension of these faults into Sop's Arm to the north resulted in later gold, base metal and uranium mineralization from the generation of hydrothermal activity when the structures were periodically reactivated during the Paleozoic orogenies (Tuach, 1987).

Molybdenum ranges from 0 - 23 ppm (Map 18). Molybdenum can behave as a granophile element or a pathfinder element for gold (similar to As). High molybdenum anomalies suggest the presence of gold in the local sedimentary environment, and are coincidentally centered on the faults in the basin, indicating the pathways for fluid movement; also observed by the magnetic residual shaded relief map (Map 3). Tuach (1987) states that the Gull Lake Granite (located between the Wigwam and Birchy Ridge Faults north of Turner's Ridge, (Map 1)) has high fluorine and molybdenum content. Minor re-mobilization in the area of the Gull Lake granite may have occurred; since the granite is younger than the fault structures in the Deer Lake Basin this suggests that the

fluids which flowed along the faults were not granite related. The fluorine contents map ranging from 0 - 1713 ppm (Map 14), lanthanum ranging from 0 - 148 ppm (Map 16) and cerium ranging from 0 - 356 ppm (Map 9) all show elevated values in the northern portion of the basin corresponding to the Gull Lake granite.

There are several uranium deposits known in the basin (Hyde. 1982). Map 25 is of uranium distribution which ranges from 0 - 37 ppm. Positive uranium anomalies correspond to areas with bitumen (samples 24, 19, (Map 1)) in the South-West coinciding with a magnetic gradient minimum (Map 4), positive gravity residuals (Map 2) and low positive to slightly negative magnetic residuals (Map 3); this is also true of bitumen in the Howley Formation (sample d3) with the exception that little or no uranium is present. Bitumen and coal are indicative of a reducing environment that could cause uranium precipitation from oxidized fluids. The coal sample W89-37A in the Howley Formation, has moderate to low concentrations of uranium with magnetic gradient maxima (Map 4), low gravity and magnetic residuals (Maps 2 and 3). Since uranium movement is suggested to have occurred early in the diagenetic history of the basin (Hyde, 1984), this could explain why little or no uranium is found in conjunction with the organic samples located in the youngest stratigraphic unit, the Howley Formation.

Another uranium anomaly occurs at latitude 49°20' and 49°10' and longitude 57°00' with a magnetic gradient minimum (Map 4), negative magnetic residuals (Map 3) and positive to slightly negative gravity residuals (Map 2). These anomalous areas are

fault related as uranium highs are centered near mapped faults (Hyde, 1982). This further suggests that uranium movement occurred early in the diagenetic history of the basin.

Ultramafic and mafic igneous rocks of older units in the basin (Hyde, 1982) have a magnetic gradient maximum (Map 4), slightly positive magnetic residual (Map 3) and a high gravity residual (Map 2). Elemental anomalies which coincide with the rock types include nickel ranging from 0 - 76 ppm (Map 19), chromium ranging from 0 - 305 ppm (Map 11), and copper (Map 12) ranging from 0 - 95 ppm. Copper anomalies also occur on mapped faults (Hyde, 1982), as suggested by the magnetic residual shaded relief map.

Nickel, chromium, ytterbium (ranging from 0 - 6 ppm (Map 26)), and thorium (ranging from 0 - 14 ppm (Map 24)), have elevated contents in the Howley Formation-Sandy Lake area (Map 1). These elements are presumably related to organic matter (coal/bitumen) present in the area.

Map 21 shows the distribution of rubidium which ranges from 0 - 62 ppm. Rb is fault related as highs are centered over the mapped faults (Hyde, 1982). Rough elemental ratios of Rb/Sr from XRF data (Appendix B.1.4; Samples 20, 21) (Rb/Sr = 1.28) indicate that Rb reflects the influence from the Pre-Cambrian basement.

Map 23 is the Samarium anomaly map which ranges from 0 - 37 ppm. The elevated Sm values are probably due to outside granitic influence. Rough elemental ratios of Sm/Nd (1.26) from XRF data (Appendix B.1.4; Samples 20, 21) indicate that the Sm values are mildly radioactive and presumably reflect a granitic influence.

The cobalt content map ranges from 0 - 100 ppm (Map 10) and Map 8 illustrates the barium distribution which ranges from 0 - 2253 ppm. The cobalt map appears to reflect Pre-Carboniferous rocks near bitumen (samples 19, 24) and also the Adies Pond high in the north. The barium distribution coincides with the North Brook Formation in the Humber syncline corresponding to barium observed by Hyde (1982). Both maps have magnetic gradient maximas (Map 4), low positive to slightly negative magnetic residuals (Map 3) and positive to slightly negative gravity residuals (Map 2).

3.4.3 - Summary

This summary deals with the correlation of potential field and geochemistry data with specific paleotopographic domains observed in the basin. The combined potential field and geochemical data show that some forms of mineralization in the basin occur near residual gravity and magnetic highs, while other forms are correlated with high magnetic gradients. The trends suggest an association of elements and bitumen / coal deposits with the underlying basement topography and the faults and fractures that formed structural conduits along which these fluids migrated. Gravity and magnetic residuals suggest that the basement within the basin is block faulted (Howley Fm. - down-thrown block and Birchy Ridge - up-thrown block).

Based on the NDME regional map of Newfoundland, mafic volcanics or a mafic phase of a pluton are mapped adjacent to the western edge of the Deer Lake Basin while granites are mapped on the eastern edge of the Basin. Due to the negative magnetic

anomalies correlating with smaller positive to slightly negative gravity anomalies on the east compared with positive gravity and magnetic anomalies on the west. both gravity and magnetic highs (Maps 2. 3. and 4) suggest that the mafics continue beneath the surficial cover on the west while the eastern edge of the study area appears to have a granitic influence. This is also indicated by rough elemental ratios of Sm / Nd (from XRF data) which suggest a granitic influence on the eastern side. and rough elemental Rb / Sr ratios (from XRF data) suggesting a mafic influence on the western side of the basin.

Overall the Howley Formation has negative Bouguer residual and magnetic residual signature. Coals within the Howley Formation appear to have a slightly positive gravity residual with low magnetic residual and magnetic gradient minimum. The bitumen and coal deposits (sample 24. 19) in the western side of the basin also have slightly positive gravity and slightly negative magnetic signatures. Magnetic maps (Maps 3. 4) support the geological mapping suggesting that the Deer Lake Basin area is fault-bounded (Hyde. 1982). and also show a marked contrast on either side of the Humber syncline due to the presence of mafics on the west limb and granites on the east limb. Maps 3 and 4 also show the presence of an E-W trending structure perpendicular to the Humber syncline suggesting a later stage structural event; it appears that the southern portion of the basin is down-thrown with respect to the northern portion.

The lowest magnetic values appear to be associated with the southern end of Wild Cove pond igneous suite rather than the Howley Fm (Miller and Wright, 1984). Birchy

Ridge (NE) has a small positive residual gravity anomaly and positive magnetic anomalies indicating that Birchy Ridge is underlain by denser magnetic material beneath a sediment cover (Miller and Wright, 1984). Uranium occurrences in the northern part of the basin correlate with magnetic and gravity residual highs.

The geochemical anomaly maps in combination with potential field data support the presence of large fault-bounded blocks of subsurface material and help delineate edges of faults which are serving as possible structural conduits for migrating fluids and/or structural traps for hydrocarbons in the basin. The basin can be divided up into eight distinct paleotopographic domains of fault-bounded blocks based on the character of the magnetic residual horizontal gradient, magnetic shaded relief, magnetic residual anomaly, Bouguer residual gravity anomaly maps, and the geochemistry anomaly maps.

The first paleotopographic domain is located between latitudes 49°00' and 49°15 and longitudes 56°45' and 57°20' bounded by the Grand Lake fault as shown by the magnetic shaded relief map (Map 3). This domain has a magnetic gradient maxima (Map 4) occurring on the fault, with a high-moderate gradient on the east side of the fault and a low-moderate on the west side of the fault. The gravity residual (Map 2) shows a positive gravity anomaly along the fault increasing in signature towards the east, with moderate-low gravity signature on the west side. The magnetic residual (Map 3) anomaly is low (negative) on the fault itself, with an extremely low signature on the west and a moderate-high signature on the east. Lake sediment elements with elevated contents in this domain include Ba, Ce, Co, La, Mn, Mo, Pb, Rb, U and Zn. These elements are usually high on

the fault structures or on the ends of the domain rather than in the middle with the exception of a barium high in the middle of the domain.

Paleotopographic domain 2 is located between latitudes 49°15' and 49°40 and longitudes 56°50' and 57°00' bounded by the Hampden and Grand Lake Faults and the north-east edge of Sandy Lake as seen by the magnetic shaded relief map (Map 3). This paleotopographic domain has a horizontal gradient (Map 4) maximum along its edges, at the faults, and edge of Sandy Lake. The magnetic residual (Map 3) is moderate to high along the faults, low along the Sandy Lake edge and low to high within the subsurface block. The gravity residual (Map 2) has a moderate to high signature along the bounding edges but decreases away from the edges toward the center of the section. Lake sediment elements with elevated contents in this paleotopographic domain include Rb, F, Cr, Th, Sm, Pb, Ni, La, Fe, Cu, Ce, Ba and Zn.

Paleotopographic domain 3 is located between latitudes 49°15' and 49°40 and longitudes 56°55' and 57°10' bounded by the Birchy Ridge fault on the west, Hampden fault on east and cuts across the southern end of Sandy Lake as seen by the magnetic shaded relief (Map 3). This paleotopographic domain has a horizontal gradient (Map 4) maximum along its edges, at the faults, low-moderate gradient inside the paleotopographic domain near Sandy Lake and gradually increases between the two bounding faults to the north. The magnetic residual (Map 3) is moderate to high along the faults, and low to moderate near Sandy Lake. The gravity residual (Map 2) is moderately high along most of the bounding edges and in the middle of the paleotopographic domain

with relative lows near the Sandy Lake edge. Lake sediment elements with elevated contents in this section include As, Ba, Cr, Ce, Co, Cu, La, Mn, Mo, Ni, Pb, Rb and Zn. These elements are observed to have low anomalies in the north and moderate-high anomalies in the south, especially along the faults.

Paleotopographic domain 4 is located between latitudes 49°15' and 49°40' and longitudes 57°15' and 57°50' bounded by the Birchy Ridge fault and the Humber syncline as seen by the magnetic shaded relief (Map 3). This paleotopographic domain has a horizontal gradient (Map 4) maximum along its edges and inside the domain. The magnetic residual (Map 3) is high along the edges of the domain and low to moderate inside the domain. The gravity residual (Map 2) is moderate to high along the bounding edges and in the center of the domain but has a low signature near Turners Ridge. Lake sediment elements with elevated contents in this section include Ag, Ba, Ce, Co, Cr, Cu, Fe, F, Mn, Mo, U and Zn.

Paleotopographic domain 5 is located between latitudes 49°10' and 49°25 and longitudes 57°30' and 57°10' and is composed mostly of the Humber syncline. The magnetic shaded relief (Map 3) shows a structure running through the middle of the syncline. This domain has a horizontal gradient (Map 4) maximum along the edges of the syncline with a minimum in the center. The magnetic residual (Map 3) has a moderate to high signature while the gravity residual (Map 2) shows a moderate to low signature in the middle of the syncline with a higher gravity residual on the north-west side. Lake

sediment elements with elevated contents in this domain include Ag, Au, Ba, Mn, Mo, and Zn.

Paleotopographic domain 6 includes the Adies Pond area located between latitudes 49°15' and 49°35' and longitudes 57°35' and 57°10'. This domain has a horizontal gradient (Map 4) maximum, a low magnetic residual (Map 3) on Adies Pond with a high signature in the rest of the domain and has a positive gravity residual (Map 2). Lake sediment elements with elevated contents in this domain include Mn, Sm, Th, La, Yb, Fe, Rb, F, Pb, Cr, Cu, Ni, Co, Mo, Ce, Ba and Zn.

Paleotopographic domain 7 is located between latitudes 49°12' and 49°00' and longitudes 57°40' and 57°15' beneath the Humber syncline bounded by the Cabot fault. This domain has a horizontal gradient (Map 4) minimum in the E-W direction at the top of the section (seen on the magnetic shaded relief (Map 3) as an E-W structure) and increases to a maximum southward. The magnetic residual (Map 3) has a high in the edges of the section, low in the middle and is shown as moderate on the E-W structure. The gravity residual (Map 2) shows a moderate to low signature on the E-W structure, and a moderate to high signature throughout the rest of the domain. Lake sediment elements with elevated contents in this domain include Ag, As, Au, Ba, Ce, Co, Cr, Cu , La, Mn, Mo, Ni, Pb, Rb, Th, Yb, U and Zn.

The last paleotopographic domain (8) is located between latitudes 49°15' and 49°00' and longitudes 57°50' and 57°30' bounded by the Cabot fault on the west, the Grand Lake fault on the east and the southern end of Sandy Lake, as seen by the magnetic

shaded relief (Map 3). This paleotopographic domain has a horizontal gradient (Map 4) maximum along the faults and a low toward the middle of the domain. The magnetic residual (Map 3) is positive on the faults and low in the middle of the domain with an isolated maximum occurring at the southern end of Sandy lake located at latitude 49°05' and longitudes 57°20' to 57°15'. The gravity residual (Map 2) is moderate to high along the faults, low at Sandy Lake and Grand lake with an isolated high at the southern end of Sandy Lake at latitude (49°05') and longitudes (57°20' and 57°15'). Lake sediment elements with elevated contents in this domain include La, Ag, As, Au, Ce, Cr, Rb, Mn, Mo, Cu, Ni, Pb, F, Fe, Sm, U and Zn. The interpretation of these paleotopographic domains, based on analysis completed by the author, will be discussed in subsequent chapters.

CHAPTER 4 - Hydrocarbon Potential

4.1.1 - Introduction

The faintly petroliferous odour of certain rocks in the Deer Lake Basin attracted the interest of local people and explorers early in this century (Baird. 1950). The presence of petroleum in the Deer Lake basin was further confirmed by the presence of oil seeps and bituminous residues in the basin. A total of seven wells have been drilled in the Deer Lake Basin; three encountered appreciable gas shows in the Rocky Brook and North Brook Formations of the Deer Lake Group (Fleming, 1970; Hamblin et al., (in prep)). Although equipment was not available at the time to measure pressures or flow rates, one of the wells was observed to still have flowing gas one year after drilling had been completed (Langdon, 1993).

Liquid and gaseous hydrocarbons from the shallow subsurface have also been observed. Mills # 1 well had a gas blowout at the time of drilling and flowed gas for a year after abandonment (Hamblin et al., (in prep.)). The author visited the site in 1996, and noted that the well still had flowing gas. Hamblin et al., (in prep.) analyzed the gas from the well and found that the it consisted of mostly methane ($\delta\ ^{13}C$ = -70.1‰) with minor carbon dioxide ($\delta\ ^{13}C$ = -28.8‰) and trace ethane ($\delta\ ^{13}C$ = -42.2 ‰). The predominance of methane and depleted carbon isotopic signature strongly suggest that the methane is of biogenic rather than thermogenic origin (Hamblin et al., (in prep.)). Claybar # 1 well near Big Falls encountered gas in the basal conglomerate unit (North Brook Formation) beneath the Rocky Brook Formation, and Claybar # 3 approximately

2.5 miles south east of the Claybar # 1 well encountered gas in the Rocky Brook Fm (Langdon, 1993); this Winkie # 37 borehole encountered a tar area at a depth of 40-50 m.

The gas shows in the North Brook Formation indicate the presence of older source rocks which probably include the carbonaceous fine grained siltstones and black mudstones of the Anguille Group and the black mudstones and limestones of the Wigwam Brook and Wetstone Point Formations (Hyde, 1984).

Paleotemperatures for the Anguille and Deer Lake Groups are estimated to have been approximately 200°C and 100°C respectively, suggesting that the Anguille Group rocks are overmature whereas the Deer Lake Group strata are within the oil-generating window (Hyde et al., 1988). Thermal maturation of the Anguille and Deer Lake Groups (measured by vitrinite reflectance, clay mineral assemblages, illite crystallinity and Rock-Eval pyrolysis) indicate a much higher level of maturation for the Anguille than the Deer Lake Group. Paleocurrent data from Hyde (1979) indicate that the paleocurrent direction was mostly in a NW-SE direction.

Sandstones and conglomerates of the Humber Falls Formation (Deer Lake Group) may provide reservoirs for any hydrocarbons generated from the source rocks of the Rocky Brook Formation (Deer Lake Group). The North Brook and Howley Formations have fair to good porosity as well as a high percentage of sandstone. Other potential reservoirs include the numerous fine-grained sandstone units (up to 3 m thick) which occur within the Rocky Brook Formation and the Howley Formation coals. The

probability of petroleum in the Anguille Group is less likely as this group is more highly deformed and non-porous than the Deer Lake Group sediments.

Trapping mechanisms for hydrocarbons in the Deer Lake Basin could involve the occurrence of anticlinal structures, flower structures, and fault traps, all of which are present. Traps may also be provided by pinchout and facies variations, especially in the upper part of the Rocky Brook Formation. If oil is contained in the Deer Lake Basin, it was probably originally generated and trapped in minor stratigraphic traps in the Carboniferous, and subsequently buried, and disrupted by strike-slip movements along the Cabot Fault system. The following sections cover the occurrence and significance of hydrocarbons as analyzed from the Basin.

4.1.2 - Oil Shales

Oil shales of the Deer Lake Basin are contained in the lower Carboniferous Rocky Brook Formation of the Deer Lake Group, and were deposited as lacustrine beds between fluvial deposits of the overlying Humber Falls and underlying North Brook Formations. Oil shale is defined as fine-grained sedimentary rock containing indigenous organic matter, mostly insoluble in ordinary petroleum solvents from which significant amounts of shale oil can be extracted by pyrolysis (Kalkeuth and Macauley, 1989). Economic considerations are that there must be 5 % total organic content (or 25 litres / ton) for oil shales to be favorable. Hyde (1984) reports that geochemical studies on source rock potential have been confined to the oil shales of the Rocky Brook Formation

(Deer Lake Group), and that rock eval pyrolysis indicates that sediments of this formation contain a type 1 (oil prone) carageen. Hydrocarbon yields of the oil shales average 55 litres / ton and range up to 155 litres / ton. The level of maturity of the oil shales ranges from immature to moderately mature.

Macauley et al. (1985) state that the Rocky Brook Formation oil shales occur as thin interbeds generally 2 - 5 cm thick, within sequences of allochemical dolostones, stromatolitic carbonates, dolomitic siltstones, and mudstones. As seen in thin section, the oil shales have abundant orange-brown amorphous carageen intermixed with fine-grained dolomite (Hyde, 1984). Disseminated quartz grains and opaque organic matter are also present. Two well- exposed sections of the Rocky Brook Formation containing oil shales occur in the Deer Lake region along the Humber River and along Rocky Brook where rocks are exposed in a synclinal feature (Kalkreuth and Macauley, 1989). The oil shales are located in paleotopographic domain 5 of the basin and have a moderate gravity residual anomaly, low magnetic residual anomaly and magnetic gradient minimum. Hatch (1919) reported better oil shales to the south along the shore of Grand Lake, that were once exposed, but now are under water due to dam construction (Hayes, 1949).

4.1.3- Coal

Krauskopf (1979) defines coal as a mixture of compounds of high molecular weight and complex structure containing a large percentage of carbon and small amounts of hydrogen, oxygen, and nitrogen. Some coals also contain sulphur, phosphorous, and

traces of other elements. Krauskopf (1979) further defines coal as the product of partial decomposition under anaerobic conditions of buried, largely terrestrial, vegetation from a swamp environment.

Hayes (1949) reported 9 coal seams on Coal Brook. 15 coal seams on Aldery Brook and 20 on Goose Brook in the Deer Lake area (Map 1). These deposits are located in paleotopographic domain 1 in the basin and have positive gravity and moderate magnetic residual signatures coinciding with a moderate magnetic horizontal gradient character. The seams are lenticular and contain shale partings and are offset by faults. The thickest coal seem is reported as 4 feet 4 inches in drill hole # 6 drilled in the Howley area (Hayes, 1949). Coal analysis (Hayes, 1949) on one seam yielded 54.03 % carbon, 8.66 % ash, 1.04 % sulphur, and is ranked as a high volatile B bituminous coal. This coal is similar to the CHN analysis of sample 24(Table 2, Map 1). The coals are thought to be the product of in situ plant growth and decay of paleosols.

About 7300 tonnes of coal from the Howley Formation were produced from 1898 -1900 and underground prospecting for more coal was attempted at Howley between 1902 - 1918. The work was stopped because of the lack of mineable coal, and adverse conditions where the coal seams were too thin, mixed with too much shale or lost due to faults. The demand for coal lessened due to the development of hydro-electric power and fuel-oil burners on trains.

4.1.4 - Bitumen

The term bitumen is poorly defined in the literature. For the purposes of this thesis the definition from Parnell (1994) will be employed, which states that bitumen is a solid/viscous migrated organic material. In other words organic matter that was mobilized and transported throughout the basin.

Crude oils and bitumens contain many trace elements. Nickel and vanadium are usually the most abundant, with values ranging up to 200 ppm for nickel and 2000 ppm for vanadium (Nakai et al., 1993). Abundances of other trace elements are generally less than 100 ppm and include copper, cobalt, chromium, molybdenum, lead, manganese, and iron. The metal enrichments probably reflect the nature of the underlying basement rocks or surrounding rocks such as granite intrusions which would release uranium, molybdenum, tungsten, and lead through weathering into the hydrological system. Epigenetic organic materials (migrating bitumens and petroleum) can cause the reduction or complexing of metals, thereby making it possible for the organic material to become metal-enriched.

There are numerous bitumen occurrences in the Deer Lake Basin (Map 1), mostly located in paleotopographic domains 5 and 7 of the basin with a moderate gravity and magnetic residual signature and a magnetic gradient minimum. The most significant occurrence is located approximately 100 m north of Goose Arm Road near Nicholsville (Map 1 - sample 24) where bitumen in the form of narrow veins or fracture fillings occurs in fractured carbonate host rocks of the North Brook Formation.

Solid bitumen also occurs as pore fillings in the grey sandstones of the Howley beds. Although these zones are quite rich, they are less than 1 m thick in the Howley Beds with little lateral extent (Hyde and Ware, 1981). Abundant bitumen has been noted in boreholes D2 and D3 located near Grand Lake in the Howley Formation (Map 1). The occurrence of bitumen at several different stratigraphic levels and structural situations suggest that the migration paths were complex (Langdon, 1993). Langdon also suggests that since bitumen is found in several localities in the basin, it indicates that there have been significant and widespread episodes of maturation of source rocks and generation of liquid petroleum in or beneath the Deer Lake Basin.

4.2.1 - Analytical Data For Bitumen and Coal Samples

Organic samples were analyzed using CHN analysis, ICP-MS, carbon isotope analysis, and LAM-ICP-MS. Table 1 lists the carbon isotope analysis values for bitumen and coal samples. Carbon isotope analyses define a range in $\delta\ ^{13}C$ values of -22.9 to -32.4 ‰ relative to PDB. These carbon values indicate a probable terrigenous source. Hydrocarbons in saline systems have high V/Ni ratios, high $\delta\ ^{13}C$ values (-26.9 to -23 ‰), whereas hydrocarbons in freshwater systems have low S and V/Ni values, and low $\delta\ ^{13}C$ values (-27 to -31 ‰) (Nakai et al., 1993). The carbon values for the Deer Lake Basin indicate that the hydrocarbons evolved from a freshwater system, which is in agreement with Hyde's original interpretation (Hyde, 1984).

Table 1 Carbon isotope analysis for bitumen and coal in the Deer Lake Basin

Sample #	Rock Type	$\delta^{13}C$ (‰)
24	Bitumen	-32.4
37A (1)	Coal	-22.9
37A (2)	Coal	-22.9
D3 (1)	Bitumen	-27.4
D3 (2)	Bitumen	-27.4

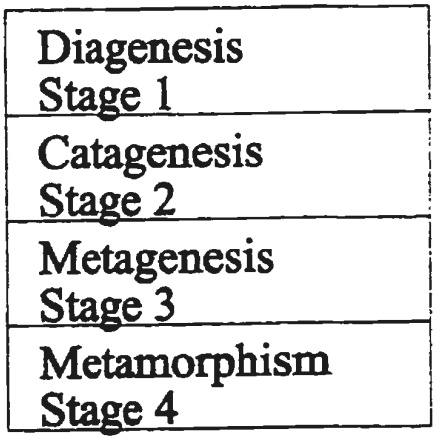

Figure 3 - Possible stages of organic matter maturation.
Depth and temperature increase with each stage.
Modified from Parnell (1994).

Figure 3 illustrates the stages that organic material can go through from organic matter to diagenesis, catagenesis, and metagenesis (Hunt, 1996). During diagenesis a series of low-temperature reactions can occur, namely decarboxylation, deamination, polymerization and reduction. Some of the results of diagenesis are early carbonate cements, dolomitization, quartz cementation, and clay coating on grains.

Catagenesis usually occurs at depths of 1000 m, and temperatures between 50 - 150°C (Hunt, 1996). This is normally referred to, in petroleum terms, as the oil window. During this stage organic material can be transformed into oil. Organic matter (kerogen) is subjected to increasingly higher temperatures with greater depth of burial. Over time the higher temperatures cause thermal degradation of organic matter to yield hydrocarbons (Hunt, 1996). Some of the reactions that can occur during this process are silica diagenesis, clay diagenesis, feldspar dissolution, kaolinite precipitation, albitization, illite growth, and chlorite precipitation. During metagenesis, quartz overgrowths occur as well as carbonate dissolution and thermal degradation of hydrocarbons. Gall (1984) noted many of these thermal reaction characteristics in his petrographic and diagenetic study of the Deer Lake Basin. Nearly complete dehydrogenation takes place as greenschist facies conditions are encountered. Higher levels of metamorphism lead to the development of graphite.

Kerogens are classified as types 1-3 based on their carbon, hydrogen, and oxygen contents (Parnell, 1994). Types 1 and 2 generate most of the world's oil, and type 3 primarily generates gas, condensate, and waxy oil. Type 1 is derived from

microbiological debris, initially hydrogen rich with H/C ratios near 1.7 or more. Type 2 has intermediate H/C ratios. Type 3 is derived from higher plant debris and bacterial reworking and has initial H/C ratios of 0.8 and lower.

Table 2 lists the CHN analysis for the bitumens and coal samples from the Deer Lake Basin. In the Deer Lake Basin, the H/C ratios which correlate with type 3 kerogens are >0.5; thus matching with catagenesis stage of maturation, which is the 'oil window' for hydrocarbons. H/C ratios larger than 0.8 have liquid-generating ability. The H/C ratio analysis of samples in the Deer Lake Basin indicates that hydrocarbons in the basin have liquid-generating ability (with the exception of W89-37A) and will probably be in the form of oil, while hydrocarbons near W89-37A in the Howley Fm will be degraded oil or in the form of gas. H/C Ratios > 0.5 (e.g. Elliot Lake, Ontario, 0.57) also correlate with the catagenesis stage of maturation (Figure 3) (Mancuso et al., 1989). H/C ratios < 0.5 (e.g. Sudbury Ontario, 0.09) correlate with the metagenesis and metamorphic stage (Figure 3) (Mancuso et al., 1989).

Table 2 CHN Analyses For Bitumen And Coal in the Deer Lake Basin

Sample	Formation/Rock Type	C(ug)	H(ug)	N(ug)	H/C Atomic ratios
D3	Howley Fm/Bitumen	176.2	13.4	2.1	0.9
D3	Howley Fm/Bitumen	70.5	5.1	1.4	0.9
24	Rocky Brook Fm/Bitumen	856.4	54.1	4.7	0.8
37A	Howley Fm/Coal	433.7	24	10.5	0.7

Results of ICP-MS Procedure for the bitumen and coal samples

Appendix B.1.1 lists the data from the ICP-MS analytical procedure waters package in two sets of numbers. The first set of numbers are the coal-leach concentrations while the last set of numbers are the residue concentrations, both of which have been calculated to account for loss on ignition and concentration due to ashing. Most of the elements are recorded as concentrations in ppm, while carbon and nitrogen are recorded as counts per second as a quantitative concentration cannot be determined due to a problem in the analytical technique.

The coal/bitumen samples have appreciable Mg, Al, P, S, Ca, Fe, Ti, and Mn contents, while the residue samples have appreciable B, Al, Ca, Ti, Fe, Ba, and Sr contents. Separation of the coal and bitumen samples from other rock material (calcite, quartz, and feldspars) was difficult and probably accounts for the high concentrations of calcium and magnesium etc. The other elements had low concentrations of less than 100 ppm which agree with the results of oil analysis from the Western Canadian Sedimentary Basin in Table 3 (Hitchon and Filby, 1983).

Figure 4 is a diagram of the individual concentrations of elements for each sample normalized to average coal concentrations, in log scale. This diagram shows that the Deer Lake Basin samples have trace element concentrations greater than the average coal standard, listed in Table 3 (Hitchon and Filby, 1983).

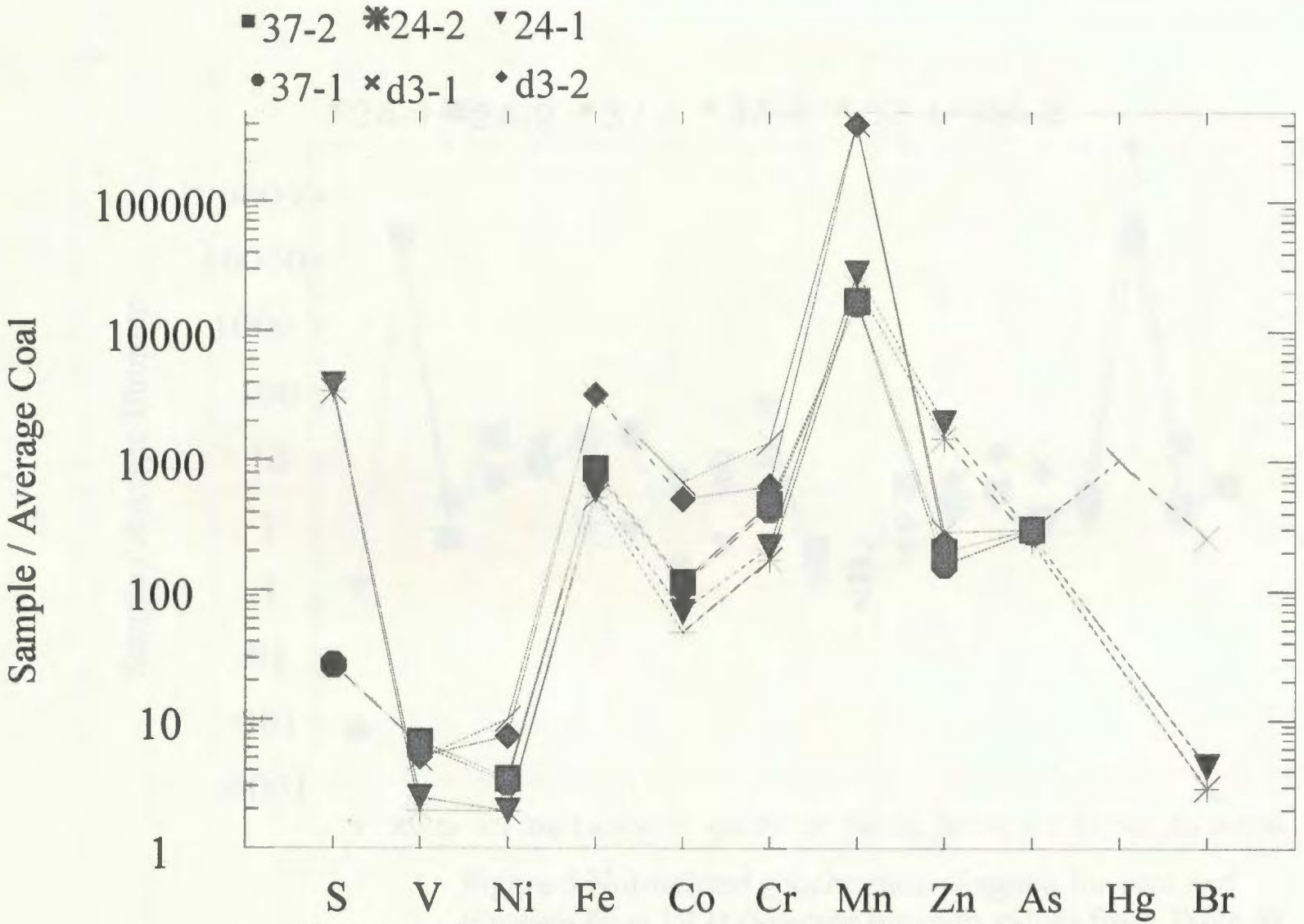

Figure 4 Normalized geochemical diagram for coal and bitumen samples from the DLB (average coal values from Table 3).

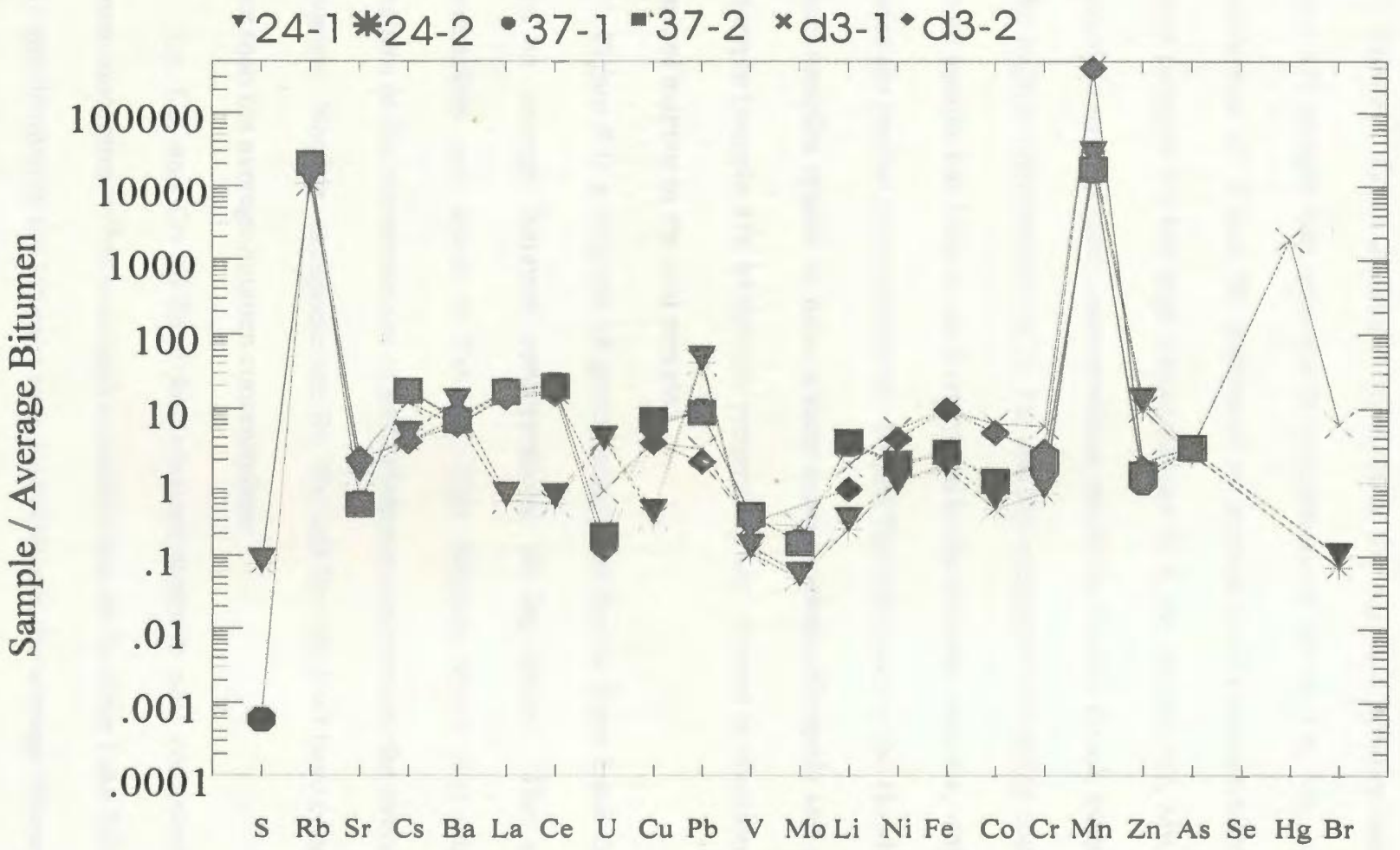

Figure 5 Normalized geochemical diagram for coal and bitumen from DLB (average bitumen values from Table 4).

Figure 4 shows distinct differences in the coal and bitumen samples. The coal (sample 37) sample has appreciable concentrations of Fe, Cr, Mn, and As, and low concentrations of V and Ni, compared to average coal concentrations. The Howley Bitumen (sample d3) has high concentrations of S, Fe, Ni, Co, Cr, Mn, Zn, Hg, and Br compared to average coal concentrations, while the Rocky Brook bitumen (sample 24) has the highest concentration of S, Fe, and Zn compared to average coal concentrations. The coal sample has little or no S compared to the bitumen samples, while the rest of the elements are similar in concentration. Br and Hg only occur in the Howley bitumen. The bitumen samples appear to have greater concentrations of metals and sulphur than the coal sample (sample 37). Metals are presumably not present in abundance in coal due to the lack of sulphur in the coal sample.

Figure 5 is a diagram of geochemical data for the Deer Lake Basin occurrences related to average bitumen concentrations, in log scale. The average bitumen concentrations are listed in Table 4. This diagram shows that there are no great differences in the concentrations of most elements compared to the average concentration in bitumen. Notable exceptions are Rb, Pb, and Br which all have concentrations much greater than the average bitumen concentration.

La, Ce, and Co all have low concentrations in coal compared to the average bitumen concentration but have high concentrations in the Deer Lake Basin bitumens. Zn and U are elevated in the bitumen samples relative to the average bitumen concentrations but lower in the coal samples. Pb is elevated in all the samples especially the Rocky

Brook bitumen. These trends of elevated elements in the ICP-MS results, coincide with the lake sediment data set, showing that, in the location of the samples on the geochemical maps (Map 5 - 27), the enriched elements are present. Overall, the bitumen samples have more elevated sulphur and metal contents than the coal samples, suggesting that either the bitumen samples had more interaction with metal-carrying aqueous solutions or that the bitumens were formed coevally with the metals in solution. Fluid inclusion studies (Chapter 5) indicate that the bitumen and minerals were not generated coevally in the basin. Therefore the bitumen samples (located on or adjacent to the porous-permeable fault pathways) are inferred to have undergone more interaction with the migrating fluids, in the basin.

Results of LAM ICP-MS procedure for bitumen and coal samples

Appendix B.1.2 lists the calculated elemental concentrations derived via the laser ablation microprobe (LAM) ICP-MS process. The samples contain appreciable V, Cr, Ni, Zn, Sr, Ba, W, Pb, and U contents. This is probably due to mineral inclusions that were ablated during the laser ablation process, as there were minor spikes in the data. Comparing the coal and bitumen samples, the bitumen samples have higher concentrations of elements than coal samples, while within the bitumen samples, sample 24 contains higher concentrations of elements than d3. Again this presumably is due to the fact that the coal sample has low concentrations of sulphur compared to the average coal sample and to bitumens.

The numbers are internally consistent between the two techniques even though the laser ablation technique analyzes individual micro pits that are ablated while the ICP-MS technique analyses the whole sample dissolved in solution.

Problems with the LAM-ICP-MS system for analyzing coals or bitumens include the inhomogeneity of the bitumen standard, and the validity of the internal standard. The bituminous coal standard used for this LAM-ICP-MS technique is the National Institute of Standards and Technology, Standard Reference Material 1632b Bituminous Coal. This reference material was intended primarily for use in the calibration of apparatus and the evaluation of techniques employed in the analysis of coal and similar materials. The problem with using this standard is that a minimum sample mass of 250 mg (dry mass) should be used for analytical determinations to be correlated to the certified values provided. However in preparing the standard for the LAM -ICP-MS technique, only 5 mg (dry mass) was used to make a pellet from a press designed for the laser ablation technique; thus the validity of the bituminous coal standard used in the LAM analysis can be questioned. Also, since the standard was somewhat inhomogeneous, an average ablation had to be used rather than individual results.

Organic material had not been analyzed at Memorial by either the LAM-ICP-MS or ICP-MS systems; thus trial experiments were undertaken. Pros and cons of each technique include: 1) The LAM-ICP-MS technique allows the researcher to pick up to 40 elements to analyze while the ICP-MS technique has set packages for elemental analyses. This is important for analyzing individual elements such as vanadium and nickel, in oil,

or uranium in coal/bitumen; 2) As mentioned above, in the analyses of organic material, the preparation and validity of standards will have to be addressed in the LAM-ICP-MS system before reliable results can be achieved; 3) Overall the ICP-MS results display higher elemental concentrations than the LAM-ICP-MS; this is interpreted as being due to the ICP-MS technique analyzing the whole sample dissolved in solution while the LAM-ICP-MS technique analyzes individual micro pits that are ablated; 4) While ablating samples in the LAM-ICP-MS technique, the researcher carefully picks each point within the sample to be analyzed, which may lead to biased results, while the ICP-MS technique analyzes the whole sample dissolved in solution; 5) In the ICP-MS technique, leaching of the coal/bitumen sample, after ashing, may have leached out minerals present in the material surrounding the coal/bitumen, resulting in overall higher concentrations of heavy minerals. When analyzing the bitumen/coal samples, the sample must be free of surrounding host rock material.

Both techniques can give viable results in terms of precision and accuracy, depending on the scope of the applied research; however, to deduce an overall understanding of the elements present in the coal/bitumen samples, the author recommends the ICP-MS technique rather than the LAM-ICP-MS technique at the beginning of the study. For detailed research into individual elemental concentrations, the author then recommends the LAM-ICP-MS system.

4.2.2 - Discussion

Metals and hydrocarbons may migrate from a common source rock, and lacustrine sedimentary rocks in rift basins such as the Deer Lake Basin are plausible as a source of both metals and hydrocarbons. The organic samples analyzed are located in different paleotopographic domains of the basin. The d3 sample is located in paleotopographic domain 2 of the basin bounded by the Hampden and Grand Lake faults with moderate to low gravity and magnetic signatures and a magnetic gradient minimum. Sample 24 is located in paleotopographic domain 7 of the basin bounded by the Birchy Ridge fault and has moderate gravity and magnetic residuals and a magnetic gradient minimum, and sample 37A is located in paleotopographic domain 8 of the basin bounded by the Birchy Ridge and Grand Lake faults; and has low gravity and magnetic residuals and a moderate magnetic horizontal gradient. The coal samples are in situ in the basin, while the bitumens have migrated to their present location. The author suggests that fluids flowed through the organic matter which provided a reducing environment for concentrating metals. Overall the coal samples have lower concentrations of metals than the bitumens which is due to lower content of sulphur in the coal. Co-migration of the metals and organic material is not plausible as hydrocarbon inclusions were not found in any of the fluid inclusion sections (Chapter 5). The bitumen / coal samples are located close to faults in the basin which have possibly served as the structural conduits for the migrating fluids, this suggests that interaction between organics and metal-carrying aqueous

solutions is possible, and that the organics provided a reducing environment for metal deposition.

Bitumens found in or near ore deposits have been described as integral components in ore genesis and have been used as a source of information about the geochemical and thermal conditions of mineralization (Parnell, 1994). When making inferences about the role or significance of organic matter, it is important to look at paragenesis, since the bitumen may be temporally unrelated to the mineralization process and may simply have used the same migration pathway.

Often in fracture systems, bitumen contains significant quantities of in situ authigenic minerals including illite clays, feldspars, and pyrite. The minerals must be authigenic because they are too delicate to survive long travel. This implies that the bitumens were deposited from fluids with an aqueous component substantial enough to transport the metallic ions that ultimately precipitate mineral phases (Parnell, 1994). In general bitumens in mineralized fracture systems tend to be paragenetically late because they take advantage of pre-existing fluid pathways.

Groundwater flowing through rocks containing vanadium, nickel, lead, zinc, and copper can transport and dissolve these metals and then re-precipitate them in organic-rich sediments including coals. Bitumen and coals have a great potential for sulphide precipitation after the early diagenetic stage, due to the movement of porewaters and release of ions during organic maturation (Spears, 1994); and may have acted in the Deer Lake Basin as a reductant for several mineral occurrences.

If hydrocarbons leak from a reservoir into a metalliferous groundwater system as in Mississippi Valley -Type (MVT) deposits, mixing can occur and the result can be precipitation of coeval bitumen and ore minerals (Ewbank et al., 1995). In another example, coeval cinnabar and bitumen in epithermal mercury deposits has led to the use of bitumen in mercury exploration (Parnell, 1994). Interaction between reservoir hydrocarbons and metalliferous groundwater, can result in formation of copper, uranium, and vanadium ores (i.e. those metals that are mobile in oxidizing conditions and are likely to be precipitated by contact with reducing hydrocarbon - rich rocks).

Commonly the source of metals in vein-hosted mineral deposits is attributed to host or adjacent sedimentary rocks rather than magmatic fluids despite the often close relationship between the mineral veins and intrusive igneous rocks (Parnell, 1994). The most likely sedimentary source rocks include limestones and organic - rich shales. Faults associated with vein systems in sedimentary basins would be important in these cases as a conduit for mineralizing fluids derived within the basin rather than as a direct source of metals.

Parnell (1986) suggests that mineral deposits in rift systems, form where metals are eroded from uplifted areas and contemporaneous volcanic rocks, are concentrated in tectonic lakes with high biological productivity. Anoxic bottom waters in tectonic lakes preserve metal-bearing organic tissues and horizons; this is a situation similar to the Deer Lake Basin. Later metals and organic components can be remobilized into vein deposits with remobilization being promoted by high heat flow and post-depositional faulting

which brings organic and metal source rocks into juxtaposition with coarse host/reservoir rocks (Parnell, 1993).

Table 3 Mean Concentrations and ranges (ppm) of selected trace elements in crude oils from the Western Canadian Sedimentary Basin (Hitchon And Filby, 1983).

Element	Mean Conc (ppm)	Range (ppm)
S (%)	0.83	0.05-3.9
V	13.6	0.1-177
Ni	9.38	0.1-74.1
Fe	10.8	0.1-254
Co	0.054	0.0002-2.0
Cr	0.093	0.005-1.68
Mn	0.010	0.003-3.85
Zn	0.459	0.025-5.92
As	0.111	0.002-1.99
Sb	0.006	0.0001-0.035
Se	0.052	0.003-0.511
Hg	0.051	0.002-0.399
Na	3.62	0.01-64.7
Cl	39.3	0.1-1010
Br	0.491	0.002-12.5
I	0.719	0.01-9.0

Table 4 - Mean concentrations and ranges of selected trace elements for bitumens in the U.S., Canada, Trinidad and Tobago, and Venezuela (modified from Hosterman et al., 1989).

Element	Mean (ppm)	Element	Mean (ppm)
Cr	22.47	Fe	3617
Co	5.88	Ni	18.7
Zn	69.81	As	11.0
Se	20.1	Br	20.5
Rb	0	Sr	146.6
Sb	0.7	Cs	0.139
Ba	36.85	La	7.46
Ce	14.53	Nd	0
Sm	0.96	Eu	0.271
Tb	0.1755	Yb	0.674
Lu	0.09	Hf	0.212
Ta	0.213	W	5.71
Th	1.80	U	12.8
Cu	13.85	Hg	0.0275
Pb	7.5	V	247.5
Mo	18.2	Nb	12.05
Y	14.05	Li	17.25
S	37850	Sc	1.538

CHAPTER 5 - Economic Mineral Potential

5.1-1 - Introduction

Base and other metallic minerals have been noted throughout the Deer Lake Basin. Most of the mineralization occurs in paleotopographic domains 1, 3, 5 and 8 of the basin, coinciding with the edges of the paleotopographic domains, which are usually marked by faults. This suggests that the faults served as possible conduits for fluids, and provided an ideal environment for base metal concentration.

The most significant copper mineralization is the Birchy Ridge showing (paleotopographic domain 3 of the basin) consisting of bornite, chalcopyrite, chalcocite, and minor uranium in a limestone bed in the Wigwam Brook Formation. The Deer Lake Group has smaller copper showings in gossan zones (Hyde et al., 1994). Up to 1.4% copper also occurs in a uraniferous bitumen nodule in the Rocky Brook Formation west of the town of Deer Lake. Hyde (1980) observed malachite staining in the North Brook and Humber Falls Formations. One boulder in the Humber Falls Formation near a drill site on Wigwam Brook yielded 700 ppm copper (Hyde, 1980). There are numerous gossans in the Howley beds (section 8) along the western side of Grand Lake containing chalcopyrite and scattered malachite, bornite and pyrite (Hyde, 1980). Hyde (1979) also observed chalcopyrite (up to 2 % copper in whole - rock samples) with malachite staining in the Rocky Brook Formation, near an uranium anomaly.

The largest known base metal occurrence in the vicinity of the Deer Lake Basin is the Turners Ridge lead prospect (paleotopographic domain 3) containing 200,000 tonnes

of 3-4% galena mineralization in fractures in tectonically brecciated limestone (Tuach 1987). A smaller galena deposit, the Side Pond showing, is located in Silurian limestones on the edge of the basin (paleotopographic domain 3).

Precious metals have only been reported in a few localities in the Deer Lake Basin. Silver (up to 1250 g/t) occurs as acanthite in some of the uraniferous till boulders of the Humber Falls Formation (Hyde, 1979); although this does not correspond to regional geochemical data of the Deer Lake Basin. Gold has been reported in quartz veins just outside the basin in White Bay (Tuach, 1987).

The presence of significant fault - controlled lead mineralization of probable Carboniferous age in carbonate horizons outside the basin, as well as minor fault - controlled Cu (- Zn) mineralization in carbonates within the basin, indicate that base metals were mobile through the basin (Hyde et al., 1994). The following sections describe in detail mineralization throughout the basin.

5.1.2 - Pre-Carboniferous Mineralization

Hyde (1979) reported Pre-Carboniferous zinc concentrations (approximately 0.06 % Zn) near Grand Lake in intermediate, grey-green, massive volcanic flows with disseminated pyrite and minor chalcopyrite (Little Pond Brook Formation) (Map 1). The gossan zone containing the mineralization is approximately 10 m long, and assays on the base metal content revealed zinc at 26 - 28 ppm, lead 10 - 13 ppm and copper 6 - 7 ppm

(op cit.). This zone is located in section 8 of the basin bounded by faults. In this same area near Grand Lake, asbestos occurs in small quantities in serpentinites.

5.1.3 -Uranium Mineralization

Hyde (1984) postulated that there are three main types of uranium mineralization in the Deer Lake Basin which he termed types I to III. Type I mineralization occurs in paleokarst breccias and bituminous carbonate rocks at the unconformity between the North Brook Formation and Cambro-Ordovician carbonate rocks. This mineralization is of epigenetic origin. The type I mineralization has relatively low grades (10 - 45 g/t range) (Hyde, 1984).

Type II mineralization consists of uranium concentrations in gray, lacustrine mudstones and carbonate layers of the Rocky Brook Formation (Hyde, 1984). This type of occurrence is stratiform and possibly extends for several kilometers. The stratiform nature of the mineralized zones and the presence of mineralization on a basin - wide scale suggests a mainly syngenetic or early diagenetic origin. A solid nodule from the Rocky Brook Formation contained the highest uranium contents at 0.46 % determined for the Deer Lake Basin (op.cit).

Type III occurs as uraniferous sandstones in the Humber Falls Formation. Gall (1984) states that the uranium occurs as uraninite cement in association with pyrite and hematite. Gall (1984) also reports that post-mineralizing iron-rich fluids may have caused extensive remobilization of the uranium so that now only small concentrations of

highly reduced, organic-bearing, subsurface mineralization remain. This fact is supported by the low uranium grades in types I - III. Gall (1984) further suggested that, through correlation of paleomagnetic data with the paragenetic sequence in the basin, between 40 - 80 Ma passed before the uranium developed completely and that a post - mineralization episode of hematite cementation may mean that economic quantities of uranium no longer exist in the sandstones.

Ore-forming processes in sedimentary environments frequently involve organic material of different origins and chemical compositions. The roles of organic material in uranium ore - forming processes are: transport, remobilization, reduction, concentration, and preservation. Uranium is readily mobile in oxidizing fluids as U^{+6} ions and can be precipitated in reducing environments as U^{+4} ions to form sediment-hosted mineral deposits (Parnell and Monson, 1990). The humic acid content of type 3 coals (type 3 are found in the Deer Lake Basin) and fossil plant debris can cause the fixation of uranium on organic matter from very dilute solutions of uranium (Parnell, 1994).

The uranium occurrences are mostly found in paleotopographic domain 5 of the basin bounded by faults. Hyde (1979) reported that there are radioactive uraniferous zones within the Deer Lake Group (specifically the Rocky Brook Formation), approximately 35 cm thick and near the base of a 3 m thick bed of dolomitic grey mudstone, which sharply overlies a thin limestone bed (Hyde, 1979) (Map 1). Assays of this zone yielded 24 ppm uranium. The thickest uranium anomaly (1.8 m) in the Rocky Brook Formation produced the most anomalous uranium assays of 4600 ppm uranium

and contained nodules of solid hydrocarbon material within calcareous grey mudstones. These nodules, only a few centimeters in diameter, are widely scattered in the host rock, while solid hydrocarbon with pyrite was observed as fracture-filling (Hyde, 1979). Another uraniferous zone (approximately 80 cm thick) in the North Brook Formation consists of two calcareous grey mudstones surrounding a mud-cracked algal limestone; assays from the algal limestone yielded 105 and 109 ppm uranium, while the mudstone yielded 130 and 74.5 ppm uranium (Hyde, 1979). Other uranium occurrences were examined; unfortunately when assayed, these showed only background values of uranium.

5.1.3 - Discussion of Uranium Models

Several models have been put forward to try to explain the origin of the uranium occurrences. The first model (Hyde, 1984) suggests that uranium and other metals accumulated at sites of plant and wood debris concentration in stream paleochannels, mostly in the Humber Falls Formation. The second model (Hyde, 1984) involves the Wigwam Fault which separates the Humber Falls and Wigwam Brook Formations. H_2S - bearing fluids flowing along the faults, induced chemical reduction of the adjacent strata setting the stage for precipitation of uranium and other metals from subsequent metal-bearing fluids (Hyde, 1984). This second model is supported by the presence of minor copper-uranium mineralization in the Wigwam Brook Formation to the east of the

Wigwam Fault, and also by some oxidized pyrite which occurs adjacent to a minor fault within the Humber Falls Formation (Hyde, 1984).

The ultimate source of the uranium is still unknown. Hyde (1984) suggested that the uranium could be from outside the basin and have been brought in by hydrothermal fluids along faults, or that the uranium could have been recycled from the underlying Rocky Brook Formation. There seems to be a connection between the bitumen and uranium occurrences perhaps due to the organic matter acting as a reductant for the uranium.

5.1.4 - Birchy Ridge Copper Mineralization

The Birchy Ridge Prospect (Map 1) is in paleotopographic domains 3 of the basin bounded by faults. The showing consists of vugs and fractures in the Wigwam Formation limestone adjacent to the Wigwam Fault which contain bornite, chalcocite, chalcopyrite, and minor uranium. Geochemical analysis yielded 5 % copper and 60 g/t silver (Hyde et al., 1994). Since the occurrence is within the Wigwam Formation, the hydrothermal system responsible for the mineralization is inferred to postdate the Early Carboniferous (Tuach, 1987). Uranium mineralization is also present within Carboniferous sandstone and conglomerate west of the Wigwam Fault, and contains 1-2 % U_3O_8, up to 0.05 % Vanadium, 100 g/t silver, trace copper, and up to 0.4 g/t gold (Tuach, 1987).

5.1.5 - Turners Ridge Lead Mineralization

The Turners Ridge lead deposit is located along the Sops Arm road (Map 1) in paleotopographic domain 3 with low gravity and magnetic residuals and a magnetic gradient maximum. This deposit is known to contain at least 200.000 tons of ore-grading 3-4 % lead, and drilling had traced mineralization over a distance of several kilometers (Saunders et al., 1992). The deposit is hosted by the Lower Volcanic Formation of the Silurian Sops Arm Group, which consists of intensely brecciated dolostones with galena, pyrite, and sphalerite. Sheared rhyolite and rhyolite cataclasite are in fault contact with the dolostone breccia (Op.cit.).

The mineralized samples comprise fine-grained galena, and pyrite occurring in limestone matrix cement to breccia fragments and along fractures with quartz and calcite gangue. In places pale pink barite is associated with the galena.

Polished section studies suggest that the mineralization occurred in at least two stages. Pyrite formed earliest and was later brecciated, followed by deposition of galena. Galena surrounds, and sometimes replaces pyrite. Since brecciation of the pyrite resembles that of the dolostone host it probably occurred at the same time; the pyrite therefore predates the formation of the dolostone breccia. This is in general agreement with the interpretation of Saunders et al., (1992) and Hyde (1984), with the exception however that no sphalerite was found in the author's samples.

The brecciation is intense, although most of the fragments are not rotated and there is little matrix. In places where the brecciation does become disruptive (i.e.,

rotation of fragments and greater percentage of matrix) the fragments become slightly rounded and there is a higher proportion of a green limey clay matrix (Saunders et al., 1992).

Movement along low angle thrusts has resulted in emplacing the rhyolite over the dolostone and then later over the Carboniferous conglomerate. The low angle thrusts may represent late movements on the adjacent Wigwam Fault (Saunders et al., 1992: Hyde, 1984). It is also suggested that the brecciation of the dolostone is of tectonic origin. Minor galena in the brecciated rhyolite suggests mineralization postdates thrusting of the rhyolite over the dolostone, and is therefore at least as young as Carboniferous. Saunders et al., (1992) suggest that the Carboniferous Deer Lake Basin is the possible source for the Turners Ridge mineralization. The brecciated dolostone may have acted as a structural and chemical trap for upwelling lead- rich basinal fluids.

5.1.6 - Side Pond Lead Mineralization

The Side Pond occurrence is located north of the main Turners Ridge showing(Map 1) in section 3 of the basin with low magnetic and gravity residuals and a magnetic gradient maximum. Brecciation of the host dolostone is more sporadic and less intense than it is in the Turners Ridge area (Saunders et al., 1992). Mineralization is similar to that at Turners Ridge but tends to be concentrated in veinlets and along fractures rather than in the breccia matrix. The most abundant minerals are pyrite and sphalerite with minor galena. As with the Turners Ridge showing, minor galena is found

in the matrix of the rhyolite breccia, which in this case underlies the dolostone instead of being emplaced over the dolostone. Dimmel (1979) reported an assay of 2.85 % lead over a 4.6 m interval that contained mainly galena with minor pyrite.

5.2.1 - Lead isotope data

Lead isotope ratios for galena separates were determined at the GEOTOP Laboratory, Université du Quebéc á Montréal (UQAM). The analytical uncertainty limits assigned to the analyses are 0.05% for the $^{206}Pb/^{204}Pb$, $^{207}Pb/^{204}Pb$, $^{208}Pb/^{204}Pb$ and $^{207}Pb/^{206}Pb$ ratios. The lead isotope data for galena separates in the Turner's Ridge and Side Pond showings, Deer Lake Basin are presented in table 5 and are shown in the lead isotope diagrams figures 6 and 7. The growth curves for the Zartman and Doe (1979) Plumbotectonics II model and model ages calculated using the Stacey and Kramer (1975) average crustal model are shown for reference. Tables 6, 7, 8 and 9 list the galena values for other carbonate-hosted deposits in Newfoundland.

Table 5: Lead isotope data for the Deer Lake Basin Area

Sample	$^{206/204}$ Pb	$^{207/204}$ Pb	$^{208/204}$ Pb	Model Age*	Mu*
H96-10A (Gales Bk)	17.995	15.537	37.687	347	9.504
H96-10B (Gales Bk)	17.987	15.531	37.677	340	9.479
H96-10C (Gales Bk)	17.998	15.549	37.706	369	9.557
Turner's Ridge	17.995	15.537	37.681	347	9.504
Turner's Ridge(1)	17.960	15.520	37.659	338	9.437
Turner's Ridge (2)1	17.969	15.532	37.712	356	9.489
Turner's Ridge(2)2	17.975	15.541	37.741	370	9.527
Side Pond	17.978	15.546	37.748	378	9.549

* Calculated using the Stacey and Kramers (1975) average crustal model.

Table 6: Lead isotope data from mesothermal gold occurrences in the Sop's Arm area, north of the Deer Lake Basin (Wilton, unpub. data)

Sample	$^{206/204}$ Pb	$^{207/204}$ Pb	$^{208/204}$ Pb	Model Age*	Mu*
Corner Brook	18.065	15.543	37.821	305	9.512
Browning (1)1	18.020	15.541	37.768	336	9.515
Browning (1)2	18.014	15.538	37.769	334	9.503
Browning (2)	18.026	15.540	37.775	329	9.509
Simms Ridge (1)1	18.036	15.531	37.759	303	9.466
Simms Ridge (1)2	18.034	15.535	37.779	313	9.484
Simms Ridge (3)	18.057	15.554	37.832	334	9.563

* Calculated using the Stacey and Kramers (1975) average crustal model.

Table 7: Lead isotope data from mesothermal gold occurrences in the Baie Verte Peninsula area (Wilton, unpub. data)

Sample	$^{206/204}$ Pb	$^{207/204}$ Pb	$^{208/204}$ Pb	Model Age*	Mu*
El Stratos (1)	17.667	15.479	37.426	482	9.337
El Stratos (2)	17.678	15.491	37.467	497	9.389
El Stratos (3)	17.690	15.502	37.503	510	9.436
Voodoo (1)2	17.704	15.511	37.530	518	9.473
Voodoo (2)	17.687	15.500	37.499	509	9.428
Voodoo (3)	17.686	15.498	37.492	505	9.419
90-13A	17.979	15.529	37.770	342	9.472
90-13B	17.965	15.513	37.719	320	9.405
Stuckley	17.911	15.541	37.715	419	9.546
2(flat)3	17.686	15.486	37.502	481	9.364
2(flat) B1	17.690	15.500	37.556	506	9.427

* Calculated using the Stacey and Kramers (1975) average crustal model.

Table 8: Lead isotope data for carbonate hosted deposits in Western Newfoundland (Swinden et al., 1987).

Sample	Name	Host	$^{206/204}$ Pb	$^{207/204}$ Pb	$^{208/204}$ Pb	Ma*
TQ 82-23	Beaver Brook	Petit Jardin Fm	17.574	15.425	38.231	442
TQ 84-3	Pikes Feeder Pond	Petit Jardin Fm	17.294	15.388	37.871	590
TQ 84-136	Eddies Cove East	Petit Jardin Fm	17.431	15.418	37.878	542
TQ 84-22	Frying Pan Pond	Catoche Fm	17.777	15.462	38.490	359
TQ 83-84	Cooks Hr	Catoche Fm	17.772	15.462	38.517	363
TQ 84-132	Daniels Hr-1	Catoche Fm	17.857	15.475	38.438	324
TQ 84-133	Daniels Hr-2	Catoche Fm	18.124	15.471	38.680	102
TQ 84-134	Daniels Hr-3	Catoche Fm	18.116	15.515	38.663	206
TQ 84-135	Daniels Hr T-zone	Catoche Fm	17.983	15.490	38.607	256
TQ 84-1	St Johns Island	Table Point Fm	18.503	15.568	39.299	18
TQ 84-2	River Of Ponds Lake	Table Point Fm	19.339	15.613	39.901	-535
SP 365	GilliamsCove	Codroy Gp	18.217	15.581	38.307	268

Table 8: Lead isotope data for carbonate hosted deposits in Western Newfoundland (Swinden et al., 1987) cont'd.

Sample	Name	Host	$^{206/204}$ Pb	$^{207/204}$ Pb	$^{208/204}$ Pb	Ma*
SP 2980	Lead Cove (1)	Codroy Gp	18.208	15.575	38.319	263
TQ 83-21	Lead Cove (2)	Codroy Gp	18.224	15.591	38.373	252
KQ 83-84	Lead Cove (3)	Codroy Gp	18.203	15.572	38.340	284
TQ 83-19	Port Au Port	Codroy Gp	18.222	15.575	38.312	266
KQ 84-46D	Shallop Cove	Codroy Gp	18.203	15.605	38.234	260
KQ 84-53	Boswarlos	Codroy Gp	18.262	15.591	38.405	308
TQ 83-20	Picadilly	Codroy Gp	18.204	15.575	38.292	255

* Calculated according to the Stacey and Kramers (1975) average crustal model.

Table 9: Lead Isotope data for the Big Cove Fm, Port Au Port Peninsula, Western Newfoundland (Dix et al., 1996).

Sample	Place	$^{206/204}$ Pb	$^{207/204}$ Pb	Sample	Model Age*
Gc-8	Gilliams Cove	18.20	15.57	38.32	234
LeC-2	Lead Cove	18.20	15.57	38.26	257
LeC-3	Lead Cove	18.23	15.60	38.35	296
LeC-10	Lead Cove	18.20	15.57	38.26	257
LeC-22	Lead Cove	18.20	15.58	38.29	277

* Calculated according to the Stacey and Kramers (1975) average crustal model.

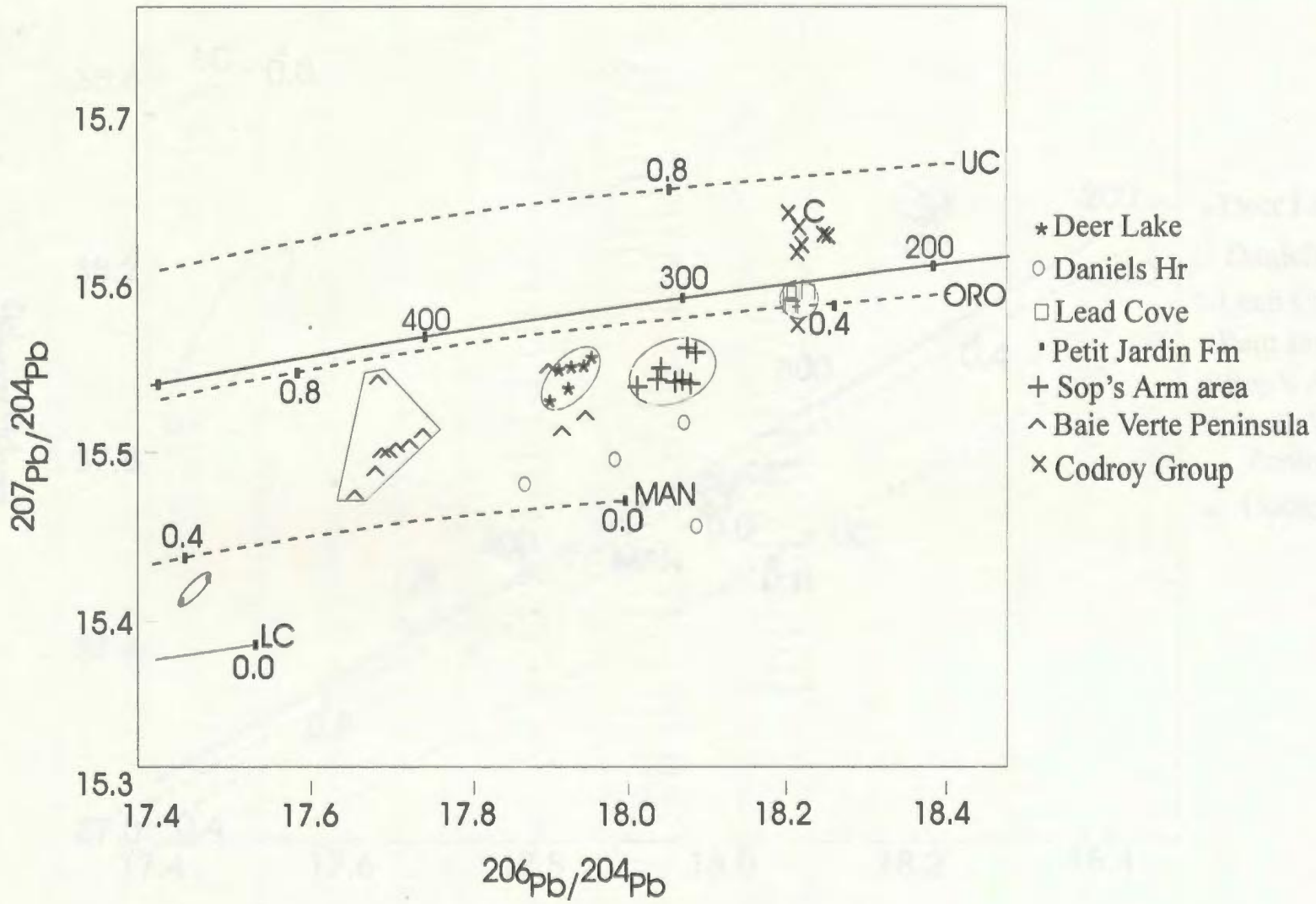

Figure 6 Lead isotope graph for galena separates from western Newfoundland. Also plotted are Stacey and Kramers model age line and the plumbotectonics curves. UC=upper crust ORO=orogen MAN=Mantle and LC=lower crust

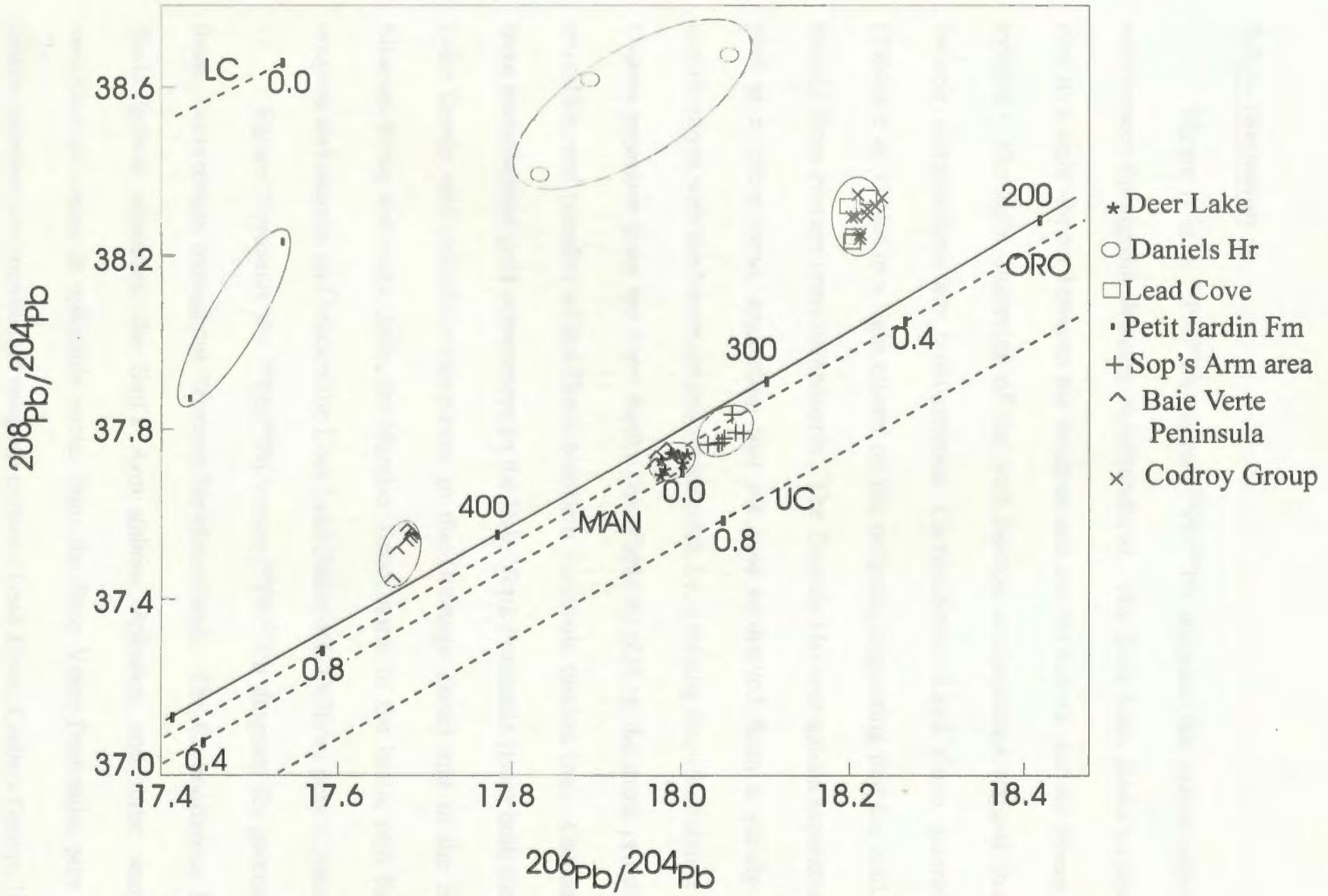

Figure 7 Lead isotope graph for galena separates from Western Newfoundland. Also plotted are Stacey and Kramers model age line and the plumbotectonics curves. UC=upper crust ORO=orogen MAN=mantle and LC=lower crust

5.2.2 - Discussion

Figure 6 is a $^{207}Pb/^{204}Pb$ versus $^{206}Pb/^{204}Pb$ diagram for galena separates from occurrences throughout Western Newfoundland. The Deer Lake Basin galena separates plot in a tight cluster between the orogene and mantle curves, and no linear trends are evident. The tight clustering of the lead isotope compositions suggest that the lead isotope compositions are homogeneous. Carboniferous Lead Cove galena separates (Tables 8 & 9) plot in a tight cluster on the orogene, suggesting that the lead is derived mainly from average crust components. The Daniels Harbour galena separates (Table 8) plot as a linear trend, suggesting that the lead is derived from a variety of source contributions with the basement and upper crust, i.e. a mixing line (Swinden et al., 1988). Galena separates from the Petit Jardin Fm (Table 8) plot as the most primitive, lower crust-like, end member of the Great Northern peninsula mixing line. Galena separates from mesothermal gold occurrences in the Baie Verte Peninsula (from both the Mic Mac Lake Group and ophiolitic complexes in the Dunnage Zone) and in the Sop's Arm Silurian felsic volcanics (from the Humber Zone) north of the basin, plot between the orogene and mantle, and bracket the Deer Lake Basin data (Wilton, pers. Comm.).

Figure 7 presents the $^{208}Pb/^{204}Pb$ versus $^{206}Pb/^{204}Pb$ diagram for galena separates from occurrences throughout Western Newfoundland. The Carboniferous Deer Lake Basin galena separates, the Sop's Arm galena separates, and three samples from mesothermal veins in ophiolitic rocks from the Baie Verte Peninsula, plot in a tight cluster between the mantle and orogene curves. Lead Cove, Codroy Group, Petit Jardin

Formation, other Baie Verte Peninsula (Mic Mac Lake Group), and Daniels Harbour galena separates plot between, and subparallel to, the orogene and lower crust curves.

Formation of Mississippi Valley Type (MVT) deposits may last 0.5 - 5 Myr (Nakai et al., 1993). Appalachian MVT deposits formed from large- scale migration of basinal brines during the late-Paleozoic Alleghanian orogeny that took place 250-330 Ma (Nakai et al., 1993). Model ages for the galena separates from western Newfoundland have been calculated according to the Stacey and Kramers (1975) model. The oldest ages (425-590 Ma) are from the Petit Jardin Formation samples. Since large- scale migration in the area occurred around 250 - 330 Ma, the model ages are obviously too old, suggesting that the lead for these galena separates originated in the Grenvillian basement.

Lead-isotope compositions clearly differentiate occurrences in Cambro-Ordovician carbonate rocks of the Northern Peninsula from those associated with the Devonian-Carboniferous Bay St. George subbasin in western Newfoundland, and also those from the Carboniferous Deer Lake Basin and surrounding areas; pointing to contrasting metal sources and processes of mineralization.

The model ages for the Great Northern Peninsula (Table 8), range from 102 - 590 Ma. Swinden et al., (1988) suggests that isotopic compositions of lead in galena from the Northern Peninsula suite (Table 8) which include the Daniels Harbour MVT deposit the Petit Jardin Formation, Lead Cove and Codroy Group, define linear trends in which the lead isotope ratios increase with stratigraphic height in the Cambro-Ordovician sequence. They further suggest that these trends are mixing lines; samples at the non-

radiogenic end (Petit Jardin Formation) have very low $^{207}Pb/^{204}Pb$ but high $^{208}Pb/^{204}Pb$ ratios relative to $^{206}Pb/^{204}Pb$ and are interpreted to represent the product of substantial evolution in high grade metamorphic rocks of the Grenville Structural Province. Swinden et al. (1988) also stated that the more radiogenic source(s) is probably located within the sedimentary pile and contributed metals to the fluids during their migration to the deposition sites. Lead isotopes ratios for the Bay St. George galena separates indicate that the lead was derived from the Carboniferous clastic sediments within the sedimentary basin.

The model for the great Northern Peninsula area involves metal-bearing fluids which ascended from the basement and/or basal clastic sequence into the overlying carbonate succession, along faults, while sulphide deposition at successively higher levels involved fluids with greater proportions of more radiogenic lead (Swinden et al., 1988). The mineralization in the Bay St. Georges's area was thought to have been formed as a consequence of fluid migration within the basin during late diagenesis, with metals, locally derived from terrigenous sediments in the basin (Swinden et al., 1988) The isotopic compositions of the lead reflect proportions of erosional products from Post-Taconian silicic volcanic and plutonic rocks with perhaps lesser inputs from PreCambrian crystalline rocks and pre-Taconian sediments and ophiolitic rocks (Swinden et al., 1988).

Dix and Edwards (1996) suggest that fluids and metals may have been mobilized from the allochthnous Humber Arm strata or from the overthrust siliciclastics that occur beneath an allochthonous Ordovician platform for the Lead Cove deposits (Table 9). Dix

and Edwards (1996) also suggest that the sulfate needed to form sulphides was supplied at the mineralization site by dissolution of nearby Mississippian evaporites.

Younger host rocks are usually the most radiogenic. The Port Au Port Peninsula lead values are more radiogenic than the Carboniferous Deer Lake Basin, whose model ages range from 338-378 Ma. The Sop's Arm, Baie Verte Peninsula and the Deer Lake Basin galena separates seem to have a common growth between the orogene and the mantle, but plot along different isochrons: with the Mic Mac Lake Group being the oldest, followed by the Deer Lake Basin and ophiolitic samples. and with the Silurian felsic volcanic hosted galena separates being the youngest. Geologically these 'ages' make no sense, i.e. Sop's Arm and Baie Verte Peninsula galena separates should be of the same geologic age, post Silurian-Devonian. Thus it may reflect a mixing line in which the primitive end-member is reflected in sediments from the Dunnage Zone (Mic Mac Lake Group etc.), while the felsic volcanics of Sop's Arm are the radiogenic end-member. The Dunnage Zone derived galena separates are more primitive than those in the Humber Zone, with the Deer Lake Basin galena separates being a mixture of the two.

The Deer Lake Basin galena separates plot between galena separates from the Mic Mac Lake Group (Sop's Arm) in the Dunnage Zone and the felsic Silurian volcanics (Baie Verte Peninsula) in the Humber Zone. Isotopic compositions of lead in galena from the these areas define a linear trend, interpreted as a mixing line; the more radiogenic source(s) is probably located within the clastic sedimentary pile and contributed metals to the fluids during their migration to the deposition sites while the

less radiogenic source(s) presumably sample the older mafic volcanic rocks. A model for the lead occurrences in the Deer Lake Basin would involve late diagenetic fluids circulating in porous clastic sediments, leaching loosely bounded metals and carrying them to sites where chemical conditions are favorable for deposition. The lead isotope compositions of the Deer Lake Basin galena separates (from the Turners's Ridge MVT galena deposit, Side Pond, and the Gales Brook galena showing) reflect proportions of erosional clastic material and/or silicic volcanic and plutonic rocks (Humber Zone) with lesser inputs from the Pre-Taconian sediments and ophiolitic rock (Dunnage Zone).

Possible sources of lead for the Deer Lake Basin are: 1) clastic sediments within the basin; or 2) the adjacent plutonic rocks and/or mafic volcanics. The lead geochemistry anomaly map (Map 20) of the Deer Lake Basin shows lead anomalies coincident with faults in the basin; suggesting that fluids migrating through the basin via the faults could have incorporated lead from the differing compositional paleotopographic domains.

Sangster and Vaillancourt (1990) state that groundwater moving slowly through sands gradually alter feldspars to clay minerals and silica thereby releasing lead contained in the feldspar crystal lattice and in the sediments too. Lead in the Deer Lake Basin is most likely derived from adjacent plutonic rocks (granitic in origin) and mafic volcanics. The lead and silica from the decomposed sandstone continue to migrate through the porous pathways as dissolved complex chemical compounds in groundwater. Galena was possibly precipitated when these groundwaters reached a zone where reducing chemical

conditions, possibly brought about by the presence of organic (coal and bitumen) material, prevailed. Under these conditions, reduced sulphur (possibly the result of bacterial activity) combined with dissolved lead compounds and precipitated galena. The presence of H_2S exerts control on the formation of Pb - Zn (and Cu) deposits through its source and availability. Thus organic- rich strata and migrated hydrocarbons can be of major importance in the production of reduced sulphur from sulphate to generate metal sulphides. To produce higher grade mineralization by this process, it is necessary to focus the basinward flow of metal-bearing groundwater through permeable fault structures.

5.3.1 - S, C and O isotopes Results and Discussion

Table 10 Sulphur isotopes for Deer Lake Basin

Sample #	Basin Section No.	$\delta^{34}S$(‰)	Mineral/ Formation
H96-10	3	6.4	Gales Brook galena
H95-05	3	-0.3	Silurian pyrite (Freeman Prospect)
H96-09	3	18.4	Gales Brook pyrite
H96-18	2	16.8	Humber Falls Fm pyrite

Sulphide samples were collected in the Deer Lake Basin for a reconnaissance sulphur isotope investigation into the similarities or dissimilarities of sulphide showings in the basin. Table 10 lists the sulphur isotope values for several sulphide separates from

the Deer Lake Basin ranging from -0.3 to +18.4 ‰ relative to Canyon Diablo Triolite. Sample H96 - 10 is a galena sample from Gales Brook in the northern part of the basin, while sample H96 - 9 is a pyrite sample just north of sample H96 - 10 (Map 1). H96-5 is a pyrite sample from the Freeman gold prospect in the northern portion of the basin. These three samples are hosted in the Sop's Arm Silurian rocks. Sample H96-18 is a pyrite sample found in micaceous sandstones of the Humber Falls Formation in the western portion of the basin (Map 1).

This discussion is based on the assumption of chemical and isotopic equilibrium among sulfur species in solution and precipitating mineral phases. Under equilibrium conditions the $\delta^{34}S$ values of the minerals respond readily to changes in the chemical environment of ore deposition as indicated by ore and wall- rock mineral assemblages (Rye and Ohmoto, 1980). Important sources of sulfur in ore deposits are deep-seated sources (mantle or homogenized crust), local country rocks, and sea-water or marine evaporites (Rye and Ohmoto, 1980).

Sample H96 - 10 has a $\delta^{34}S$ value of 6.4 ‰. The source of sulfur for this sample probably came disseminated sulphides in the local country rocks. This positive $\delta^{34}S$ value indicates that the showing is oxidized with respect to $\delta^{34}S$. Samples H96 - 09 and H96 - 18 have $\delta^{34}S$ values (16.8-18.4 ‰) closer to those of evaporite deposits. Deposition occurs as a result of reduced seawater sulphate. The sulfur was likely derived from oxidized marine evaporites. Sample H96 - 05, a pyrite sample, has a $\delta^{34}S$ value of -0.3 ‰. This sample located in Silurian volcanics is distinctly different from the other

showings in the basin. Deposition probably occurred as a result of biogenic reduction (bacterial) of seawater sulphate.

Various suggestions can be made based on the isotopic signatures of the samples. Turner's Ridge and Gales Brook galenas are assumed to be Carboniferous in age (based on the lead isotope data). The pyrite in both the Gales Brook area and the Humber Falls Formation are essentially the same according to the $\delta\ ^{34}S$ signature, suggesting that these samples are tapping into the same source of sulfur, presumably reduced seawater sulfate from oxidized marine evaporites, and that the Humber Falls pyrite is also Carboniferous in age. The Gales Brook galena is assumed to be Carboniferous in age, but the sulfur source is different from that of the pyrite. The $\delta\ ^{34}S$ value is much lower than that of the pyrite in the same area. This is due to fractionation of coexisting minerals in the basin. Higher temperatures, result in more extensive fractionation (or isotopic difference between coexisting minerals). The sulfide showings in the Gales Brook area occur in the highest temperature fluids (Sec. 5.4) suggesting fractionation between co-existing galena and pyrite, which presumably explains the widely varying $\delta\ ^{34}S$ results. Coexisting pyrite and galena, usually results in pyrite with high positive $\delta\ ^{34}S$ values, and galena with lower positive $\delta\ ^{34}S$ values, as is the case in the Deer Lake Basin.

The pyrite from the Freeman prospect is distinctly different from the other sulphide occurrences in the area. The reason for this difference is 1) the showing is assumed to be Silurian in age, not Carboniferous and 2) formed as a result of biogenic reduction (bacterial) of seawater sulfate.

Table 11 Carbon and oxygen isotopes from Deer Lake Basin

Sample #	$\delta^{13}C$ (‰)	$\delta^{18}O$ (‰)	Rock Type/Formation
W89-25A	-5.0	15.1	Sst with $CaCO_3$ veins/ WigWam Bk Fm
W89-25B	-2.1	14.1	Sst with $CaCO_3$ veins/ WigWam Bk Fm
W89-27B	-3.9	18.6	Limestone/ Humber Falls Fm
W89-28B	-2.2	11.1	Cong with $CaCO_3$ veins/ WigWam Bk Fm
W89-31A	-3.4	13.5	Sst with $CaCO_3$ veins/ WigWam Bk Fm
W89-31D	-4.2	21.8	Cong with $CaCO_3$ veins/ WigWam Bk Fm
W89-18B	-1.0	15.4	Lst/ Humber Falls Fm
W89-18C	-0.9	16.6	Lst with $CaCO_3$ veins/ Humber Falls Fm

The rationale for carbon and oxygen analyses was to deduce background isotopic values of carbon and oxygen from rocks collected in the Deer Lake Basin, and to deduce contributions to hydrothermal fluids. $\delta^{13}C$ and $\delta^{18}O$ values of carbon-bearing minerals are controlled by the physical-chemical conditions within the hydrothermal fluids (Rye et al., 1980). Important sources of carbon are deep-seated sources (mantle or homogenized crust), marine limestones, and organic matter in sedimentary rocks, while oxygen sources are from waters (Rye, 1980). Table 11 lists the carbon and oxygen isotopes analyzed for the Deer Lake Basin.

In sulfate-rich environments, such as the Deer Lake Basin, bacterial sulfate reduction is important producing diagenetic carbonates with markedly negative $\delta^{13}C$

compositions (Katz, 1990). Oxygen isotopic compositions are not significantly influenced by bacterial processes, as they preserve a record of the composition of the waters in which the host sediments were deposited. Increasing $\delta^{18}O$ values in diagenetic carbonates produced in association with bacterial sulfate reduction indicate increasingly $\delta^{18}O$-enriched pore waters and suggest that carbonates formed in this diagenetic environment also preserve an isotopic record of the waters in which the host rock was deposited (Katz, 1990).

Slightly chloritized conglomerates from the Wigwam Brook Formation found in or near fault gouges in the Deer Lake Basin, contained carbonate veinlets which were sampled. The $\delta^{13}C$ values ranged from -2 to -4 ‰ relative to PDB, and $\delta^{18}O$ values ranged from +11 to +22 ‰ relative to SMOW. The value for $\delta^{13}C$ is similar to average $\delta^{13}C$ for marine limestones (Rye et al., 1980). Since the samples are found in faults in the basin, these values are reflecting the fluids that circulated through the faults, rather than the host rock compositions. Micaceous sandstones from the Wigwam Brook Formation contained carbonate veins which were analyzed for background values of oxygen and carbon. The values ranged from $\delta^{13}C$ of -2 to -5 ‰ relative to PDB and $\delta^{18}O$ of +13 to +15 ‰ relative to SMOW; these values reflect both the fluids and host rock compositions.

Limestones from the Humber Falls Formation, with some pink dolomite veins were analyzed giving $\delta^{13}C$ values between -0.8 to -5 ‰ relative to PDB, and $\delta^{18}O$ values ranging from +14 to +18 ‰ relative to SMOW.

The $\delta^{13}C$ values for the Deer Lake Basin sediments differs from the carbon values analyzed from bitumen and coal samples (Ch 4.2.1) which had $\delta^{13}C$ values between -22.9 to -32.4 ‰. Deer Lake Basin sediment values are isotopically heavy with regards to $\delta^{13}C$ while the hydrocarbon samples are isotopically light with respect to $\delta^{13}C$. The isotopic values for the hydrocarbon samples are probably the result of reduced or organic carbon in sediments. The organic matter and sulfate rich environment, presumably played a role in the extreme negative $\delta^{13}C$ values which are displayed.

The Wigwam Brook Formation sediments (sandstones and conglomerates) isotopically, are essentially the same, with little variation in the $\delta^{13}C$ or $\delta^{18}O$ signature, reflecting either the fluid and/or host rock compositions. The limestones from the Humber Falls Formation have slightly different isotopic signatures suggesting that the sediment compositions are slightly different. A combination of organic matter present and influence from marine limestones, in the carbonates of the Humber Falls, presumably is the reason for the slightly different $\delta^{13}C$ signature, in the limestones than the sandstones and conglomerates. $\delta^{18}O$ values in all the samples have virtually the same signature, suggesting that the Deer Lake sediment isotopic values, reflect a meteoric fluid influence.

5.3.2 - Whole Rock Geochemistry

The rationale for the use of XRF analysis is to derive background geochemical information for sediments in the Deer Lake Basin to compare them to average worldwide

background concentrations of sedimentary and igneous rocks given by Hawkes and Webb, 1962; and ultimately to deduce contributions to hydrothermal fluids. Appendix B.1.3 lists the whole rock geochemical data for oil shales and various other rocks in the Deer Lake Basin. Appendix B.1.4 lists the whole rock data for samples collected by Wilton (unpub. data).

The Deer Lake Basin contains sedimentary rocks: although both igneous and sedimentary rocks can contribute metals to any mineral deposits found in the basin. Figure 8 is a diagram of the individual concentrations of elements for each sandstone sample normalized to average sandstone concentrations, in log scale. This diagram shows that the Deer Lake Basin sandstone samples, have trace element concentrations comparable to the average sandstone concentrations, listed in Table 12 (Hawkes and Webb, 1962). A notable exception is Nb, which is enriched in the Deer Lake Basin sandstones, possibly reflecting a granitic source for the sediments. The North Brook Formation, consisting of conglomerates and sandstones, is one of the hydrocarbon reservoirs for the basin. This formation has elevated concentrations of Pb, Zn, and Cu relative to the average background concentrations for sedimentary rocks (Table 12); however with respect to the lake sediment data (Ch 3), these elements were not observed to be elevated.

Figure 9 is a diagram of the individual concentrations of elements for each limestone sample, normalized to average limestone concentrations, in log scale. This diagram shows that the Deer Lake Basin limestone samples, have trace element

concentrations that are broadly comparable to the average limestone concentrations, listed in Table 12 (Hawkes and Webb , 1962). Notable exceptions are enrichments in Nb, La, and Pb, reflecting a granitic source influence of the sediments, and Ba, reflecting the evaporitic nature of the sedimentary environment. Lead has elevated concentrations in the limestone samples, as many of the lead showings occur in limestones. Arsenic is also elevated in some samples presumably reflecting pyrite and possible gold occurrences.

Figure 10 is a diagram of the individual concentrations of elements for each oil shale sample, normalized to average shale concentrations, in log scale. This diagram shows that the Deer Lake Basin oil shale samples, have trace-element concentrations comparable to the average shale concentrations, listed in Table 12 (Hawkes and Webb, 1962). Notable positive exceptions are As, S, Ba and U. This suggests that oil shales could be a source of uranium in the basin. Oil shales from the Rocky Brook Fm have source rock potential (Hyde, 1984) for generating hydrocarbons. The level of maturity ranges from immature to moderately mature. The coal and bitumen compositions (ICP-MS data) are comparable to host rocks of the oil shales. Overall the lake sediment data (Ch 3) are reflected in the average background compositions of the host rocks: metal concentrations in both the rock and lake sediments are elevated.

Table 12: Average (and/or range) of background concentrations for igneous and sedimentary (sandstones, limestones and shales) rocks (modified from Hawkes and Webb, 1962).

Element	limestone ppm	sandstone ppm	shale ppm	igneous (ppm)
Sb	0	1	3	0.3
As	0	0	4	2.0
Ba	20-200	100-500	300-600	640
Be	<1	<1	1-6	4.2
Bi	0	0.3	1	0.1
B	18	155	130	13
Cd	0	0	0.3	0.13
Cr	5	10-100	100-400	117
Co	0.2-2	1-10	10-50	18
Cu	5-20	10-40	30-150	70
F	51	290	590	660
Au	0.005-0.009	0.03	0.01-1	0.1
Fe	1.3%	3.1%	4.3%	4.65%
Pb	5-10	10-40	20	16
Li	2-20	7-29	50	50
Mn	1300	385	0	1000
Hg	0.03	0.03-0.1	0.4	0.06
Mo	0.1-0.5	0.1-1	1	1.7

Table 12: Background concentrations of average sedimentary and igneous rocks cont'd

Element	limestone ppm	sandstone ppm	shale ppm	igneous (ppm)
Ni	3-10	2-10	20-100	100
Nb	0	0	20	20
Se	0.1-1	1	0.5-1	0.09
Ag	0.2	0.4	5-50	0.2
S	8000	2200	1100	900
Sn	0	0	40	32
Ti	400	3000	4400	4400
W	1.8	1.6	0	2
U	2.5	0.45	4.1	2.6
V	2-20	10-60	50-300	90
Zn	4-20	5-20	50-300	80

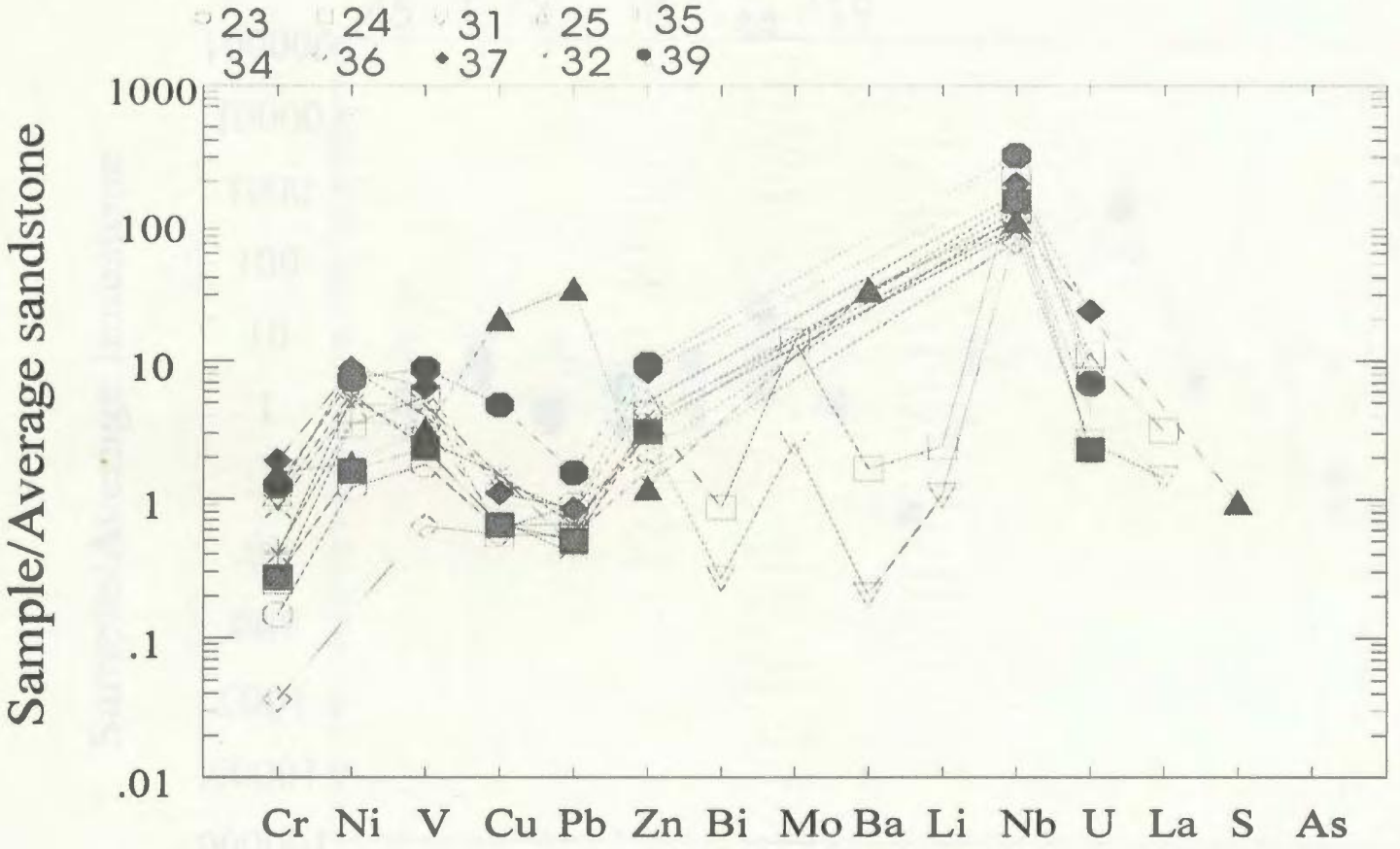

Figure 8: Normalized geochemical data for sandstone samples from the DLB (average sandstone values from Table 12).

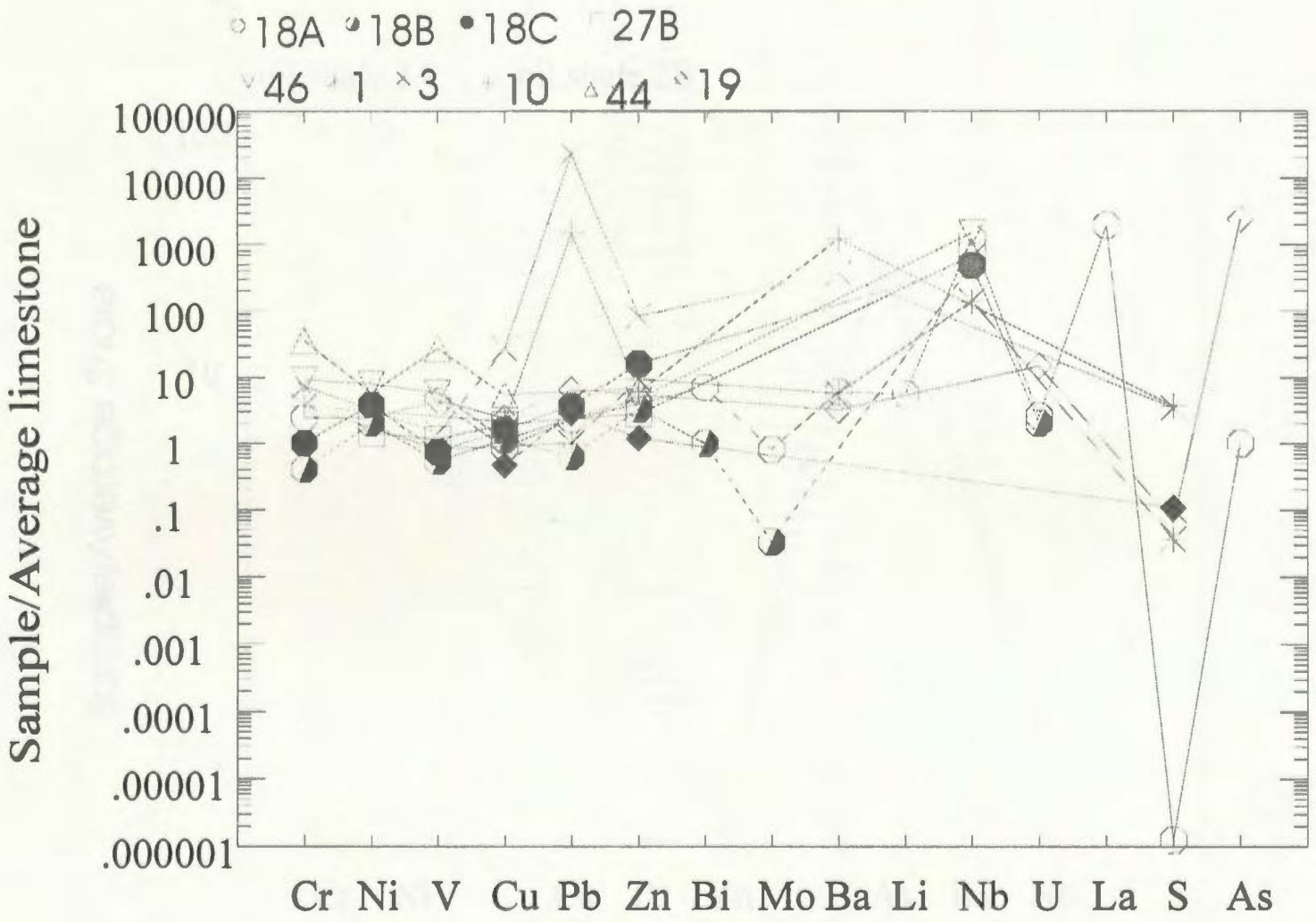

Figure 9: Normalized geochemical data for limestone samples from the DLB (average limestone values from Table 12).

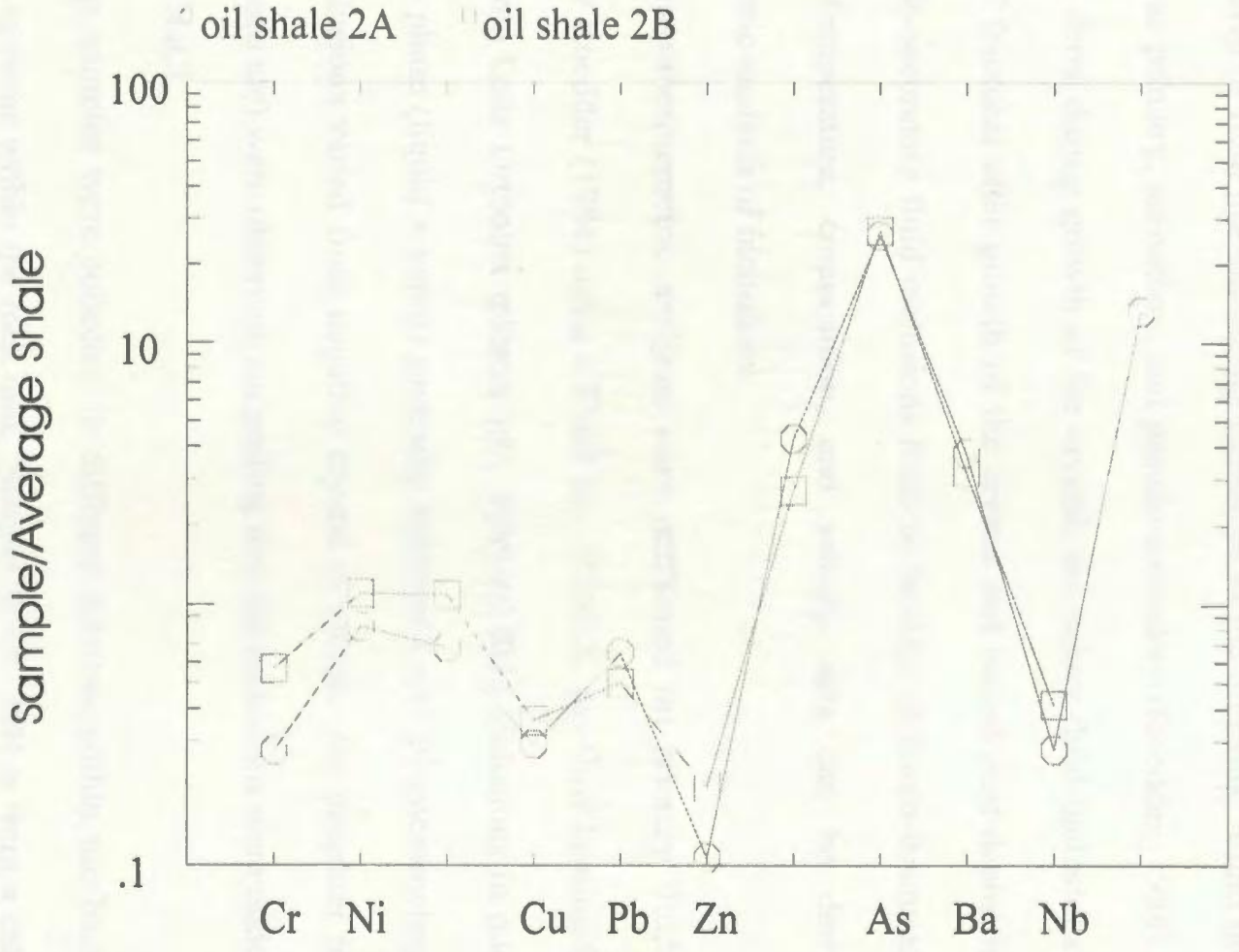

Figure 10: Normalized geochemical diagram for shale samples from the DLB (average shale values in Table 12)

5.4.1 - Fluid Inclusion Results

Fluid Inclusions are liquid and/or vapor fillings in cavities or voids within minerals such as quartz or calcite. The fluid present in the inclusion may be representative of fluid present during formation of the minerals. Fluid inclusions can be classified as primary, secondary, and pseudo-secondary (Roedder, 1984). Primary fluid inclusions form during growth of the crystal; secondary fluid inclusions form from the healing of fractures after growth of the crystal and record post-depositional conditions and pseudo-secondary fluid inclusions form by healing of micro-fractures during crystal growth. Temperature, composition, and salinity data can be derived from the thermometric analysis of inclusions.

Micro-thermometric analyses were performed on primary fluid inclusions, as defined by Roedder (1984) using a Fluid Inc. U.S.G.S. gas-flow heating-freezing system attached to a Leitz Ortholux microscope. Primary fluid inclusions in quartz and calcite were two- phase (liquid + vapor) generally between 4 and 20 micrometers in size; forms of the inclusions varied from negative crystal to oblate. No daughter minerals (halite, hydrocarbons etc) were observed, suggesting that the inclusions were undersaturated with respect to NaCl.

The samples were collected in different sections within the basin (Map 1), all were vein systems within the rock unit. Sample W89 - 39H is from a calcite vein in the Howley Formation; H96 - 9, W89 - 21B, H96 - 1 and H96 - 5 are from quartz veins in the Silurian Sop's Arm Group, in the northern part of the basin. Fluid inclusions from

sample W89 - 17B and W89 - 43B are from quartz veins in the Salt Water Cove Formation. Fluid inclusions from sample W89 - 30B are from a quartz vein in the Forty-Five Brook Formation while fluid inclusions from core 80 - 78 are from a quartz vein in the Birchy Ridge copper showing in the Wigwam Brook Formation.

Table 13: Fluid inclusion data summary for the Deer Lake Basin

Group	T_h Range (°C)	T_h Max(°C)	F. I. Sample #'s	Sec. in DLB
1	154-185	170	W89-39H, 21B, 17B, 43 H96-9, 5, 1	1 and 7
2	185-227	200	W89-30B	8
3	227-258	245	Core 80-78	3

Table 13 presents the fluid inclusion summary for the Deer Lake Basin. Thermometric analyses distinguished 3 groups of inclusions based on homogenization and last ice melting temperatures (T_h and T_m respectively). Temperatures of first observed melting of inclusions (ideally a eutectic) were recorded to determine the components present. Homogenization temperature (T_h) ranges from 154.2 to 258.4 °C with an average homogenization temperature of T_h = 206.3 °C. The first melting temperatures (T_m) ranged from -2.7° to -10.3 °C, with average T_m = -6.0 °C. Using the computer program Flincor, salinities were calculated based on the T_m, resulting in salinities in

weight % NaCl equivalent (wt. % NaCl eq.). The fluid inclusion salinities ranged from 4.4 to 14.3 wt % NaCl eq. with an average salinity of 9.1 wt. % NaCl eq.

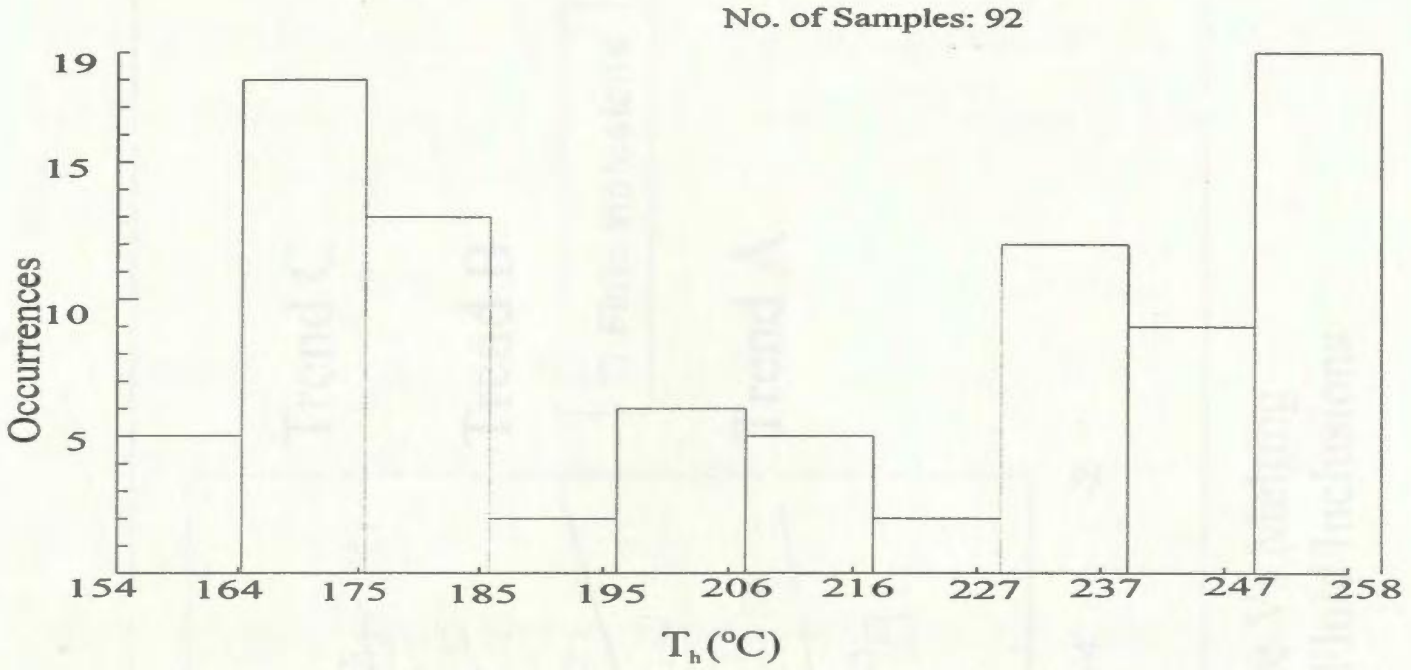

Figure 11 Histogram of Homogenization Temperature

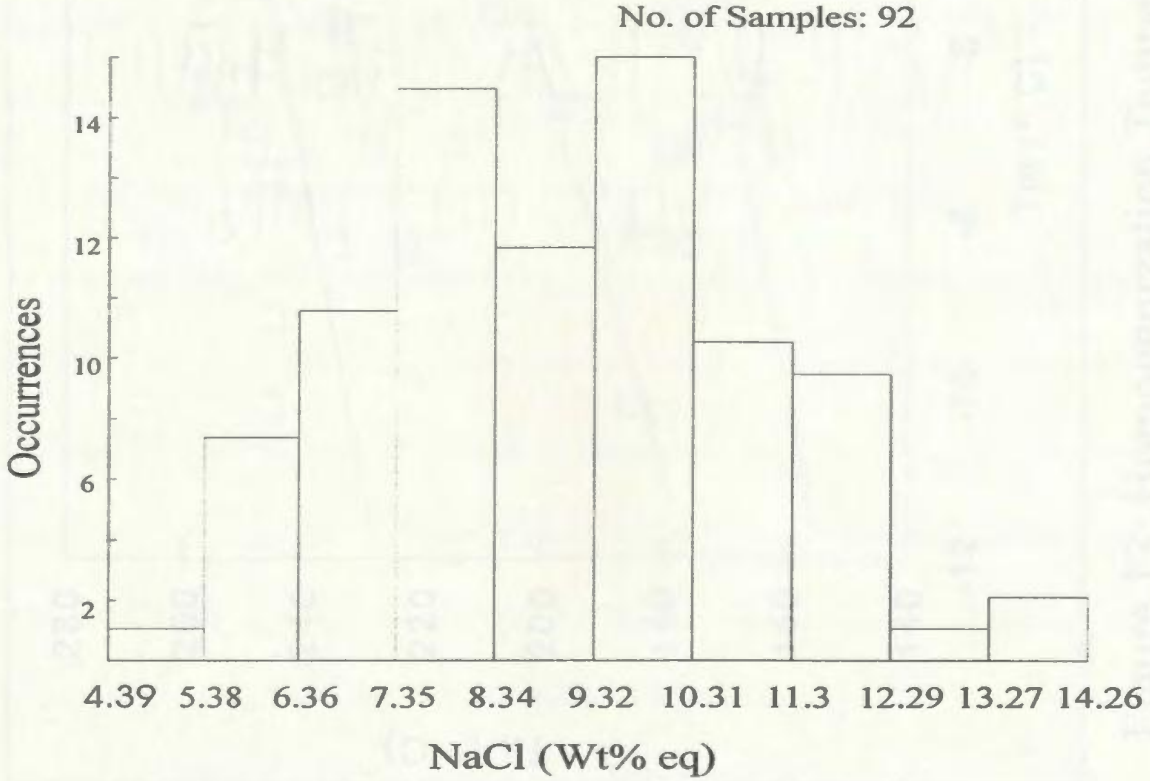

Figure 12 Histogram of salinity (NaCl wt% eq)

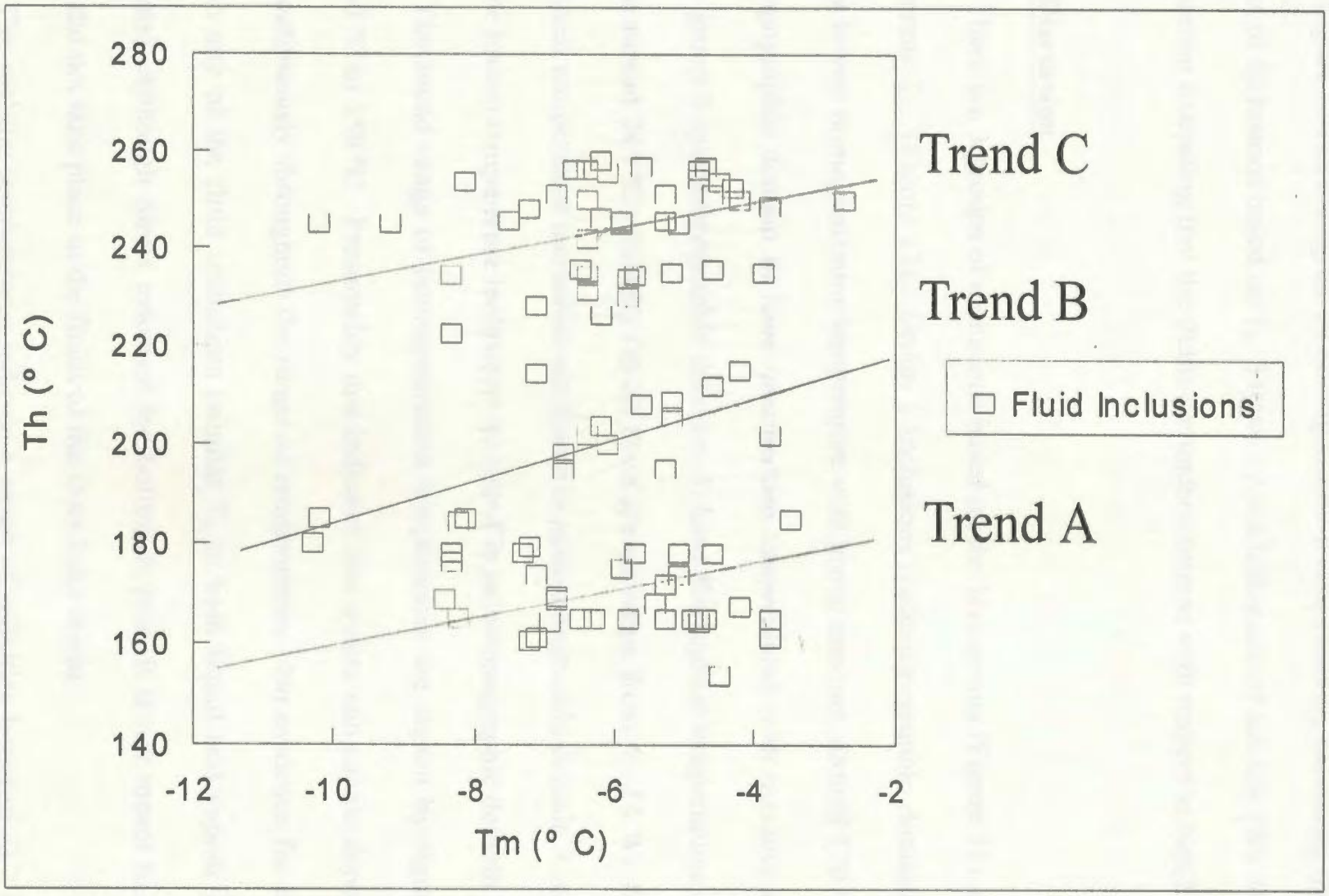

Figure 13: Homogenization Temperature Vs Melting Temperature For The Deer Lake Basin Fluid Inclusions

Figure 11 is a histogram of homogenization temperatures, indicating that there are 3 groups of inclusions based on T_h. Figure 12 is a histogram of salinity (Wt. % NaCl eq.) measurement indicating that the fluids are undersaturated with respect to NaCl.

5.4.2 - Discussion

There are 3 groups of inclusions based on the histograms (Figure 11) and the plot of T_h versus T_m (Figure 13). Group 1 inclusions (paleotopographic domains 1 and 7) have the lowest homogenization temperature with group maxima around 170 °C, group 2 (paleotopographic domain 8) have intermediate temperatures with maxima around 200 °C, and group 3 (paleotopographic domains 3) have the highest temperatures with group maxima around 245 °C. Salinity for all three groups range from 4 - 14 Wt. % NaCl eq. The highest temperature inclusions are found in paleotopographic domain 3 on the basin, while the lowest temperature inclusions are found in paleotopographic domain 1.

The broad range of homogenization temperatures are shown by figure 11 from near 250 °C to 150 °C. Presumably this indicates that quartz and calcite deposition took place continuously throughout the range of temperatures. No evidence for boiling was found in any of the fluid inclusions (similar T_h to both liquid and vapour in adjacent inclusions). Although direct evidence for boiling is rare, it is not meant to imply that boiling did not take place in the fluids of the Deer Lake Basin.

The melting temperatures indicate a range of salinities between -2.7 to -10.3 °C (4.39 to 14.26 wt. % NaCl eq.) with average T_m = -6 °C (~ 9 wt. % NaCl eq.). NaCl or

other daughter minerals were not identified in any of the samples, thus the fluids are interpreted to be undersaturated with respect to NaCl.

Figure 13 presents the plot of T_h versus T_m for inclusions in the Deer Lake Basin. Three linear trends are noted. Trend A (Group 1) is a lower temperature, low salinity trend, displaying a gentle positive slope. Trend B (Group 2) is an intermediate temperature, low salinity group displaying a slightly steeper slope, while Trend C (Group 3) contains the highest temperature, low salinity fluid inclusions displaying a steep positive slope. Each trend includes increasing homogenization temperature with increasing melting temperature (and thus salinity).

The fluid inclusion data define a linear trend in which the fluid inclusion temperatures decrease north to south in the basin. Quartz and calcite from the northern part of the basin formed under high temperatures and low salinities, while in the southern part of the basin inclusions in quartz and calcite display low temperatures and salinities. Fluid inclusions from the Birchy Ridge copper showing in the northern part of the basin, have the highest homogenization temperatures. Copper is usually transported at higher temperatures than other metals, thus confirming high homogenization temperatures.

It appears that there were several phases of fluid migration through the basin. The first was a high temperature, low salinity fluid possibly carrying metals such as Cu. It is possible that these high temperature fluids paved the way for other slightly lower temperature but similar salinity fluids, and hydrocarbons to migrate through the basin, by improving the porosity in the basin.

The thermal maturation of bitumen and coal is in the temperature range of 80 - 120°C ('oil window'). Bitumen deposition presumably postdates the deposition of quartz and calcite since no hydrocarbon inclusions were noted in any of the samples. This suggests that temperature must have decreased from the time of quartz (and/or calcite) nucleation to bitumen cracking. Hydrocarbon solubility decreases with increasing salinity of aqueous media, thus hydrocarbons are mostly transported in low salinity, high temperature fluids, similar to those found in the Deer Lake Basin. Catagenesis of organic matter bearing sediments was probably a result of heated meteoric mater flowing downward through the strata. Meteoric water (low salinity) flowed downward, presumably driven by gravity through hydrocarbon bearing units resulting in the catagenesis of the organic matter. The fluid flow was then focussed and mixed along fault planes.

CHAPTER 6 - Summary, Conclusions And Recommendations

6.1- Summary

Metals and hydrocarbons migrating from common source rocks, and lacustrine rocks, such as those in the Deer Lake Basin, are plausible, as a source of both metals and hydrocarbons. Parnell (1994) states that the metals in liquid petroleum, solid bitumens/coals, and ore deposits are all products of fluid migration of one type or another. He further states that transition metal reduction/deposition from transport media to host media is conceptionally similar whether the host medium is an oil, a solid bitumen, or an ore body; and understanding the origin of metals in, for example solid bitumens will assist in understanding the origin of the bitumens themselves, and in turn, information about bitumens, will be of use in assessing the origin of both petroleum and ore deposits.

Key factors in determining the mode and extent of mineralization include: 1) sediment/source composition; 2) fluid properties; and 3) extent of fluid-sediment reservoir contact. Mineralization patterns in different strata vary according to how these factors are inter-related, and affect the relative rates of reactions involved in deposition.

Both mineralized and unmineralized samples were collected in the basin. These samples were used to determine background values in individual strata, making it possible to determine specific changes in chemical composition of source sediments which result from the passage of mineralizing fluids; and also to determine the composition of the ore/petroleum fluids.

Host rock sediment concentrations in the basin were measured using XRF data and lake sediment data, which show that some sediments have elevated concentrations of certain metals with respect to the average background concentrations of sedimentary rocks. The metals with elevated concentrations in the Deer Lake Basin are Pb. Cu. and Zn in sandstones; Pb, and As in limestones: and As and U in the oil shales. The elevated concentrations of Pb in limestones can be explained as limestones are the host rocks of galena occurrences in the basin. The elevated concentration of U in oil shales may reflect a source of U in the basin. The XRF data for the sedimentary rocks reflect a granitic source influence due to elevated concentrations of Nb and La; elevated Sm concentrations in the lake sediment data, also reflect a granitic influence (Topsails igneous source) in the basin, especially on the eastern side of the basin. Barium has elevated concentrations in limestones in the basin, reflecting evaporitic conditions.

Lake sediment data indicate several mobile elements whose distribution is deemed to be fault controlled by including: As, Au, Cu, Pb, Mo, U, and Zn; as elevated concentrations of these elements coincide with mapped faults in the basin. Other elements are indicative of subsurface strata, which, are in most cases, fault bounded. The involvement of the Pre-Cambrian basement as a source is also reflected in elevated concentrations of Co, Rb, and As. The distribution of sample sites indicates that the geochemical anomalies defined for the basin are real anomalies. This is further substantiated by the low concentrations of manganese. Manganese is a sponge element,

(Hawkes and Webb, 1962) concentrating other elements, the low values of manganese indicate that the geochemical anomalies are not manganese induced.

ICP-MS and LAM-ICP-MS results indicate that the coal is relatively devoid of sulphur and many metals, while the bitumen contains appreciable contents of sulphur and metals, compared to the average concentrations of coal and bitumen; suggesting that either the bitumen samples had more interaction with metal-carrying fluids than the coal, or were carried coevally with metals in solution. Isotopic variations in carbon and oxygen ratios reflect a meteoric fluid influence in the basin, while sulphur isotope values suggest fractionation exists between coexisting minerals in the basin (pyrite and galena). The source of sulphur for some samples presumably comes from reduced seawater sulphate from marine evaporites, while others have a source of sulphur resulting from the reduction (bacterial) of seawater sulphate.

Based on the potential field, geology and geochemistry data, the basin was subdivided into eight sections. The combined potential field and geochemical data indicate that some forms of mineralization and hydrocarbons in the basin occur near residual gravity and magnetic highs, while other forms are correlated with high magnetic gradients. The trends indicate the association of mineralization and hydrocarbon deposits with the underlying basement topography and the faults and fractures that formed structural conduits along which the mineralized fluids migrated. The geochemical anomaly maps in combination with potential field data suggest the presence of large fault- bounded blocks of subsurface material and help delineate edges of faults which

served as possible structural conduits for migrating fluids and/or structural traps for hydrocarbons in the basin. Formation of mineral deposits is a secondary feature related to structural and stratigraphic features and are likely controlled by major basement faults. The faults may develop as or into wrench faults or major deep thrusts.

During the Devonian-Carboniferous, wrench faulting occurred in the Deer Lake Basin, followed by deposition. Deposition of sediments (basin fill) would ultimately have been controlled by faulting in the basin; i.e. the Deer Lake Group facies were deposited throughout the basin, but may be absent on the eastern edge of the basin due to steep faults. This could have implications for petroleum exploration in the basin, in terms of the hydrocarbon reservoir and traps, especially with regards to the Deer Lake Group facies. Some of the faults were later re-activated, and resulted in fluid generation, whereby several episodes of fluid migration occurred. Ore movement and deposition occurred first, followed by oil migration.

Because of age and timing constraints (i.e. mineralizing events were early Carboniferous onwards), the migration of mineralizing fluids must have been largely controlled by the regional fault system. The association of bitumen samples with the mineralizing fluids appear to be the result of their utilization of the same regional fault system for movement (migration).

This study found no hydrocarbon-bearing fluid inclusions in any of the ore fluids. This suggests that hydrocarbons were not coeval with the main mineralization event but were seemingly transported within lower temperature fluids. Bitumen cracking post-

dates calcite/quartz nucleation. Bitumen samples were subjected to temperatures of less than 120 °C (the maximum temperature for the oil window), confirming that bitumen veins formed during decreasing temperatures. Catagenesis of organic matter-bearing sediments was probably the result of meteoric water (low salinity) flowing downward through the strata, mixing and then being focussed along fault planes in the basin.

An important aspect concerning the origin of metal enrichment, is whether the metals were transported with the migrating hydrocarbons, absorbed by hydrocarbon in situ, or merely utilized the same migration pathways. The abundance of metallic minerals implies the migration of large quantities of fluid in order to transport the ions.

A genetic model for the Deer Lake Basin, must involve both hydrocarbons and ore deposits within differing compositional blocks on the edges of the basin and within the basin. While deposition was not coeval between the hydrocarbons and ore deposits, each process likely utilized the same regional fault system and required similar factors; such as source input, migration, and maturation, which control hydrocarbon and ore deposition.

Of the four factors mentioned above, migration is one of the most important in this basin. It appears that there were several phases of fluid migration through the basin. The first was a high-temperature, low-salinity fluid probably carrying metals such as Cu. It is possible that these high-temperature fluids paved the way for other, slightly lower temperature but similar salinity fluids, and hydrocarbons to migrate through the basin, by improving the porosity in the basin. The importance of bitumen and coal in the

mineralizing process is not precisely known; however the author is suggesting that when interacting with metal-carrying aqueous solutions, the bitumen/coal samples may have played the role of a reducing substrate for precipitating metals. Most of the bitumen and coal samples are located on or adjacent to faults in the basin, which are the pathways for migrating fluids. In this case, organic material present (which later became bitumen/coal) may have provided a reducing environment for concentrating metals, when it came into contact with the metal-carrying aqueous solutions. This liquidified organic material, which eventually produced bitumen, was carried by the latest low temperature, low salinity fluid movement, migrating through the porous - permeable pathways provided by the faults in the basin, to its final depositional location.

The fluid-inclusion data define a linear trend in which the fluid- inclusion temperatures decrease north to south in the basin. Quartz and calcite, from the northern part of the basin, contain inclusions that formed under high temperatures and low salinities, while in the southern part of the basin inclusions in quartz and calcite display low temperatures and salinities. Fluid inclusions from the Birchy Ridge copper showing in the northern part of the basin, has the highest homogenization temperatures. Copper is usually transported at higher temperatures than other metals, thus suggesting high temperatures of formation.

The occurrence of bitumen at several different stratigraphic levels and structural situations indicate that the migration paths were complex. Langdon (1994) suggests that since bitumen and coal are found in several localities in the basin, there has been

significant and widespread episodes of maturation of source rocks and generation of liquid petroleum in or beneath the Deer Lake Basin.

Carbon isotope data for bitumen and coal samples indicate a terrestrial source for hydrocarbons with either organic-bearing units or oil shales being the probable source for hydrocarbons in the basin. H/C ratios for samples in the basin, correlate with type 3 kerogens; thus matching the catagenesis stage of maturation, which is the 'oil window' for hydrocarbons. H/C ratios larger than 0.8 have liquid generating ability. The H/C ratio analysis of samples in the Deer Lake Basin indicate that hydrocarbons in the basin have liquid generating ability and will probably be in the form of oil, while some hydrocarbons in the Howley Formation will be degraded oil or in the form of gas.

Source related metals in sedimentary organic matter are either: 1) present in contributing organisms; 2) stripped from the aqueous depositional medium and adsorbed onto non-living organic matter; or 3) contributed from circulating groundwater coming in contact with the source or reservoir rock (Parnell, 1994). These metals can then be re-distributed from organic matter to inorganic ores.

Models have been put forward to try to explain the origin of some metal occurrences in the basin. A model for the lead occurrences in the Deer Lake Basin would involve late diagenetic fluids circulating in porous clastic sediments, leaching loosely bound metals and carrying them to sites where chemical conditions are favorable for deposition. The lead isotope compositions of the Deer Lake Basin galena separates (from the Turners's Ridge MVT galena deposit, Side Pond, and the Gales Brook galena

showing) suggest that lead was leached from erosional clastic material and/or silicic volcanic and plutonic rocks (Humber Zone) with lesser inputs from the Pre-Taconian sediments and ophiolitic rock (Dunnage Zone).

Pb-Pb model ages for the Carboniferous Deer Lake Basin, range from 338 - 378 Ma. The Sop's Arm, Baie Verte Peninsula and the Deer Lake Basin galena separates seem to have a common growth between the orogene and the mantle, but plot along different isochrons,; with the Mic Mac Lake Group being the oldest, followed by the Deer Lake Basin and ophiolitic samples, and with the Silurian felsic volcanic hosted galena separates being the youngest. Geologically these 'ages' make no sense, i.e. Sop's Arm and Baie Verte Peninsula galena separates should be of the same geologic age, post Silurian-Devonian. Thus it must reflect a mixing line in which the primitive end-member is reflected in sediments from the Dunnage Zone (Mic Mac Lake Group etc.), while the felsic volcanics of Sop's Arm are the radiogenic end-member. The Dunnage Zone derived galena separates are more primitive than those in the Humber Zone, with the Deer Lake Basin galena separates being a mixture of the two. Summarizing the isotopic composition of lead in galenas from the these areas define a linear trend, interpreted as a mixing line; a more radiogenic source(s) is probably located within the clastic sedimentary pile and contributed metals to the fluids during their migration to the deposition sites while the less radiogenic source(s) presumably sampled the older mafic volcanic rocks.

Possible sources of lead for the Deer Lake Basin are: 1) derived from clastics within the basin; or 2) derived from adjacent plutonic rocks and/or mafic volcanics. The lead geochemistry anomaly map (Map 20) of the Deer Lake Basin shows lead anomalies coincident with faults in the basin; suggesting that fluids migrating through the basin via the faults could have incorporated lead from the differing compositional blocks.

Based on the Newfoundland Department of Mines and Energy regional map of Newfoundland, mafic volcanics or a mafic phase of a pluton are mapped adjacent to the western edge of the Deer Lake Basin while granites are mapped on the eastern edge of the Basin. Due to the negative magnetic anomalies correlating with smaller positive to slightly negative gravity anomalies on the east compared with positive gravity and magnetic anomalies on the west, both gravity and magnetic highs (Maps 2, 3, and 4) suggest that the mafics continue beneath the surficial cover on the west while the eastern edge of the study area reflects a granitic influence.

6.2-Conclusions and Recommendations

There are high risks associated with exploring frontier basins. Careful evaluation of all available geological, geophysical, and geochemical data is essential in targeting the most promising areas of a prospective basin. Since the beginning of the century, the discovery i.e. of oil shales and coal, natural gas and uranium associated with solid hydrocarbons, have sparked interest in the Deer Lake Basin. Although several drilling programmes in the past have encountered shallow gas, oil staining and bitumen, except

for a brief period of coal mining there has never been any production from the basin. Exciting new seismic data have shown that the basin is now deeper than originally interpreted. Therefore there is potential for new exploration targets.

Geophysical studies (seismic, gravity and magnetics) have shown that the Deer Lake Group is thick enough for hydrocarbon generation to have occurred. Since the Deer Lake Basin is a fault bounded basin, faults could obviously have served as feeders for hydrothermal fluids. Based on the number of occurrences, their potential inter-relationships and probable fault control, the basin should be looked upon favorably for occurrences of both mineral and hydrocarbon prospects. Occurrences of target minerals even in trace amounts are potentially important, as they may be indicative of effective ore-forming processes. These trace minerals may be indicative of fluid flow paths or dilution due to surrounding geology, and a major deposit could potentially be nearby. The lead and copper mineralization is believed to be fault controlled in the carbonates both inside and outside the basin. Therefore a more detailed evaluation of the fault zones (especially in conjunction with the carbonates) might result in discovering new economically exploitable reserves of base metals.

This study used potential field, geological, and geochemical data to examine the structural controls on the type(s) and nature(s) of hydrothermal fluids that coursed through the basin. Potential economic mineral and hydrocarbon occurrences have been noted throughout the basin, and the migration of both hydrocarbons and hydrothermal solutions presumably involved fluid flow through similar porous-permeable pathways.

The potential also exists that the same migration pathways may have been used by both fluid types. If the two fluids co-migrate, then the organic matter could affect metal activity in the fluids either by reduction or by formation of metal-organic complexes.

Fluid inclusion results suggest that co-migration did not occur in most of the basin since hydrocarbon inclusions were not found in any of the fluid inclusion sections. However this does not prove that co-migration did not occur in other parts of the basin. Fluids migrating through the basin were hot, sodium poor brines (< 14 wt. % NaCl eq.) (undersaturated with respect to NaCl). It appears that the hydrocarbon migration occurred later than initial hydrothermal fluid movement. The presence of organic matter in the basin may have acted as a reductant for many of the mineral occurrences. Since the Deer Lake Basin is a fault bounded basin, as seen by the potential field maps, faults could obviously have served as feeders for hydrothermal fluids.

Based on the potential field, geology and geochemical data the basin was subdivided into eight sections. The combined potential field and geochemical data show that some forms of mineralization and hydrocarbons in the basin occur near residual gravity and magnetic highs, while other forms are correlated with high magnetic gradients. The trends suggest the association of mineralization and hydrocarbon deposits with the underlying basement topography and the faults and fractures that formed structural conduits along which the mineralized fluids migrated. Formation of mineral deposits are a secondary feature related to structural and stratigraphic features and are

controlled by major basement faults. The faults may develop as or into wrench faults or major deep thrusts.

To determine the most probable mineralization scenarios in the Deer Lake Basin, further studies should be aimed at discovering the relative importance of factors determining metal deposition, namely sediments, fluids and interaction between the two, with respect to geographic and stratigraphic location, and timing of mineralization. A complete structural analysis, to deduce timing of fault structures and fault movement in the basin, is also warranted. While the author suggests that hydrocarbons and hydrothermal fluids did not co-migrate in the basin, the specific role of organic matter in the mineralization and hydrocarbon process also merits further study. Due to the lack of outcrop in the basin, drilling and seismic programs are suggested, to further understand the complexity of the basin, in terms of its structure and economic prospects.

REFERENCES:

Adams, K., 1981. Birchy Lake Prospect-Newfoundland Reid Lot 45. Department Of Mines And Energy Report 12H/7(697).

Ahmed, K. F., 1983. The Processing And Interpretation Of Deer Lake Seismic Data. M.Sc Thesis. M.U.N, St. John's Nfld.

Baird, D. M., 1950. Oil Shales Of The Deer Lake Region. Geological Survey Of Newfoundland 12H/3(45). 23p.(Unpublished Report).

Barley, M. E., And Groves, D. I., 1992. Supercontinent Cycles And The Distribution Of Metal Deposits Through Time. Geology Vol. 20. pp. 291-294.

Biddle, K. T., And Christie-Blick, N., 1985. Strike Slip Deformation, Basin Formation And Sedimentation. Society Of Economic Paleontologists And mineralogists Special Publication No.37.

Brannon, J. C., Cole, S. C., Podosek, F. A., Ragan, V. M., Coverney Jr., R. M., Wallace, M. W., Bradley, A. J., 1996. Th-Pb And U-Pb Dating Of Ore-Stage Calcite And Paleozoic Fluid Flow. Science Vol. 271.

Brown, P. E., 1989. Flincor: A Microcomputer Program For The Reduction And Investigation Of Fluid Inclusion Data. American Mineralogist Vol 74 pp. 1390-1393.

Cathelineau, M., Oliver, R., Nieva, D., And Garfias, A., 1985. Mineralogy And Distribution Of Hydrothermal Mineral Zones In Los Azufres (Mexico) Geothermal Field. Geothermics Vol. 14. No. 1 pp. 49-57.

Christensen, J.N., Halliday, A.N., Vearncombe, J.R., And Kesler, S.E., 1995. Testing Models Of Large-Scale Crustal Fluid Flow Using Direct Dating Of Sulphides: Rb-Sr Evidence For Early Dewatering And Formation Of Mississippi Valley-Type Deposits, Canning Basin, Australia. Economic Geology Vol.90 pp.877-884.

Clendenin, C.W., 1993. Small Scale Positive Flower Structures. An Ore Control Identified In The Viburnum Trend, Southeast Missouri, USA. Mineralium Deposita. Vol 28. pp.22-27.

Dalley, D., 1981. The Relationship Between Magnetic Minerals And Uranium Mineralization In The Deer Lake Basin. B.Sc Honours Thesis, M.U.N. St. John's Nfld.

Davenport, P. H., Nolan, L. W., Butler, A. J., Wagenbauer, H. A., And Honarvar, P., 1996. Digital Geochemical Atlas Of Newfoundland. Newfoundland Department Of Mines And Energy, Geological Survey Digital Atlas 95-1, Version 1.1.

Disnar, J. R., 1996. A Comparison Of Mineralization Histories For Two MVT Deposits, Treves And Les Malines (Causses Basin, France), Based On The Geochemistry Of Associated Organic Matter. Ore Geology Reviews Vol 11 pp.133-156.

Dix, G. R., And Edwards, C., 1996. Carbonate-Hosted, Shallow-Submarine And Burial Hydrothermal Mineralization In The Upper Mississippian Big Cove Formation, Port Au Port Peninsula, Western Newfoundland. Economic Geology Vol.91 pp.180-203.

Doe, B. R., And Zartman, R. E., 1979. Plumbotectonics. In: Geochemistry Of Hydrothermal Ore Deposits.

Dunne, K. P. E., 1992. Application Of Fluid Inclusion Petrography To The Mineral Industry. Mineral Deposits Research Unit. Department Of Geological Sciences, U. B.C. MDRU Technical Report MT2.

Eidel, J. J., 1990. Basin Analysis For The Mineral Industry. Society Of Economic Geology Short Course. Chapter 1, 15p.

Ewbank, G., Manning, D. A. C., And Abbott, G. D., 1995. The Relationship Between Bitumens And mineralization In The South Pennine Orefield, Central England. Published Paper pp 751-765.

Filby, R. H., 1994. Origin And Nature Of Trace Element Species In Crude Oils, Bitumens And Kerogens: Implications For Correlation And Other Geochemical Studies. Geofluids: Origin, Migration And Evolution Of Fluids In Sedimentary Basins. Geological Society Special Publication No. 78 pp. 203-219.

Fleming, J. M., 1970. Petroleum Exploration In Newfoundland And Labrador. Mineral Resources Division, Dept. Of Mines And Energy, Nfld. Mineral Resources Report No.3.

Gall, Q., And Hyde, R. S., 1989. Analcime In Lake And Lake-Margin Sediments Of The Carboniferous Rocky Brook Formation, Western Newfoundland, Canada. Sedimentology V.36 pp. 875-887.

Gall, Q., 1984. Petrography And Diagenesis Of The Carboniferous Deer Lake Group And Howley Formation, Deer Lake Subbasin, Western Newfoundland. M.Sc Thesis, Memorial University Of Newfoundland 242p.

Galley, A. G., 1995. Target Vectoring Using Lithogeochemistry: Applications To The Exploration Of Volcanic Hosted Massive Sulphide Deposits. Canadian Institute Of Mining Bulletin.

Geological Society Of Canada, 1967 Airbourne Magnetic Survey.

Goodarzi, F., Gentzis, T., Mossman, D., And Nagy, B., 1993. Petrography And Genesis Of Organic Matter In The Paleoproterozoic Uraniferous Conglomerates Of The Elliot Lake Region, Ontario. Energy Sources Vol.15 pp.339-357.

Goodarzi, F., Fowler, M.G., Bustin, M., And Mckirdy, D. M., 1992. Thermal Maturity Of Early Paleozoic Sediments As Determined By The Optical Properties Of Marine-Derived Organic Matter - A Review. In: Early Organic Evolution: Implications For Mineral And Energy Resources. Pp.279-295.

Government Of Newfoundland And Labrador, 1989. Hydrocarbon Potential Of The Western Newfoundland, Onshore Area. Dept Of Energy.

Grossman, I., 1946. Preliminary Report On The Geology Of The Deer Lake Area: Geological Survey Of Newfoundland 12H/3(35)(Unpublished Report).

Hamblin, A. P., Fowler, M. G., Utting, J., Langdon, G. S., And Hawkins, D. (In Prep). Stratigraphy, Palynology And Source Rock Potential Of Lacustrine Deposits Of The Lower Carboniferous (Visean) Rocky Brook Formation, Deer Lake Sub-Basin, Newfoundland.

Hawkes, H. E., And Webb, J. S., 1962. Geochemistry In Mineral Exploration. Harper Row And Publishers Inc.

Hayes, A. O., 1949. Coal Possibilities Of Newfoundland. Information Circular No.6. Newfoundland Geological Survey.

Ho, E. S., And Mauk, J. L., 1996. Relationship Between Organic Matter And Copper Mineralization In The Proterozoic Nonesuch Formation, Northern Michigan. Ore Geology Reviews Vol.11 pp.71-88.

Hosterman, J. W., Meyer, R. F., Palmer, C. A., Doughten, M. W., And Anders, D. E., 1989. Chemistry And Mineralogy Of Natural Bitumens And Heavy Oils And Their Reservoir Rocks From The United States, Canada, Trinidad And Tobago, And Venezuela. Published Report pp.1-19.

Howse A. F., 1992. Barite Resources Of Newfoundland. Mineral Resource Report 6. Geological Survey Branch Department Of Mines And Energy.

Howse, A., And Fleischmann, J., 1982. Coal Assessment In The Deer Lake Carboniferous Basin. Report 82-1.

Hunt, J. M., 1996 Petroleum Goechemistry And Geology. Second Edition. W.H. Freeman And Company Ltd.

Hutchinson, R. W., 1992. Mineral Deposits And Metallogeny: Indicators Of Earth's Evolution. In: Early Organic Evolution: Implications For Mineral And Energy Resources. Springer-Verlag Publications.

Hutchinson, R. W., 1984. Archean Metallogeny: A Synthesis And Review. Journal Of Geodynamics. Vol. 1 pp.339-358.

Hyde, R. S., Langdon, G. S., Tuach, J., And Wilton, D. H. C., 1994. The Last Frontier - A Field Conference To The Deer Lake Basin, Nfld. Geological Summary And Fieldtrip Guidebook. CERR Report #1.

Hyde, R. S., 1989. The North Brook Formation: A temporal Bridge Spanning Contrasting Tectonic Regimes In The Deer Lake Basin, Western Newfoundland. Atlantic Geology 25 15-22.

Hyde, R. S., Miller, H. G., Hiscott, R. N., And Wright, J. A., 1988. Basin Architecture And Thermal Maturation In The Strike-Slip Deer Lake Basin, Carboniferous Of Nfld. Basin Research V.1 pp.85-105.

Hyde, R. S.,1984 Mineral Deposits Of Newfoundland A 1984 Prospective. Department Of Mines And Energy Report.

Hyde, R. S., 1984b. Oil Shales Near Deer Lake, Newfoundland. Geological Survey Of Canada, Open File 1114. 10p.

Hyde, R. S., And Ware, M. J., 1981. (Unpublished Report) Notes Of The Geology Of Portions Deer Lake (12H/3) and Rainy Lake (12A/4) Map Areas.

Hyde, R. S., And Ware, M. J., 1981. (Unpublished Report) Geology Of Carboniferous Strata In The Deer Lake (12H/3) and Rainy Lake (12A/4) Map Areas, Newfoundland. pp.17-31.

Hyde, R. S., 1980. Marginal Notes For Map 80-11. (Unpublished Report).

Hyde, R. S., 1979 Geology Of The Carboniferous Strata In Portions Of The Deer Lake Basin, Western Nfld. Mineral Development Division, Dept. Of Mines And Energy. Report 79-6.

Irving, E., And Strong, D. F., 1984. Paleomagnetism Of The Early Carboniferous Deer Lake Group, Western Nfld: No Evidence For Mid-Carboniferous Displacement Of 'Acadia'. Earth And Planetary Science Letters V.69 pp.379-390.

Kalkeuth, W., and Macauley, G., 1989. Organic Petrology And Rock-Eval Studies On Oil Shales From The Lower Carboniferous Rocky Brook Formation, Western Newfoundland. Bulletin Of Canadian Petroleum Geology Vol.37 No.1 p. 31-42.

Katz, B. J., 1990 Lacustrine Basin Exploration Case Studies And Modern Analogs. American Association Of Petroleum Geologists Memoir 50

Kesler, S. E., And Van Der Pluijm, B. A., 1990. Timing Of MVT mineralization: Relation To Appalachian Orogenic Events. Geology vol. 18. Pp.1115-1118.

Kettler, R. M., 1995. Incipient Bitumen Generation In Miocene Siliceous Sedimentary Rocks From The Japan Sea. Elsevier Science ltd. pp.699-708.

Kilfoil, G. J., And Bruce, P. A., 1989. Gridded Aeromagnetic Data 200m Grid Cell (Ver.1.0), Newfoundland by 1:250,000 NTS Map Area. Geosoft Grids And Histogram Files. Newfoundland Department Of Mines And Energy Open File 2063.

Klemmie, D. H., 19??. Types Of Petroliferous Basins. In: Petroleum Geology In China.

Krauskopf, K. B., 1979. Introduction To Geochemistry. International Series In The Earth And Planetary Sciences 2nd Edition.

Landais, P., 1996. Organic Geochemistry Of Sedimentary Uranium Ore Deposits. Ore Geology Reviews Vol.11 pp.33-51.

Landell-Mills, T., 1954. Report On The Oxley Oil And Oil Shale Concession In The Deer Lake District Newfoundland (Unpublished Report).

Landell-Mills, T., 1921. Notes On The Districts Of Newfoundland Containing Indications Of Subterranean Oil Pools:(Unpublished Report).G21001 Brinex (Nfld (716)

Langdon, G. S., 1996. Tectonics And Basin Deformation In The Cabot Strait Area And Implications For The Late Paleozoic Development Of The Appalachians In The St. Lawrence Promontory. Ph.D Thesis, M.U.N, St. John's Nfld.

Langdon, G. S., And Hall, J., 1994. Devonian-Carboniferous Tectonics And Basin Deformation In The Cabot Strait Area, Eastern Canada. American Association Of Petroleum Geologists. Vol 78. No.11 pp.1748-1774.

Langdon, G. S., 1993. A Study Of Petroleum Potential And Regional Petroleum Prospsectivity Of The Deer Lake Group And Howley Formation On Permits 93-103 And 93-104, Deer Lake Basin. CERR Report, Dept Of Earth Sciences, Memorial University Of Newfoundland.

Macauley, G., 1987. Geochemical Investigation Of Carboniferous Oil Shales Along Rocky Brook; Western Newfoundland. GSC Open File Report OFR-1438 (Nfld 12H/3-943) 12p.

Macauley, G., Snowdon, L. R., And Ball, F. D., 1985. Geochemistry And Geological Factors Governing Exploitation Of Selected Canadian Oil Shale Deposits. GSC Paper 85-13.

Macauley, G., 1981. Geology Of Oil Shales Of Canada. GSC Open File Report OFR-754 (Nfld 1240).

Magoon, L. B., And Dow, W. G., 1994. The Petroleum System From Source To Trap. American Association Of Petroleum Geologists Memoir 60

Mancuso, J. J., Kneller, W. A., And Quick J. C., 1989. Precambrian Vein Pyrobitumen: Evidence For Petroleum Generation And Migration 2 Ga Ago. Precambrian Research Vol 44 pp.137-146.

Mason, J. F., 1980. Petroleum Geology In China. Pennwell Books Ltd.

Mastalerz, M., Thompson, M. L., Stankiewicz, A., Bustin, R. M., And Sinclair. A. J., 1994. A Geochemical Study Of Solid Bitumen In An Eocene Epithermal Deposit: Owen Lake, British Columbia, Canada. Chemical Geology v.115 pp 249-262.

Menzie, W. D., And Mosier, D. L., 1985. Grade, Tonnage And Lithologic Data For Sediment-Hosted Submarine Exhalative Zn-Pb And Sandstone Hosted Pb-Zn Deposits. United States Department Of The Interior Geologic Survey. Open File Report 85-206.

Miller, H. G., And Wright, J. A., 1984. Gravity And Magnetic Interpretation Of The Deer Lake Basin, Nfld. Canadian Journal Of Earth Science V.21 pp.10-18.

Mossman, D. J., And Thompson-Rizer, C. L., 1993. Toward A Working Nomenclature And Classification Of Organic Matter In Precambrian (And Phanerozoic) Sedimentary Rocks. Precambrian Research Vol 61. pp.171-179.

Mossman, D. J., Goodarzi, F., And Gentziz, T., 1993. Characterization Of Insoluble Organic Matter From The Lower Proterozoic Huronian Supergroup, Elliot Lake Ontario. Precambrian Research Vol 61 pp.279-293.

Nakai, S., Halliday, A. N., Kesler, S. E., Jones, H. D., Kyle, J. R., And Lane, T. E., 1993. Rb-Sr Dating Of Sphalerites From Mississippi Valley-Type (MVT) Ore Deposits. Geochemica Et Cosmochimica Acta Vol.57 pp.417-427.

Nesbitt, B. E., 1995. Crustal Paleo-Hydrogeological Mapping As A tool In Exploration For Mineral Deposits. Journal Of Geochemical Exploration Vol.54 pp.153-165.

Nesbitt, B. E., And Muehlenbachs, K., 1992. Geochemical Studies Of Syntectonic Fluids Along The Southern Cordilleran Lithoprobe Transect. Southern Cordillera Transect Report No. 24.

Nesbitt, B. E., And Muehlenbachs, K., 1989. Origins and movements Of Syntectonic Fluids, Eastern Half Of The Southern Cordilleran Lithoprobe Transect: Initial Results. In: Transect Workshop Southern Canadian Cordillera.

Pagel, M., And Poty, B., 1984. The Evolution Of Composition, Temperature, And Pressure Of Sedimentary Fluids Over Time. A Fluid Inclusion Reconstruction. Thermal Phenomena In Sedimentary Basins. No. 64 pp.71-87.

Pagel, M., Walgenwitz, F., And Dubessy, J., 19??. Fluid Inclusions In Oil And Gas bearing Sedimentary Formations. From Thermal Modelling In "Sedimentary Basins" vol. 99 pp.565-583.

Parnell, J., 1994. Hydrocarbons And Other Fluids: Paragenesis, Interactions And Exploration potential Inferred From Petrographic Studies. Geological Society Special Publication No 78 pp.275-291.

Parnell, J., Kucha, H., And Landais, P., 1993. Bitumens In Ore Deposits. Society For Geology Applied To Mineral Deposits. Special Publication No.9.

Parnell, J., And Monson, B.. 1990. Sandstone-Hosted Thorium-Bitumen Mineralization In The Northwest Irish Basin. Sedimentology Vol 37. pp.1011-1022.

Parnell, J., 1990. Metal Enrichments In Organic Materials As A Guide To Ore Mineralization. Sediment Hosted Mineral Deposits Special Publication No.11 pp.183-192.

Parnell, J., 1986. Hydrocarbons And Metalliferous Mineralization In A Lacustrine Rift Basin: The Hartford-Deerfield Basin, Connecticut Valley. Neues Jahrbuch Mineralogical Abh. Vol.154 No.1 pp.93-110.

Plumlee, G. S., Goldhaber, M. B., And Rowan, E. L.,1995. The Potential Role Of Magmatic Gases In The Genesis Of Illinois-Kentucky Fluorspar Deposits: Implications From Chemical Reaction Path Modeling. Bulletin Of The Society Of Economic Geologists. Vol.90. No.5. pp.999-1011.

Plumlee, G. S., Leach, D. L., Hofstra, A. H., Landis, G. P., Rowan, E. L., And Viets, J. G., 1994. Chemical Reaction Path Modelling Of Ore Deposition In Mississippi Valley type Pb-Zn Deposits Of The Ozark Region Us Midcontinent. Economic Geology Vol 89. pp.1361-1383.

Rasmussen, B., And Glover, J. E., 1994. Diagenesis Of Low-Mobility Elements (TI,REES,TH) And Solid Bitumen Enveiopes In Permian Kennedy Group Sandstone, Western Australia. Journal Of Sedimentary Research Vol.A64 No.3 pp.572-583.

Roedder, E., 1984. Fluid Inclusions; Mineralogical Society Of America, Reviews In Mineralogy V.12 644pp.

Rye, R. O., And Ohmoto, H., 1980. Sulfur And Carbon Isotopes And Ore Genesis: A Review. Economic Geology pp.826-842.

Sangster, D. F., And Vaillancourt, P. D., 1990. Paleo-Geomorphology In The Exploration For Undiscovered Sandstone-Lead Deposits, Salmon River Basin, Nova Scotia. Canadian Institute Of Mining Bulletin. pp. 62-68.

Saunders, C. M., Strong, D. F., And Sangster, D. F., 1992. Carbonate Hosted Lead-Zinc Deposits Of Western Newfoundland. Geological Survey Of Canada Bulletin 419.

Saunders, C. M., And Strong, D. F., 1986. Assessment Of Lead-Zinc Deposits Of The Western Newfoundland Carbonate Platform. In Current Research, Part A Geological Survey Of Canada, Paper 86-1A pp.229-237.

Spears, D. A., 1994. Geochemistry And Mineralogy Of Some British Coals. Mineralogical Magazine, Vol 58A. pp.870-871.

Strong, D. F., 1987. Metallogeny. Encyclopedia Of Physical Sciences And Technology V.8.2

Swinden, H. S., Lane, T. E., And Thorpe, R. I., 1988. Lead-Isotope Compositions Of Galena In Carbonate-Hosted Deposits Of Western Newfoundland: Evidence For Diverse Lead Sources. Canadian Journal Of Earth Sciences Vol 25. pp.593-602.

Telford, W. M., Geldart, L. P., And Sheriff, R. E., 1990. Applied Geophysics 2nd Edition.
Cambridge University Press.

Thompson, C. L., 1993. Optical Description Of Amorphous Carageen In Both Thin Sections And Isolated Carageen Preparations Of Precambrian To Eocene Shale Samples. Precambrian Research Vol 61. Pp.181-190.

Thomson, M. L., Mastalerz, M., And Bustin, R. M., 1992. Fluid Source And Thermal History Of An Epithermal Vein Deposit, Owen Lake, Central British Columbia: Evidence From Bitumen And Fluid Inclusions. Springer-Verlag. pp.219-225.

Tuach, J., 1987. Stratigraphy Structure And Mineralization, Western White Bay. Road Log And Field Guide. GAC Newfoundland Branch.

Tuach, J., 1987. Mineralized Environments, Metallogenesis And The Doucers Valley Fault Complex, Western White Bay: A Philosophy For Gold Exploration In Newfoundland. Current Research Newfoundland Dept Of Mines And Energy Mineral Development Division Report 87-1. pp 129-144.

Waples, D. W., 1980. Time And Temperature In Petroleum Formation: Application Of Lopatin's Method To Petroleum Exploration. The American Association Of Petroleum Geologists Bulletin vol.64. pp.916-926.

Weaver, D. F.1967. A geological Interpretation Of The Bouguer Anomaly Field Of Newfoundland. Publication Of The Dominion Observatory, Ottawa, Ontario., Vol.XXXV. No.5 pp.223-251.

Werner, H. J., 1956. Oil And Gas Investigations In Western Newfoundland (Unpublished Report).

Werner, H. J., 1956. The Geology Of Humber Valley, Newfoundland. Summary And Final Report To The Newkirk Mining Corporation, Toronto, Ontario. (Unpublished Report).

Williams, H., 1979. Appalachian Orogeny In Canada. Canadian Journal Of Earth Science vol.16 pp.792-807.

Williams, R. M., 1958. Claybar Uranium And Oil Ltd. Humber Valley Area, Western Newfoundland. (Nfld 311)(Unpublished Report).

Wilton, D. H. C., 1996. Paleoproterozoic, ~1.88-2.0 Ga, Organic Matter From the Mugford/Kaumajet Mountain Group, Northern Labrador. Precambrian Research Vol 77 pp.131-141.

Wright, J. A., Hoffe, B. H., And Quinlan, G. M. (in Prep). The Deer Lake Basin Newfoundland: Structural Constraints From New Seismic Data. CERR Report, Dept Of Earth Sciences, M.U.N, Newfoundland.

Appendix A1 - Analytical Procedures:

A.1.1 - ICP-MS Procedure For Bitumen And Coal

A series of filtration and acidification processes were first undertaken to prepare the samples for the ICP-MS. The samples were crushed, placed in the oven at 500 °C for ashing and loss on ignition. 2.0 grams were weighed out in Teflon screw cap jars, leached with 8.0 nitric acid and left to evaporate on a hot plate. The samples were then re-dissolved in nitric acid and filtered. This solution was the coal leach. The coal residue was reweighed, and then 8.0 normal nitric acid and hydrofluoric acid was added, and left to evaporate again. The samples were then analyzed by the Perkin-Elmer SCIEX ELAN model 250 ICP-MS as a waters package to determine the concentration of 39 elements.

The ICP-MS system uses an autosampler to supply the system with standards, samples and wash acids to calculate the concentrations. The data from the ICP-MS was then reduced using in-house computer software programs.

A.1.2 - LAM-ICP-MS Procedure For Bitumen And Coal

The LAM-ICP-MS method was also a trial experiment for the coal and bitumen samples, again with encouraging results. Figure 14 presents the setup of the LAM-ICP-MS system. First the samples were cut and mounted in epoxy rings to be ablated. The samples were then polished using aluminum oxide lapping film (15 - 0.3 microns). Once polished the samples are then put in a beaker of nanopure water and placed in a sonic bath for 5 minutes to remove any excess particles from the polishing procedure. The samples

were then ablated by the laser at a firing power varying between 0.1 - 0.3 mj / pulse. The ablated particles are removed by argon gas which is flowing through the system, and concentrations are analyzed by the mass spectrometer.

An in-house computer software program calculated the data by comparing each sample to a bitumen standard (1632b- Bituminous Coal) and an internal standard for each sample based upon the CHN analysis completed at the Ocean Sciences Center, Logy Bay by Elizabeth Hatfield. The bituminous coal standard used for this LAM ICP-MS technique is the National institute of Standards and Technology, Standard Reference material 1632b Bituminous Coal. This reference material was intended primarily for use in the calibration of apparatus and the evaluation of techniques employed in the analysis of coal and similar materials. The standard was made by pressing 5 mg of dry mass into a pellet and then mounting the pellet in epoxy.

A.1.3 X-Ray Fluorescence

Whole rock analysis was carried out at the XRF lab at Memorial University of Newfoundland using a fisons/ARL model 8420+ sequential wavelength dispersive x-ray spectrometer on pressed powder pellets.

Samples were first crushed and 5.0 g of rock powder and 0.7 g of BRP-5933 Bakelite™ phenolic resin were placed into a 100 ml glass jar. Two stainless steel ball bearings (~ 0.5 inch in diameter) were added to the mixture. This mixture was thoroughly mixed on a roller mixer for approximately 10 minutes, and then added to a

pellet press (~ 29 mm diameter). The pellets were then placed in an oven for 15 minutes at 200 °C and then labeled.

Elemental analysis was completed as a traces package. Elements included TiO_2, Fe_2O_3, CaO, K_2O, MnO, Sc, V, Cr, Ni, Cu, Zn, Ga, As, Rb, Sr, Y, Zr, Nb, Ba, Ce, Pb, Th, and U. SiO_2, Al_2O_3, MgO, P_2O_5, Na_2O, S, and Cl were analyzed on a semi-quantitative basis. Data was collected by a computer attached to the XRF and placed in a computer software program for data reduction.

A.1.4 - CHN Analysis

The samples were first hand picked and crushed using a morter and pestle. Carbon isotope data were obtained from Memorial University's Marine Ocean Sciences Center on Marine Drive in Logy Bay. The samples were combusted in the CHN analyzer and analyzed using a mass spectrometer.

A.1.5 - Sulphur, Carbon, and Oxygen Isotopes

Sulphur, carbon and oxygen isotopes were analyzed by Memorial University of Newfoundland stable isotope group. All samples were hand picked, prepared and isotopes were separated under vacuum conditions. The isotopic values were then analyzed by a mass spectrometer.

Figure 14: LAM - ICP-MS System Setup

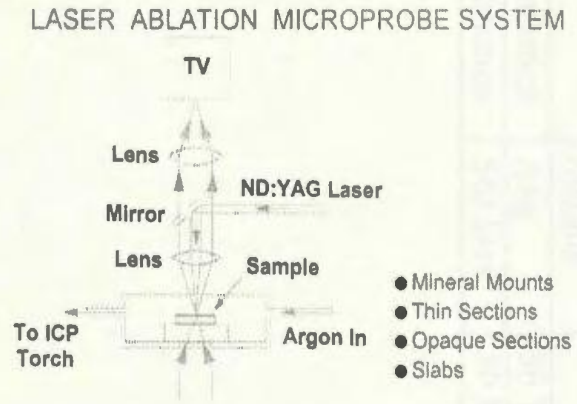

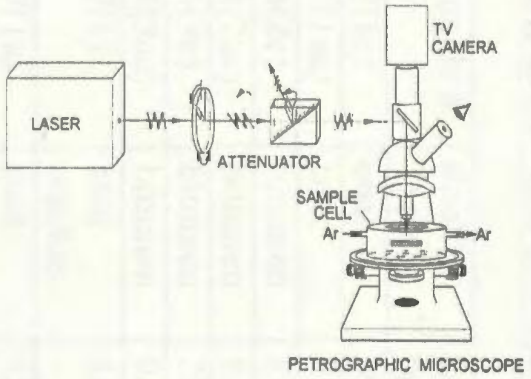

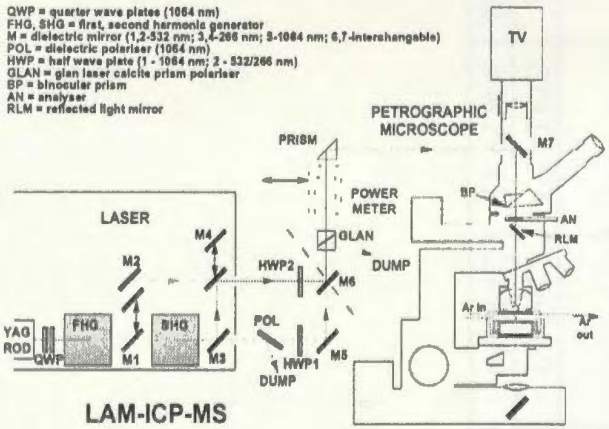

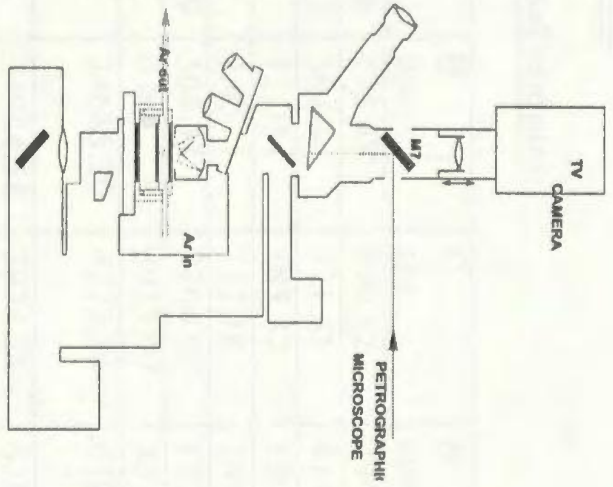

Appendix B: Tables Of Geochemical Data

Table B.1.1 - ICP-MS data for bitumen and coal samples

Sample #	Rock Type	Li 6 ppm	Li 7 ppm	Be ppm	B ppm	C cps	N cps
37(1c)	coal	69.80	58.43	10.88	178.48	490.12	3964.43
37(1ac)	coal	81.15	61.46	13.15	36.03	521.31	4192.86
24(2c)	bitumen	8.41	5.41	0.35	12.05	185.32	1507.08
24(2ac)	bitumen	6.15	4.00	0.22	7.45	152.18	1498.38
d3(3c)	bitumen	297.97	29.78	50.69	304.31	2264.02	17221.37
d3(3ac)	bitumen	0.00	13.96	1.82	0.00	3973.97	38757.55
37(1)	coal residue	12.94	6.13	3.44	34685.20	4273.86	6102.09
37(1a)	coal residue	15.28	4.93	2.94	34944.58	3974.24	6288.37
24(2)	bitumen residue	110.51	11.65	5.04	93750.52	8753.23	13853.82
24(2a)	bitumen residue	58.01	8.26	4.10	60944.35	6143.68	10052.67
d3(3)	bitumen residue	16.34	3.73	3.47	47478.48	5168.73	7723.81
d3(3a)	bitumen residue	0.00	2.66	4.23	57838.15	6861.60	10692.33
Statistics	Avg	56.31	17.53	8.36	27514.97	3563.52	10154.56
Statistics	Std Dev	80.84	20.24	13.28	30879.15	2758.70	9759.19

Table B.1.1 - ICP-MS data for bitumen and coal samples cont'd

Sample #	Rock Type	Mg ppm	Al ppm	Si ppm	P ppm	S ppm	Cl ppm
37(1c)	coal	1799.97	0.00	46.84	652.49	0.00	0.00
37(1ac)	coal	1815.94	0.00	21.43	623.28	0.00	0.00
24(2c)	bitumen	2134.34	5298.88	2.28	5761.78	3176.3	22.38
24(2ac)	bitumen	1628.23	3998.99	2.67	4389.49	2847.5	0.00
d3(3c)	bitumen	12695.03	53676.25	47.62	1190.70	0.00	2133.9
d3(3ac)	bitumen	14659.39	62106.73	29.41	1679.87	0.00	0.00
37(1)	coal residue	204.10	14800.69	52.91	82.26	0.00	0.00
37(1a)	coal residue	182.62	12723.69	48.78	92.5	0.00	0.00
24(2)	bitumen residue	334.34	10215.36	112.68	118.94	0.00	0.00
24(2a)	bitumen residue	235.14	6952.39	73.69	88.96	0.00	0.00
d3(3)	bitumen residue	869.83	0.00	143.17	40.97	0.00	0.00
d3(3a)	bitumen residue	622.18	0.00	135.13	47.53	0.00	0.00
Statistics	Avg	3098.43	14147.75	59.72	1230.73	501.99	179.7
Statistics	Std Dev	4795.73	20236.50	45.71	1811.64	1124.5	589.27

Table B.1.1 - ICP-MS data for bitumen and coal samples cont'd

Sample #	Rock Type	Ca 42 ppm	Ca 43 ppm	Ti ppm	V ppm	Cr 52 ppm	Cr 53 ppm
37(1c)	coal	1863.3	1460.8	532.6	85.53	38.08	39.67
37(1ac)	coal	1869.3	1259.8	638.7	91.39	42.89	43.39
24(2c)	bitumen	59446.4	59903.3	118.8	33.55	19.67	20.21
24(2ac)	bitumen	43082.4	44571.9	96.3	26.45	15.66	16.04
d3(3c)	bitumen	87124.2	81684.4	1367.3	66.67	60.15	129.25
d3(3ac)	bitumen	88361.9	94001.8	1937.4	69.26	50.87	59.17
37(1)	coal residue	0.00	1579.1	2008.4	12.64	8.61	8.52
37(1a)	coal residue	0.00	1462.8	2051.8	10.8	7.46	7.69
24(2)	bitumen residue	388.23	2845.8	1734.3	9.35	9.37	9.50
24(2a)	bitumen residue	290.7	1972.1	1099.3	6.37	6.30	6.25
d3(3)	bitumen residue	6852.77	8734.6	2634.6	16.3	13.90	13.95
d3(3a)	bitumen residue	5881.2	8394.13	1640.1	13.15	8.64	8.75
Statistics	Avg	24596.7	25655.9	1321.6	36.79	23.47	30.2
Statistics	Std Dev	33686.3	33356.8	788.9	30.7	18.3	34.1

Table B.1.1 - ICP-MS data for bitumen and coal samples cont'd

Sample #	Rock Type	Fe 54 ppm	Mn ppm	Fe 56 ppm	Fe 57 ppm	Co ppm	Ni ppm
37(1c)	coal	10259.9	164.8	0.00	10384.9	5.88	31.61
37(1ac)	coal	11073.8	172.1	0.00	11397.5	6.25	34.04
24(2c)	bitumen	7526.4	281.7	0.00	7956.2	3.68	19.22
24(2ac)	bitumen	6653.44	221.7	0.00	6695.9	2.56	18.79
d3(3c)	bitumen	41281.5	4079.8	0.00	40379.7	37.04	98.61
d3(3ac)	bitumen	41200.3	4002.9	34903	40810.8	27.68	72.65
37(1)	coal residue	1074.4	7.11	1064.3	1051.6	0.21	2.05
37(1a)	coal residue	921.9	6.21	895.7	917.9	0.16	2.20
24(2)	bitumen residue	1089.8	8.63	1071.6	1071.99	0.00	2.08
24(2a)	bitumen residue	1015.7	6.29	1002.7	1022	0.00	1.56
d3(3)	bitumen residue	2250.4	412.8	2205.0	2323.27	0.53	3.14
d3(3a)	bitumen residue	1643.9	41.9	1591.3	1717.17	0.41	3.49
Statistics	Avg	10499.3	783.8	3561.2	10477.4	7.03	24.12
Statistics	Std Dev	14199.8	1462.1	9476.2	13955.6	11.69	30.19

Table B.1.1 - ICP-MS data for bitumen and coal samples cont'd

Sample #	Rock Type	Cu ppm	Zn ppm	As ppm	Br ppm	Se ppm	Rb ppm
37(1c)	coal	81.54	73.05	32.11	0.00	0.00	19.2
37(1ac)	coal	97.92	92.29	33.02	0.00	0.00	20.41
24(2c)	bitumen	5.54	906.33	30.62	2.13	0.00	12.38
24(2ac)	bitumen	4.51	683.7	26.85	1.44	0.00	10.61
d3(3c)	bitumen	47.73	130.16	32.82	125.07	218.98	18.64
d3(3ac)	bitumen	47.20	108.77	0.00	0.00	0.00	19.18
37(1)	coal residue	8.39	6.54	6.34	0.00	0.00	11.64
37(1a)	coal residue	7.28	28.49	4.92	0.00	0.00	9.91
24(2)	bitumen residue	5.49	45.87	1.52	0.00	0.00	12.41
24(2a)	bitumen residue	3.33	21.74	1.28	0.00	0.00	8.31
d3(3)	bitumen residue	7.96	7.69	0.00	0.00	0.00	32.95
d3(3a)	bitumen residue	4.92	6.10	0.00	0.00	0.00	33.82
Statistics	Avg	26.82	175.89	14.12	10.72	18.25	17.45
Statistics	Std Dev	32.17	283.4	14.53	34.48	60.52	8.15

Table B.1.1 - ICP-MS data for bitumen and coal samples cont'd

Sample #	Rock Type	Sr ppm	Mo ppm	Ag ppm	Cd ppm	Sn ppm	Sb ppm
37(1c)	coal	75.83	2.86	0.57	0.26	2.75	0.39
37(1ac)	coal	72.69	2.71	0.59	0.28	2.98	0.39
24(2c)	bitumen	215.68	1.01	0.22	3.08	1.11	0.04
24(2ac)	bitumen	191.07	0.89	0.18	2.50	0.93	0.03
d3(3c)	bitumen	320.80	4.67	3.97	17.83	27.87	7.29
d3(3ac)	bitumen	302.65	0.00	0.25	0.00	5.7	0.00
37(1)	coal residue	5.78	2.66	1.98	0.00	23.81	26.52
37(1a)	coal residue	4.91	2.35	1.92	0.00	23.0	24.25
24(2)	bitumen residue	324.33	0.39	0.30	0.00	1.66	0.33
24(2a)	bitumen residue	270.76	0.36	0.24	0.00	1.04	0.26
d3(3)	bitumen residue	413.9	0.17	0.23	0.00	4.03	0.00
d3(3a)	bitumen residue	369.17	0.00	0.10	0.00	3.25	0.00
Statistics	Avg	213.97	1.51	0.88	2.00	8.18	4.96
Statistics	Std Dev	137.04	1.44	1.12	4.88	9.8	9.35

Table B.1.1 - ICP-MS data for bitumen and coal samples cont'd

Sample #	Rock Type	I ppm	Cs ppm	Ba ppm	La ppm	Ce ppm	Hg ppm
37(1c)	coal	0.00	2.39	274.99	129.34	298.8	0.00
37(1ac)	coal	0.00	2.39	256.39	125.88	290.4	0.00
24(2c)	bitumen	0.07	0.63	462.43	5.13	9.53	0.00
24(2ac)	bitumen	0.00	0.50	258.96	4.11	7.40	0.00
d3(3c)	bitumen	9.31	1.68	214.06	115.01	242.7	51.75
d3(3ac)	bitumen	0.08	0.49	214.73	104.09	226.0	0.00
37(1)	coal residue	0.00	0.59	58.92	2.02	4.63	0.00
37(1a)	coal residue	0.00	0.52	49.55	1.45	3.74	0.00
24(2)	bitumen residue	0.00	0.39	17004	2.13	2.70	0.00
24(2a)	bitumen residue	0.00	0.25	9231.9	1.26	1.82	0.00
d3(3)	bitumen residue	0.00	0.15	1371.3	10.76	30.96	0.00
d3(3a)	bitumen residue	0.00	0.49	1253.9	7.74	24.17	0.00
Statistics	Avg	0.7	0.87	2554.3	42.41	95.3	4.3
Statistics	Std Dev	2.29	0.77	5000.6	54.22	121.3	14.3

Table B.1.1 - ICP-MS data for bitumen and coal samples cont'd

Sample #	Rock Type	Tl ppm	Pb ppm	Bi ppm	U ppm
37(1c)	coal	0.68	69.04	0.46	2.25
37(1ac)	coal	0.61	65.91	0.42	2.33
24(2c)	bitumen	0.34	356.76	0.00	48.54
24(2ac)	bitumen	0.28	308.34	0.00	47.57
d3(3c)	bitumen	7.92	21.26	7.14	9.55
d3(3ac)	bitumen	0.00	14.37	0.00	1.49
37(1)	coal residue	0.00	2.15	0.00	2.74
37(1a)	coal residue	0.00	1.98	0.00	2.50
24(2)	bitumen residue	0.00	40.91	0.00	2.39
24(2a)	bitumen residue	0.00	29.0	0.00	2.00
d3(3)	bitumen residue	0.00	13.44	0.00	0.71
d3(3a)	bitumen residue	0.00	12.77	0.00	0.44
Statistics	Avg	0.8	77.9	0.67	10.2
Statistics	Std Dev	2.15	116.2	1.95	17.07

Table B.1.2 - LAM-ICP-MS data for bitumen and coal samples

Sample #	Rock Type	C02 wt%	MgO wt%	SiO2 wt %	CaO wt %	TiO2 wt %	V ppm
24	Bitumen	53	0.03	0.66	0.07	0.07	68.29
24	Bitumen	53	0.02	0.65	0.09	0.09	75.77
24	Bitumen	53	0.00	0.03	0.05	0.00	62.22
24	Bitumen	53	0.00	0.05	0.05	0.00	79.59
24	Bitumen	53	0.00	0.02	0.04	0.01	88.29
24	Bitumen	53	0.00	0.06	0.04	0.04	93.61
24	Bitumen	53	0.01	0.11	0.08	0.07	104.86
24	Bitumen	53	0.01	0.06	0.07	0.00	98.14
37	Coal	42	0.00	0.01	0.00	0.00	0.4
37	Coal	42	0.03	0.07	0.04	0.00	2.14
37	Coal	42	0.00	0.01	0.00	0.00	0.00
d3	Bitumen	53	0.00	0.01	0.00	0.00	0.00
d3	Bitumen	53	0.00	0.01	0.00	0.00	0.00
d3	Bitumen	53	0.00	0.01	0.00	0.00	0.00
Statistics	Avg	50.6	0.007	0.125	0.037	0.02	48.1
Statistics	Std Dev	4.5	0.010	0.218	0.031	0.031	42.6

Table B.1.2 - LAM-ICP-MS data for bitumen and coal samples cont'd

Sample #	Rock Type	Cr ppm	MnO wt %	FeO wt%	Co ppm	Ni ppm	Zn ppm
24	Bitumen	20.56	17.52	0.79	1.49	22.41	29.33
24	Bitumen	23.85	15.43	2.17	1.45	25.85	31.04
24	Bitumen	11.42	7.44	0.05	1.82	7.32	36.5
24	Bitumen	13.45	5.83	0.09	1.7	7.19	34.64
24	Bitumen	13.51	5.34	0.04	1.74	14.93	28.47
24	Bitumen	15.77	6.16	0.05	1.63	14.59	31.67
24	Bitumen	30.27	9	0.06	3.36	32.46	20.96
24	Bitumen	31.02	9.02	0.06	5.11	33.97	19.51
37	Coal	1.18	1.16	0.00	0.23	9.46	3.35
37	Coal	1.99	9	0.07	0.42	6.76	139.4
37	Coal	0.86	0.00	0.00	0.00	0.00	0.09
d3	Bitumen	0.97	0.00	0.00	0.00	0.03	0.2
d3	Bitumen	0.88	0.01	0.00	0.00	0.02	0.22
d3	Bitumen	0.79	0.00	0.00	0.00	0.01	0.22
Statistics	Avg	11.89	6.13	0.24	1.35	12.5	26.8
Statistics	Std Dev	10.82	5.46	0.57	1.41	11.5	34.2

Table B.1.2 - LAM-ICP-MS data for bitumen and coal samples cont'd

Sample #	Rock Type	Rb ppm	Sr ppm	Mo ppm	Cs ppm	Ba ppm	La ppm
24	Bitumen	2.3	21.26	1.5	0.31	53.14	14.17
24	Bitumen	2.39	27.5	2.17	0.29	66.54	12.34
24	Bitumen	0.01	15.94	5.16	0.00	47.02	0.66
24	Bitumen	0.01	14.78	5.78	0.00	43.36	1.69
24	Bitumen	0.01	16.91	4.32	0.00	66.71	0.62
24	Bitumen	0.07	19.78	3.65	0.00	69.19	0.56
24	Bitumen	0.01	20.48	1.99	0.00	34.03	3.26
24	Bitumen	0.01	23.77	1.87	0.00	42.15	0.99
37	Coal	0.09	0.1	0.13	0.00	0.28	0.01
37	Coal	2.14	5.08	0.12	0.14	4.93	0.13
37	Coal	0.00	0.01	0.00	0.00	0.00	0.00
d3	Bitumen	0.00	0.06	0.00	0.00	0.01	0.00
d3	Bitumen	0.00	0.00	0.00	0.00	0.00	0.00
d3	Bitumen	0.00	0.00	0.00	0.00	0.00	0.00
Statistics	Avg	0.50	11.83	1.91	0.05	30.5	2.46
Statistics	Std Dev	0.927	10.02	1.99	0.107	27.4	4.5

Table B.1.2 - LAM-ICP-MS data for bitumen and coal samples cont'd

Sample #	Rock Type	Ce ppm	Sm ppm	Eu ppm	W ppm	Pb ppm	Th ppm	U ppm
24	Bitumen	30.21	3.11	0.47	2.15	46.08	2.55	1.92
24	Bitumen	26.04	3.03	0.37	1.43	25.92	2.4	1.83
24	Bitumen	1.51	0.44	0.08	34.34	8.99	0.08	1.2
24	Bitumen	3.21	0.54	0.1	35.15	12.49	0.19	1.32
24	Bitumen	1.39	0.51	0.09	35.56	7.29	0.09	1.34
24	Bitumen	1.26	0.49	0.08	31.49	7.11	0.12	1.27
24	Bitumen	5.07	0.95	0.14	2.87	11.4	0.38	1.17
24	Bitumen	1.64	0.51	0.07	1.36	8	0.35	0.03
37	Coal	0.02	0.00	0.00	0.00	1.02	0.00	0.38
37	Coal	0.43	0.04	0.01	0.02	11.82	0.06	0.00
37	Coal	0.00	0.00	0.00	0.00	0.02	0.00	0.00
d3	Bitumen	0.00	0.00	0.00	0.00	0.03	0.00	0.00
d3	Bitumen	0.01	0.00	0.00	0.00	0.02	0.00	0.00
d3	Bitumen	0.00	0.00	0.00	0.00	0.01	0.00	0.00
Statistics	Avg	5.05	0.69	0.1	10.1	10.0	0.44	0.85
Statistics	Std Dev	9.55	1.01	0.14	14.8	12.1	0.83	0.71

Table B.1.3 - XRF data from DLB

Sample #	Rock Type	SiO2 wt %	TiO2 wt %	Al2O3 wt %	Fe2O3 wt %	MnO wt %	MgO wt %
13	cong/sltst	40.39	0.81	8.70	4.10	0.31	4.12
1	carb/vol	11.78	0.11	1.73	6.92	1.22	27.3
3	carb/vol	26.9	0.16	4.76	5.05	1.11	10.5
9	barite	90.41	0.00	0.15	9.31	0.00	0.00
5	py/quartz	15.41	0.09	1.22	13.11	3.39	21.3
10	vol/carb	5.58	0.05	0.96	7.27	1.29	24.3
17	cong.	80.59	0.24	9.92	2.90	0.04	1.77
19	carbonate	6.36	0.06	0.95	0.96	0.13	19.8
oil shale 2a	oil shale	42.05	0.39	6.89	4.75	0.21	16.2
oil shale 2b	oil shale	44.13	0.54	9.10	5.81	0.17	15.5
26	carbonate	12.54	0.03	0.42	0.53	0.10	0.95
Statistics	Avg	31.34	0.21	3.73	5.06	0.66	11.8
Statistics	Std Dev	28.21	0.24	3.72	3.66	0.95	0.94

Table B.1.3 - XRF data from DLB cont'd

Sample #	Rock Type	CaO wt %	Na2O wt %	K2O wt %	P2O5 wt %	Cr ppm	Ni ppm
13	cong/sltst	37.89	1.74	1.86	0.08	85	9
1	carb/vol	49.99	0.52	0.39	0.02	18	0
3	carb/vol	49.38	0.22	1.93	0.03	36	0
9	barite	0.11	0.00	0.02	0.00	0	16
5	py/quartz	44.57	0.30	0.61	0.02	19	96
10	vol/carb	60	0.27	0.25	0.02	18	0
17	cong.	1.37	1.82	1.31	0.03	37	0
19	carbonate	70.01	0.32	0.41	1.01	0	0
oil shale 2a	oil shale	26.39	1.99	0.93	0.26	69	49
oil shale 2b	oil shale	20.77	2.40	1.41	0.13	142	66
26	carbonate	85.17	0.10	0.15	0.01	0	0
Statistics	Avg	37.14	0.81	0.77	0.15	38.6	21.5
Statistics	Std Dev	26.9	0.86	0.67	0.28	42.12	31.9

Table B.1.3 - XRF data from DLB cont'd

Sample #	Rock Type	Sc ppm	V ppm	Cu ppm	Pb ppm	Zn ppm	S ppm
13	cong/sltst	26	96	405	668	18	2121
1	carb/vol	19	12	0	8	140	293.7
3	carb/vol	26	21	397	180642	1242	27570
9	barite	0	9	13247	27	0	48805
5	py/quartz	22	52	2967	50	346	12951
10	vol/carb	22	0	32	11983	91	29494
17	cong.	11	51	7	19	0	3376
19	carbonate	18	66	36	52	0	517
oil shale 2a	oil shale	21	119	22	13	16	4702
oil shale 2b	oil shale	23	190	27	10	30	2986
26	carbonate	47	0	7	23	18	865
Statistics	Avg	21.47	55.95	1558.8	17590	172.96	12153
Statistics	Std Dev	10.86	56.65	3788.5	51673	352.14	15383

Table B.1.3 - XRF data from DLB cont'd

Sample #	Rock Type	As ppm	Rb ppm	Ba ppm	Sr ppm	Ga ppm	Nb ppm
13	cong/sltst	0	54	8152	170	6	10.4
1	carb/vol	0	10	626	213	0	1.4
3	carb/vol	0	67	40672	1046	1070	0
9	barite	45.40	0	0	3	0	1.5
5	py/quartz	250.96	27	30759	860	0	1.5
10	vol/carb	0	8	134279	1379	0	0
17	cong.	19.7	36	281	83	11	8.7
19	carbonate	24.29	4	345	1603	0	0
oil shale 2a	oil shale	103.1	33	1129	1515	7	5.6
oil shale 2b	oil shale	108.4	51	957	1167	11	8.3
26	carbonate	0.00	2	0	791	0	0
Statistics	Avg	50.14	26.52	19745	802.7	100.5	3.40
Statistics	Std Dev	74.23	22.51	38626	570.8	306.6	3.87

Table B.1.3 - XRF data from DLB cont'd

Sample #	Rock Type	Zr ppm	Y ppm	Th ppm	U ppm	Ce ppm	Cl ppm
13	cong/sltst	215	25	0	0	109.5	170.1
1	carb/vol	28	4	0	0	0	270.8
3	carb/vol	0	6	0	0	3992	522.0
9	barite	0	0	0	0	0	137
5	py/quartz	10	14	0	0	0	160.1
10	vol/carb	0	16	0	0	90.7	231.9
17	cong.	150	23	5.86	0	66.5	77.68
19	carbonate	0	7	13	37.31	0	546.3
oil shale 2a	oil shale	17	17	10.33	54.63	109.5	313.0
oil shale 2b	oil shale	35	14	7.56	34.94	145.4	278.1
26	carbonate	0	17	0	0	0	104.5
Statistics	Avg	41.3	12.9	3.3	11.5	410.4	255.6
Statistics	Std Dev	68.8	7.6	4.7	19.4	1134	149.3

Table B.1.4 - XRF data from DLB (Wilton, unpub. data)

Sample Name	Sc ppm	V ppm	Cu ppm	Pb ppm	Zn ppm	Bi ppm
W89-018A	3	64	13	18	60	0.07
W89-018B	0	8	17	5	49	0.00
W89-018C	0	11	24	29	242	0.00
W89-019D	0	32	15	8	25	0.00
W89-019.1	3	42	16	16	27	0.11
W89-019.2	3	32	16	10	24	0.15
W89-020	9	77	12	6	145	0.13
W89-021A	0	0	11	33	43	0.00
W89-021B.1	0	3	18	6	29	0.00
W89-021B.2	0	2	11	22	30	0.00
W89-022D	0	21	50	8	52	0.00
W89-023	0	53	12	18	34	0.00
W89-024	13	164	11	11	62	0.26
W89-025A	0	120	27	16	76	0.00
W89-025B	0	116	22	8	70	0.00
W89-026	0	46	21	21	56	0.00
W89-027A	0	88	20	12	41	0.00
W89-027B	0	17	29	0	42	0.00
W89-028A	0	247	18	5	107	0.00
W89-028B	0	202	36	75	104	0.00
W89-028C	0	204	33	46	99	0.00
W89-031A	0	69	13	9	31	0.00
W89-031B	8	69	13	13	45	0.08
W89-031C	0	141	17	9	68	0.00
W89-031D1	0	94	14	6	46	0.00
W89-031D2	0	50	20	6	39	0.00
W89-031E	9	63	0	13	0	0.08
W89-032	0	80	30	13	52	0.00
W89-032A	0	154	37	6	66	0.00
W89-033	13	118	33	20	70	0.79
W89-034A	0	143	30	9	60	0.00

Table B.1.4 - XRF data from DLB (Wilton, unpub. data) cont'd

Sample Name	Sc ppm	V ppm	Cu ppm	Pb ppm	Zn ppm	Bi ppm
W89-34B	0	114	39	6	48	0.00
W89-035	0	100	14	8	57	0.00
W89-036	0	19	11	11	24	0.00
W89-037B	0	193	22	17	125	0.00
W89-039H	0	263	96	31	142	0.00
W89-043	0	1	12	0	27	0.00
W89-044	0	399	81	0	100	0.00
W89-045	4	15	10	4	75	0.06
W89-046	9	106	16	9	60	0.09
W89-046.1	0	86	17	0	70	0.00
W89-047	0	70	13	10	46	0.00
W89-048	0	57	14	4	51	0.00
W89-049	0	22	9	16	67	0.00
avg	2	90	23	14	63	0
std dev	4	82	17	13	41	0

Table B.1.4 - XRF data from DLB (Wilton, unpub. Data) cont'd

Sample Name	SiO2 wt %	TiO2 wt %	Al2O3 wt %	Fe2O3 wt %	FeO wt %	MnO wt %
W89-018A	73.48	0.18	14.23	0.31	1.58	0.06
W89-018B	11.84	0.00	1.88	0.15	0.81	0.32
W89-018C	17.01	0.06	4.61	0.37	1.89	0.21
W89-019D	76.52	0.15	10.98	0.17	0.88	0.12
W89-019.1	76.28	0.15	11.20	0.17	0.88	0.12
W89-019.2	78.81	0.17	10.61	0.27	1.36	0.18
W89-020	73.90	0.38	12.09	0.53	2.70	0.10
W89-021A	79.04	0.00	11.94	0.14	0.71	0.02
W89-021B.1	78.05	0.00	12.12	0.13	0.68	0.01
W89-021B.2	94.90	0.00	2.95	0.06	0.32	0.01
W89-022D	74.19	0.17	8.57	0.36	1.82	0.04
W89-023	78.82	0.36	11.74	0.28	1.47	0.03
W89-024	63.51	1.29	15.80	1.01	5.16	0.09
W89-025A	67.00	0.69	15.16	1.09	5.56	0.16
W89-025B	71.18	0.51	14.15	0.91	4.66	0.07
W89-026	75.32	0.17	11.60	0.48	2.45	0.08
W89-027A	74.27	0.50	12.31	0.46	2.31	0.05
W89-027B	7.46	0.13	1.62	0.07	0.35	0.27
W89-028A	66.58	0.85	13.15	1.36	6.94	0.17
W89-028B	66.18	0.83	16.28	1.15	5.89	0.15
W89-028C	0.00	0.00	0.00	0.00	0.00	0.00
W89-031A	78.14	0.29	10.30	0.36	1.83	0.05
W89-031B	77.03	0.74	10.84	0.51	2.63	0.09
W89-031C	0.00	0.00	0.00	0.00	0.00	0.00
W89-031D1	72.93	0.68	11.22	0.54	2.77	0.12
W89-031D2	78.34	0.21	10.06	0.29	1.47	0.07
W89-031E	75.46	0.53	11.81	0.49	2.49	0.07
W89-032	69.92	0.56	12.51	0.41	2.07	0.06
W89-032A	70.51	0.84	12.96	0.91	4.64	0.21
W89-033	72.13	0.84	12.74	0.84	4.30	0.21
W89-034A	72.56	0.62	12.48	0.82	4.19	0.26

Table B.1.4 - XRF data from DLB (Wilton, unpub. Data) cont'd

Sample Name	SiO2 wt %	TiO2 wt %	Al2O3 wt %	Fe2O3 wt %	FeO wt %	MnO wt %
W89-34B	72.23	0.63	13.65	0.56	2.87	0.09
W89-035	76.22	0.53	11.82	0.53	2.68	0.06
W89-036	81.56	0.20	10.10	0.20	1.03	0.05
W89-037B	64.41	0.77	15.02	2.06	10.50	0.53
W89-039H	1.39	0.99	23.41	2.57	13.03	1.39
W89-043	81.35	0.04	11.29	0.15	0.78	0.03
W89-044	0.00	0.00	0.00	0.00	0.00	0.00
W89-045	75.84	0.21	12.21	0.57	2.95	0.02
W89-046	75.96	0.45	11.78	0.61	3.12	0.07
W89-046.1	67.99	0.39	12.78	0.58	3.01	0.09
W89-047	78.11	0.37	12.10	0.41	2.07	0.02
W89-048	74.47	0.57	13.33	0.46	2.34	0.04
W89-049	72.30	0.41	14.22	0.37	1.86	0.05
avg	63.4819	0.3967	10.8995	0.5388	2.7517	0.1332
std dev	25.9154	0.3175	4.6686	0.5049	2.5701	0.2168

Table B.1.4 - XRF data from DLB (collected by Wilton, 1989) cont'd

Sample Name	MgO wt %	CaO wt %	Na2O wt %	K2O wt %	P2O5 wt %	Cr ppm
W89-018A	1.04	0.39	4.08	4.51	0.13	12
W89-018B	1.56	82.74	0.00	0.61	0.08	2
W89-018C	1.62	72.85	0.21	0.96	0.21	5
W89-019D	0.83	3.63	4.11	2.60	0.03	5
W89-019.1	0.83	3.66	4.10	2.60	0.02	7
W89-019.2	0.59	1.39	3.67	2.92	0.03	5
W89-020	1.65	2.86	2.94	2.75	0.11	34
W89-021A	0.04	0.00	4.08	4.03	0.00	2
W89-021B.1	0.04	0.18	4.29	4.49	0.01	1
W89-021B.2	0.05	0.00	0.48	1.22	0.00	9
W89-022D	0.79	8.92	2.61	2.36	0.16	4
W89-023	0.67	0.34	3.32	2.89	0.07	8
W89-024	2.99	2.14	5.60	1.96	0.44	14
W89-025A	2.89	2.75	2.00	2.58	0.11	60
W89-025B	2.83	1.06	2.18	2.34	0.12	54
W89-026	1.55	2.42	5.85	0.06	0.02	8
W89-027A	0.90	2.52	3.46	3.17	0.06	12
W89-027B	0.71	88.73	0.39	0.25	0.02	0
W89-028A	3.60	3.07	2.94	1.19	0.15	119
W89-028B	3.17	0.91	1.55	3.73	0.16	106
W89-028C	0.00	0.00	0.00	0.00	0.00	114
W89-031A	1.42	2.41	2.94	2.21	0.04	19
W89-031B	1.95	1.29	2.59	2.26	0.06	55
W89-031C	0.00	0.00	0.00	0.00	0.00	70
W89-031D1	1.97	5.10	3.03	1.58	0.07	41
W89-031D2	1.12	2.96	2.83	2.64	0.01	15
W89-031E	1.87	1.08	3.51	2.41	0.26	0
W89-032	1.52	7.61	3.74	1.52	0.09	22
W89-032A	2.79	2.23	3.67	1.12	0.12	62
W89-033	2.16	1.38	3.35	1.94	0.11	46
W89-034A	2.39	1.16	3.19	2.25	0.07	48

Table B.1.4 - XRF data from DLB (collected by Wilton, 1989) cont'd

Sample Name	MgO wt %	CaO wt %	Na2O wt %	K2O wt %	P2O5 wt %	Cr ppm
W89-34B	1.72	2.15	4.58	1.49	0.03	35
W89-035	1.47	1.06	3.11	2.45	0.08	23
W89-036	0.54	0.90	3.12	2.26	0.01	2
W89-037B	2.03	1.48	1.06	2.08	0.05	104
W89-039H	2.91	47.31	2.26	4.74	0.00	68
W89-043	0.23	0.26	4.00	1.84	0.02	2
W89-044	0.00	0.00	0.00	0.00	0.00	175
W89-045	0.96	0.47	2.55	4.19	0.03	9
W89-046	1.88	0.52	3.21	2.27	0.11	29
W89-046.1	2.30	7.04	2.39	3.32	0.11	45
W89-047	0.55	0.37	3.62	2.32	0.07	15
W89-048	0.83	0.37	3.59	3.92	0.09	6
W89-049	0.39	0.71	3.95	5.69	0.07	5
avg	1.40	8.37	2.82	2.31	0.08	33.64
std dev	0.98	21.05	1.46	1.33	0.08	39.06

Table B.1.4 - XRF data from DLB (Wilton, unpub. Data) cont'd

Sample Name	Rb ppm	Cs ppm	Ba ppm	Sr ppm	Tl ppm	Ga ppm
W89-018A	183	3.00	654	295	1.32	19
W89-18B	37	0.00	0	638	0.00	3
W89-018C	64	0.00	0	825	0.00	8
W89-019D	63	0.00	0	188	0.00	12
W89-019.1	71	1.08	3452	152	0.43	14
W89-019.2	65	0.84	1760	188	0.27	12
W89-020	123	2.46	472	94	0.56	14
W89-021A	323	0.00	0	0	0.00	29
W89-021B.1	75	0.00	0	1	0.00	8
W89-021B.2	239	0.00	0	13	0.00	28
W89-022D	35	0.00	0	161	0.00	15
W89-023	76	0.00	0	235	0.00	13
W89-024	53	1.03	415	159	0.27	22
W89-025A	106	0.00	0	119	0.00	20
W89-025B	91	0.00	0	114	0.00	20
W89-026	1	0.00	0	46	0.00	11
W89-027A	85	0.00	0	153	0.00	18
W89-027B	8	0.00	0	705	0.00	3
W89-028A	48	0.00	0	179	0.00	18
W89-028B	117	0.00	0	44	0.00	23
W89-028C	114	0.00	0	38	0.00	22
W89-031A	51	0.00	0	232	0.00	12
W89-031B	51	0.59	717	217	0.30	12
W89-031C	93	0.00	0	180	0.00	17
W89-031D1	43	0.00	0	276	0.00	14
W89-031D2	65	0.00	0	201	0.00	11
W89-031E	56	0.68	645	244	0.36	0
W89-032	45	0.00	0	203	0.00	13
W89-032A	31	0.00	0	198	0.00	17
W89-033	63	4.23	547	139	0.70	15
W89-034A	65	0.00	0	204	0.00	15
W89-034B	45	0.00	0	151	0.00	15

Table B.1.4 - XRF data from DLB (Wilton, unpub. Data) cont'd

Sample Name	Rb ppm	Cs ppm	Ba ppm	Sr ppm	Tl ppm	Ga ppm
W89-35	74	0.00	0	2	0.00	13
W89-036	64	0.00	0	205	0.00	13
W89-037B	115	0.00	0	53	0.00	24
W89-039H	198	0.00	0	455	0.00	31
W89-043	65	0.00	0	71	0.00	12
W89-044	0	0.00	0	0	0.00	20
W89-045	160	3.00	143	36	0.92	22
W89-046	58	1.60	475	144	0.31	16
W89-046.1	105	0.00	0	161	0.00	15
W89-047	67	0.00	0	162	0.00	14
W89-048	53	0.00	0	202	0.00	13
W89-049	224	0.00	0	73	0.00	22
avg	86	0	211	189	0	16
std dev	63	1	591	170	0	6

Table B.1.4 - XRF data from DLB (Wilton, unpub.data) cont'd

Sample Name	Mo ppm	K ppm	Ni ppm	Li ppm	Ta ppm
W89-018A	0.24	37467	12	61.51	0.70
W89-018B	0.00	5056	10	0.00	0.00
W89-018C	0.00	7993	19	0.00	0.00
W89-019D	0.00	21553	5	0.00	0.00
W89-019.1	1.14	21575	3	1.47	0.99
W89-019.2	0.24	24253	5	2.38	0.63
W89-020	0.31	22795	27	21.67	1.22
W89-021A	0.00	33437	1	0.00	0.00
W89-021B.1	0.00	37299	0	0.00	0.00
W89-021B.2	0.00	10112	0	0.00	0.00
W89-022D	0.00	19600	2	0.00	0.00
W89-023	0.00	24023	6	0.00	0.00
W89-024	1.39	16309	17	36.24	1.50
W89-025A	0.00	21427	44	0.00	0.00
W89-025B	0.00	19462	33	0.00	0.00
W89-026	0.00	520	1	0.00	0.00
W89-027A	0.00	26277	11	0.00	0.00
W89-027B	0.00	2100	7	0.00	0.00
W89-028A	0.00	9857	39	0.00	0.00
W89-028B	0.00	30998	68	0.00	0.00
W89-028C	0.00	0	64	0.00	0.00
W89-031A	0.00	18375	23	0.00	0.00
W89-031B	0.25	18768	29	16.79	0.84
W89-031C	0.00	0	51	0.00	0.00
W89-031D1	0.00	13092	32	0.00	0.00
W89-031D2	0.00	21909	29	0.00	0.00
W89-031E	0.20	20035	0	14.61	0.96
W89-032	0.00	12602	27	0.00	0.00
W89-032A	0.00	9274	35	0.00	0.00
W89-033	0.45	16119	25	36.21	5.27
W89-034A	0.00	18641	24	0.00	0.00

Table B.1.4 - XRF data from DLB (Wilton, unpub.data) cont'd

Sample Name	Mo ppm	K ppm	Ni ppm	Li ppm	Ta ppm
W89-34B	0.00	12373	28	0.00	0.00
W89-35	0.00	20301	18	0.00	0.00
W89-036	0.00	18797	0	0.00	0.00
W89-037B	0.00	17288	44	0.00	0.00
W89-039H	0.00	39322	37	0.00	0.00
W89-043	0.00	15279	0	0.00	0.00
W89-044	0.00	0	29	0.00	0.00
W89-045	0.60	34759	4	15.01	1.39
W89-046	0.44	18875	21	22.93	0.59
W89-046.1	0.00	27593	39	0.00	0.00
W89-047	0.00	19230	8	0.00	0.00
W89-048	0.00	32513	3	0.00	0.00
W89-049	0.00	47205	2	0.00	0.00
avg	0	19192	20.06	5	0
std dev	0	11003	17.69	13	1

Table B.1.4 - XRF data from DLB (Wilton, unpub. Data) cont'd

Sample Name	Nb ppm	Hf ppm	Zr ppm	Ti ppm	Y ppm	La ppm
W89-018A	12.3	2.36	165	1104	4	19.65
W89-018B	5.1	0.00	52	0	7	0.00
W89-018C	4.8	0.00	13	385	14	0.00
W89-019D	4.2	0.00	95	885	8	0.00
W89-019.1	8.5	1.15	93	886	12	32.77
W89-019.2	4.2	0.86	91	997	8	17.28
W89-020	14.8	2.72	360	2288	15	41.04
W89-021A	80.0	0.00	157	0	130	0.00
W89-021B.1	6.1	0.00	25	0	17	0.00
W89-021B.2	74.1	0.00	170	0	70	0.00
W89-022D	15.2	0.00	125	1039	48	0.00
W89-023	11.1	0.00	138	2184	13	0.00
W89-024	21.8	3.91	343	7728	38	53.82
W89-025A	16.1	0.00	195	4127	29	0.00
W89-025B	18.0	0.00	355	3039	31	0.00
W89-026	4.2	0.00	81	1002	27	0.00
W89-027A	9.3	0.00	168	2977	18	0.00
W89-027B	6.7	0.00	74	810	35	0.00
W89-028A	13.8	0.00	207	5085	30	0.00
W89-028B	14.5	0.00	200	4975	27	0.00
W89-028C	15.0	0.00	189	0	26	0.00
W89-031A	5.1	0.00	105	1729	9	0.00
W89-031B	8.2	1.03	108	4415	16	24.04
W89-031C	12.0	0.00	216	0	25	0.00
W89-031D1	9.5	0.00	194	4061	23	0.00
W89-031D2	5.2	0.00	87	1251	11	0.00
W89-031E	8.1	1.32	123	3174	14	21.22
W89-032	8.6	0.00	177	3332	19	0.00
W89-032A	11.6	0.00	167	5055	34	0.00
W89-033	9.2	2.86	153	5051	28	19.17
W89-034A	9.4	0.00	164	3739	26	0.00
W89-034B	8.3	0.00	149	3749	24	0.00

Table B.1.4 - XRF data from DLB (Wilton, unpub. Data) cont'd

Sample Name	Nb ppm	Hf ppm	Zr ppm	Ti ppm	Y ppm	La ppm
W89-35	12.2	0.00	190	3176	19	0.00
W89-36	7.2	0.00	97	1228	16	0.00
W89-037B	19.3	0.00	215	4640	46	0.00
W89-039H	31.0	0.00	570	5938	93	0.00
W89-043	15.3	0.00	103	244	53	0.00
W89-044	0.0	0.00	0	0	0	0.00
W89-045	36.9	15.75	627	1231	52	52.86
W89-046	8.3	2.47	144	2726	13	18.53
W89-046.1	15.2	0.00	329	2337	36	0.00
W89-047	14.4	0.00	209	2212	28	0.00
W89-048	19.3	0.00	148	3415	15	0.00
W89-049	45.7	0.00	333	2435	58	0.00
avg	15	1	180	2378	29	7
std dev	16	2	125	1903	24	14

Table B.1.4 - XRF data from DLB (Wilton, unpub. Data) cont'd

Sample Name	Th ppm	U ppm	Tb ppm	Dy ppm
W89-018A	16.32	6.48	0.15	0.84
W89-018B	0.00	5.08	0.00	0.00
W89-018C	8.02	0.00	0.00	0.00
W89-019D	6.33	0.00	0.00	0.00
W89-019.1	5.75	3.18	0.55	2.93
W89-019.2	4.44	1.26	0.30	1.67
W89-020	11.64	2.90	0.62	3.63
W89-021A	37.45	7.08	0.00	0.00
W89-021B.1	5.05	0.00	0.00	0.00
W89-021B.2	36.54	8.12	0.00	0.00
W89-022D	5.42	0.00	0.00	0.00
W89-023	11.13	1.01	0.00	0.00
W89-024	14.64	4.96	1.20	7.22
W89-025A	11.83	4.30	0.00	0.00
W89-025B	11.62	3.17	0.00	0.00
W89-026	5.22	1.04	0.00	0.00
W89-027A	10.34	1.03	0.00	0.00
W89-027B	8.43	0.00	0.00	0.00
W89-028A	5.30	0.00	0.00	0.00
W89-028B	9.34	2.07	0.00	0.00
W89-028C	13.00	2.00	0.00	0.00
W89-031A	8.24	0.00	0.00	0.00
W89-031B	6.72	1.17	0.48	2.95
W89-031C	10.00	1.00	0.00	0.00
W89-031D1	9.53	0.00	0.00	0.00
W89-031D2	4.17	0.00	0.00	0.00
W89-031E	6.44	1.10	0.43	2.73
W89-032	7.48	0.00	0.00	0.00
W89-032A	8.43	0.00	0.00	0.00
W89-033	9.88	1.44	0.67	4.51
W89-034A	8.32	0.00	0.00	0.00
W89-034B	7.30	0.00	0.00	0.00

Table B.1.4 - XRF data from DLB (Wilton, unpub. Data) cont'd

Sample Name	Th ppm	U ppm	Tb ppm	Dy ppm
W89-35	9.17	2.04	0.00	0.00
W89-036	6.15	0.00	0.00	0.00
W89-037B	9.10	10.24	0.00	0.00
W89-039H	18.58	3.10	0.00	0.00
W89-043	20.34	3.05	0.00	0.00
W89-044	0.00	0.00	0.00	0.00
W89-045	17.93	5.70	1.34	8.88
W89-046	5.58	1.85	0.40	2.61
W89-046.1	11.91	0.00	0.00	0.00
W89-047	13.33	1.03	0.00	0.00
W89-048	1.02	0.00	0.00	0.00
W89-049	24.37	2.03	0.00	0.00
avg	10	2	0.14	0.86
std dev	8	2	0.32	2.00

Table B.1.4 - XRF data from DLB (Wilton, unpub. Data) cont'd

Sample Name	Ce ppm	Pr ppm	Nd ppm	Sm ppm	Eu ppm	Gd ppm
W89-018A	55.89	2.61	8.12	1.26	0.32	1.37
W89-018B	0.00	0.00	0.00	0.00	0.00	0.00
W89-018C	0.00	0.00	0.00	0.00	0.00	0.00
W89-019D	0.00	0.00	0.00	0.00	0.00	0.00
W89-019.1	58.57	7.66	28.24	5.45	1.46	5.09
W89-019.2	35.86	4.20	15.56	2.89	0.73	2.80
W89-020	86.33	10.00	37.43	6.65	1.23	5.47
W89-021A	0.00	0.00	0.00	0.00	0.00	0.00
W89-021B.1	0.00	0.00	0.00	0.00	0.00	0.00
W89-021B.2	0.00	0.00	0.00	0.00	0.00	0.00
W89-022D	0.00	0.00	0.00	0.00	0.00	0.00
W89-023	0.00	0.00	0.00	0.00	0.00	0.00
W89-024	112.87	13.13	47.49	8.84	2.07	8.30
W89-025A	0.00	0.00	0.00	0.00	0.00	0.00
W89-025B	0.00	0.00	0.00	0.00	0.00	0.00
W89-026	0.00	0.00	0.00	0.00	0.00	0.00
W89-027A	0.00	0.00	0.00	0.00	0.00	0.00
W89-027B	0.00	0.00	0.00	0.00	0.00	0.00
W89-028A	0.00	0.00	0.00	0.00	0.00	0.00
W89-028B	0.00	0.00	0.00	0.00	0.00	0.00
W89-028C	0.00	0.00	0.00	0.00	0.00	0.00
W89-031A	0.00	0.00	0.00	0.00	0.00	0.00
W89-031B	46.65	5.38	19.25	3.52	0.91	3.35
W89-031C	0.00	0.00	0.00	0.00	0.00	0.00
W89-031D1	0.00	0.00	0.00	0.00	0.00	0.00
W89-031D2	0.00	0.00	0.00	0.00	0.00	0.00
W89-031E	54.99	5.04	19.08	3.44	0.86	3.10
W89-032	0.00	0.00	0.00	0.00	0.00	0.00
W89-032A	0.00	0.00	0.00	0.00	0.00	0.00
W89-033	35.10	4.58	17.33	3.88	1.13	4.39
W89-034A	0.00	0.00	0.00	0.00	0.00	0.00

Table B.1.4 - XRF data from DLB (Wilton, unpub. Data) cont'd

Sample Name	Ce ppm	Pr ppm	Nd ppm	Sm ppm	Eu ppm	Gd ppm
W89-34B	0.00	0.00	0.00	0.00	0.00	0.00
W89-035	0.00	0.00	0.00	0.00	0.00	0.00
W89-036	0.00	0.00	0.00	0.00	0.00	0.00
W89-037B	0.00	0.00	0.00	0.00	0.00	0.00
W89-039H	0.00	0.00	0.00	0.00	0.00	0.00
W89-043	0.00	0.00	0.00	0.00	0.00	0.00
W89-044	0.00	0.00	0.00	0.00	0.00	0.00
W89-045	113.71	13.88	51.65	10.57	0.44	9.15
W89-046	37.90	4.53	16.80	3.29	0.73	3.05
W89-046.1	0.00	0.00	0.00	0.00	0.00	0.00
W89-047	0.00	0.00	0.00	0.00	0.00	0.00
W89-048	0.00	0.00	0.00	0.00	0.00	0.00
W89-049	0.00	0.00	0.00	0.00	0.00	0.00
avg	14.50	1.61	5.93	1.13	0.22	1.05
std dev	30.14	3.56	13.14	2.53	0.49	2.29

Table B.1.4 - XRF data from DLB (Wilton, unpub. Data) cont'd

Sample Name	Ho ppm	Er ppm	Tm ppm	Yb ppm	Lu ppm	Be ppm
W89-018A	0.15	0.50	0.07	0.47	0.07	3.10
W89-018B	0.00	0.00	0.00	0.00	0.00	0.00
W89-018C	0.00	0.00	0.00	0.00	0.00	0.00
W89-019D	0.00	0.00	0.00	0.00	0.00	0.00
W89-019.1	0.54	1.46	0.22	1.60	0.21	0.70
W89-019.2	0.31	0.84	0.13	0.79	0.12	0.81
W89-020	0.64	1.87	0.28	1.93	0.30	2.45
W89-021A	0.00	0.00	0.00	0.00	0.00	0.00
W89-021B.1	0.00	0.00	0.00	0.00	0.00	0.00
W89-021B.2	0.00	0.00	0.00	0.00	0.00	0.00
W89-022D	0.00	0.00	0.00	0.00	0.00	0.00
W89-023	0.00	0.00	0.00	0.00	0.00	0.00
W89-024	1.43	4.17	0.59	3.83	0.56	2.92
W89-025A	0.00	0.00	0.00	0.00	0.00	0.00
W89-025B	0.00	0.00	0.00	0.00	0.00	0.00
W89-026	0.00	0.00	0.00	0.00	0.00	0.00
W89-027A	0.00	0.00	0.00	0.00	0.00	0.00
W89-027B	0.00	0.00	0.00	0.00	0.00	0.00
W89-028A	0.00	0.00	0.00	0.00	0.00	0.00
W89-028B	0.00	0.00	0.00	0.00	0.00	0.00
W89-028C	0.00	0.00	0.00	0.00	0.00	0.00
W89-031A	0.00	0.00	0.00	0.00	0.00	0.00
W89-031B	0.61	1.79	0.25	1.62	0.24	1.07
W89-031C	0.00	0.00	0.00	0.00	0.00	0.00
W89-031D1	0.00	0.00	0.00	0.00	0.00	0.00
W89-031D2	0.00	0.00	0.00	0.00	0.00	0.00
W89-031E	0.56	1.55	0.23	1.51	0.24	1.71
W89-032	0.00	0.00	0.00	0.00	0.00	0.00
W89-032A	0.00	0.00	0.00	0.00	0.00	0.00
W89-033	0.93	2.98	0.41	2.77	0.42	1.88
W89-034A	0.00	0.00	0.00	0.00	0.00	0.00
W89-034B	0.00	0.00	0.00	0.00	0.00	0.00

Table B.1.4 - XRF data from DLB (Wilton, unpub. Data) cont'd

Sample Name	Ho ppm	Er ppm	Tm ppm	Yb ppm	Lu ppm	Be ppm
W89-35	0.00	0.00	0.00	0.00	0.00	0.00
W89-036	0.00	0.00	0.00	0.00	0.00	0.00
W89-037B	0.00	0.00	0.00	0.00	0.00	0.00
W89-039H	0.00	0.00	0.00	0.00	0.00	0.00
W89-043	0.00	0.00	0.00	0.00	0.00	0.00
W89-044	0.00	0.00	0.00	0.00	0.00	0.00
W89-045	1.96	6.26	1.02	6.92	1.07	3.01
W89-046	0.52	1.62	0.23	1.67	0.24	1.42
W89-046.1	0.00	0.00	0.00	0.00	0.00	0.00
W89-047	0.00	0.00	0.00	0.00	0.00	0.00
W89-048	0.00	0.00	0.00	0.00	0.00	0.00
W89-049	0.00	0.00	0.00	0.00	0.00	0.00
avg	0.17427	0.523979	0.0779	0.52526	0.0787	0.433325
std dev	0.4046974	1.245276	0.19119	1.28759	0.19559	0.900755

Appendix B.1.5- Geosoft Statistics

File	Min Value	Max Value	Average	Std Dev
gravity residual Map2	-16.9 mGal	19.6 mGal	0.001	5.3
magnetic residual Map3	-585.5 nT	1256 nT	-0.65	128.2
Ag Map 5	0.03 ppm	0.6 ppm	0.1	0.06
As Map 6	0 ppm	73.7 ppm	6.7	7.7
Au Map 7	0 ppb	10.3 ppb	1.5	1.04
Ba Map 8	0 ppm	2253.9 ppm	235.2	189.5
Ce Map 9	0 ppm	356 ppm	50.4	39.3
Co Map 10	0 ppm	100.6 ppm	7.6	9.4
Cr Map 11	0 ppm	305.8 ppm	29.9	30.8
Cu Map 12	0 ppm	95 ppm	16.3	11.6
Eu Map 13	0 ppm	4.3 ppm	0.8	0.5
F Map 14	0 ppm	1713.1 ppm	128.9	209.1
Fe Map 15	0 %	35.9 %	2.5	3.3
La Map 16	0 ppm	148.5 ppm	31.4	22.1
Mn Map 17	0 ppm	44175 ppm	1168.1	2947.4
Mo Map 18	0 ppm	23.1 ppm	3.03	2.05
Ni Map 19	0 ppm	76 ppm	15.7	11.1
Pb Map 20	0 ppm	53.2 ppm	5.8	5.1
Rb Map 21	0 ppm	62 ppm	8.5	8.6
Sb Map 22	0 ppm	1.7 ppm	0.2	0.1
Sm Map 23	0 ppm	37.2 ppm	6	4.7
Th Map 24	0 ppm	14.6 ppm	3.2	1.6
U Map 25	0 ppm	37.2 ppm	4	4.1
Yb Map 26	0 ppm	6.6 ppm	1.5	0.95
Zn Map 27	0 ppm	313.1 ppm	91.6	45.1

LEGEND TO GEOLOGICAL UNITS

CARBONIFEROUS

23 Howley Formation Sandstone, pebble-boulder conglomerate, siltstone, black carbonaceous shale, minor bituminous coal.

VISEAN

Deer Lake Group

22 Little Pond Brook Formation Red, gray, green and tan sandstone, red to gray, pebble to boulder conglomerate, and red, grey, and green siltstone.

21 Humber Falls Formation very light gray, light orange, and red sandstone, pink to gray, pebble to cobble conglomerate, and mostly red, but also gray siltstone.

20 Rocky Brook Formation 20a, Squires Park Member: gray to green siltstone, gray to green and black mudstone, gray dolomitic limestone and calcareous dolostone, dark brown oil shale, very rare gypsum in drill core; 20b, The Spillway Member: gray to red and brown, calcareous siltstone, grey to green mudstone, gray to green calcareous dolostone and dolomitic limestone, rare gray to red sandstone and dark brown oil shale.

19 North Brook Formation 19a, Mainly red to gray, pebble to boulder conglomerate and interbedded red to gray sandstone;19b, mainly red to gray sandstone, but also red to gray pebble to cobble conglomerate and pebbly sandstone, red siltstone, gray and pink limestone; 19c, red to gray sandstone and interbedded red siltstone, lithologies arranged in fining-upward sequences; 19d, mainly red sandstone and siltstone, minor gray to pink limestone, thin gypsum layers reported in drill hole near Humber Canal; 19e, gray limestone breccia, limestone.

TOURNAISIAN

18 Wetstone Point Formation Gray to green and red sandstone and siltstone, gray pebbly sandstone and pebble-cobble conglomerate, minor green and dark gray to black mudstone and gray limestone.

17 Wigwam Brook Formation Red, brown and gray sandstone, gray to red, pebble to boulder conglomerate, gray limestone.

TOURNAISIAN AND OLDER?

Anguille Group

16 Thirty-Fifth Brook Formation gray to pink, very arkosic, sandstone, pebbly sandstone, and pebble to boulder conglomerate, dark gray siltstone and sandstone, rare limestone.

15 Cape Rouge Formation Tan to orange-weathering dolomitic sandstone (with graded bedding), gray, reddish-brown, and red dolomitic siltstones, minor tan dolostone.

14 Saltwater Cove Formation Dark gray sandstone and siltstone, black carbonaceous shale and mudstone, interbedded with light gray sandstone, pebbly sandstone, and pebble to cobble conglomerate, very rare limestone and dolostone.

13 Anguille Bay Members: Gray and tan-weathering sandstones (with graded bedding) interbedded with dark-gray siltstones and black carbonaceous shales.

12 Forty-five Brook Formation Dark to light gray sandstone, dark gray siltstone, black carbonaceous shale, tan to orange-weathering dolostone, minor pebble to cobble conglomerate.

11 Gold Cove Formation Red and gray sandstones, pebbly sandstones, pebble to cobble conglomerates, and siltstones.

10 Blue Gulch Brook Formation gray, carbonate-and quartz pebble to cobble conglomerate, gray sandstone and siltstone, calcareous and dolomitic sandstone, quartzose and dolomitic limestone.

PRE-CARBONIFEROUS BASEMENT (PRECAMBRIAN-DEVONIAN?)

9 Granitic (mainly?) to gabbroic rocks

8 Mic Mac Lake Group 8a, Felsic to intermediate volcanic rocks; 8b, mafic to intermediate volcanic rocks; 8c, reddish conglomerate and sandstone.

7 Sops Arm Group 7a, Felsic to intermediate volcanic rocks; 7b, mafic to intermediate volcanic rocks; 7c, sandstones, siltstones, carbonate rocks.

6 Undivided volcanic, sedimentary and plutonic rocks; 6a, Foliated granitoid rocks; 6b, felsic to intermediate rocks; 6c, mafic to intermediate volcanic rocks, gabbro and diorite; 6d, chloritic metaconglomerate, metasandstone, and metasiltstone.

5 Glover Formation mafic to intermediate volcanic rocks; 5b, ultramafic rocks; 5c, gabbroic rocks.

4 4a, Undivided carbonate rocks; 4b, Boucers Formation variably recrystallized limestone and dolostone; 4c, Labrador Group quartzite, quartz-mica schist, mica schist.

3 Fleur-de-Lys Supergroup 3a, Metasandstone, mica schist, phyllite, and metaconglomerate; 3b, White Bay Group: Quartz-mica schist and mica schist; 3c, Doby Mountain Amphibolite Amphibolite with screens of granitic gneiss.

2 2a, Gabbro, trondhjemite, schistose dolomitic marble; 2b, shaly melange, tan to orange recrystallized carbonate rocks, mafic rocks (dikes?); 2c, flaggy, gray metasandstone interbedded with lesser amounts of green, gray, and red slate; 2d, carbonatized (?) greenschist, minor gabbro and shaly melange like rocks.

1 1a, Granitic gneiss and undivided granitic plutons; 1b, metagabbro and gabbroic dikes.

MINERAL OCCURRENCE ABBREVIATIONS

Ag	silver	mrb	marble
Asb	asbestos	Ni	nickel
Au	gold	Pb	lead
Ba	barite	Po	pyrrhotite
btm	hydrocarbons	Py	pyrite
cly	clay	sls	silica
Col	coal	sls	slate
Cr	chromite	stn	dimension stone
Cu	copper	Th	thorium
Fe	iron	Ti	titanium
Fl	fluorite	U	uranium
lst	limestone	Zn	zinc
Mo	molybdenum		

LEGEND TO SYMBOLS

- Highway/road
- Geological contact
- Fault
- Thrust Fault
- ●13 Rock sample location
- △Py Mineral occurrence site
- Borehole location
- Paleotopographic Domain (PD#)

N

Scale: 1:125,000

0 10 Kilometres

PD1 PD2 PD3 PD4 PD5 PD6 PD7 PD8

Adies Pond · Sir Richards Squires Memorial Park · Deer Lake · Grand Lake · Glover Island · Sandy Lake · White Bay · Turners Ridge · Spruce Ridge · Jade Pond · Claybank · Claybank #3 · Claybank #4 · Mals #1 · Mals #2 · Mals #3 · Mals #4 · Mals #5 · Mals #6 · Mals #7 · Mals #8 · Mals #9 · Mals #10 · Mals #11 · Mals #12 · Mals #13 · Mals #14 · Mals #15 · Mals #16 · Mals #17 · Mals #18 · Mals #19 · Mals #20 · Mals #21 · Mals #22 · Mals #23 · Mals #24 · Mals #25 · Mals #26 · Mals #27 · Mals #28 · Mals #29 · Mals #30 · Mals #31 · Mals #32 · Mals #33 · Mals #34 · Mals #35 · Mals #36 · Mals #37 · Mals #38 · Mals #39 · Mals #40 · Mals #41 · Mals #42 · Mals #43 · Mals #44 · Mals #45 · Mals #46 · Mals #47 · Mals #48 · Mals #49 · Mals #50 · Mals #51 · Mals #52 · Mals #53 · Mals #54 · Mals #55 · Mals #56 · Mals #57 · Mals #58 · Mals #59 · Mals #60 · Mals #61 · Mals #62 · Mals #63 · Mals #64 · Mals #65 · Mals #66 · Mals #67 · Mals #68 · Mals #69 · Mals #70 · Mals #71 · Mals #72 · Mals #73 · Mals #74 · Mals #75 · Mals #76 · Mals #77 · Mals #78 · Mals #79 · Mals #80 · Mals #81 · Mals #82 · Mals #83 · Mals #84 · Mals #85 · Mals #86 · Mals #87 · Mals #88 · Mals #89 · Mals #90 · Mals #91 · Mals #92 · Mals #93 · Mals #94 · Mals #95 · Mals #96 · Mals #97 · Mals #98 · Mals #99 · Mals #100 · Mals #101 · Mals #102 · Mals #103 · Mals #104 · Mals #105 · Mals #106 · Mals #107 · Mals #108 · Mals #109 · Mals #110 · Mals #111 · Mals #112 · Mals #113 · Mals #114 · Mals #115 · Mals #116 · Mals #117 · Mals #118 · Mals #119 · Mals #120 · Mals #121 · Mals #122 · Mals #123 · Mals #124 · Mals #125 · Mals #126 · Mals #127 · Mals #128 · Mals #129 · Mals #130 · Mals #131 · Mals #132 · Mals #133 · Mals #134 · Mals #135 · Mals #136 · Mals #137 · Mals #138 · Mals #139 · Mals #140 · Mals #141 · Mals #142 · Mals #143 · Mals #144 · Mals #145 · Mals #146 · Mals #147 · Mals #148 · Mals #149 · Mals #150 · Mals #151 · Mals #152 · Mals #153 · Mals #154 · Mals #155 · Mals #156 · Mals #157 · Mals #158 · Mals #159 · Mals #160 · Mals #161 · Mals #162 · Mals #163 · Mals #164 · Mals #165 · Mals #166 · Mals #167 · Mals #168 · Mals #169 · Mals #170 · Mals #171 · Mals #172 · Mals #173 · Mals #174 · Mals #175 · Mals #176 · Mals #177 · Mals #178 · Mals #179 · Mals #180 · Mals #181 · Mals #182 · Mals #183 · Mals #184 · Mals #185 · Mals #186 · Mals #187 · Mals #188 · Mals #189 · Mals #190 · Mals #191 · Mals #192 · Mals #193 · Mals #194 · Mals #195 · Mals #196 · Mals #197 · Mals #198 · Mals #199 · Mals #200 · Mals #201 · Mals #202 · Mals #203 · Mals #204 · Mals #205 · Mals #206 · Mals #207 · Mals #208 · Mals #209 · Mals #210 · Mals #211 · Mals #212 · Mals #213 · Mals #214 · Mals #215 · Mals #216 · Mals #217 · Mals #218 · Mals #219 · Mals #220 · Mals #221 · Mals #222 · Mals #223 · Mals #224 · Mals #225 · Mals #226 · Mals #227 · Mals #228 · Mals #229 · Mals #230 · Mals #231 · Mals #232 · Mals #233 · Mals #234 · Mals #235 · Mals #236 · Mals #237 · Mals #238 · Mals #239 · Mals #240 · Mals #241 · Mals #242 · Mals #243 · Mals #244 · Mals #245 · Mals #246 · Mals #247 · Mals #248 · Mals #249 · Mals #250 · Mals #251 · Mals #252 · Mals #253 · Mals #254 · Mals #255 · Mals #256 · Mals #257 · Mals #258 · Mals #259 · Mals #260 · Mals #261 · Mals #262 · Mals #263 · Mals #264 · Mals #265 · Mals #266 · Mals #267 · Mals #268 · Mals #269 · Mals #270 · Mals #271 · Mals #272 · Mals #273 · Mals #274 · Mals #275 · Mals #276 · Mals #277 · Mals #278 · Mals #279 · Mals #280 · Mals #281 · Mals #282 · Mals #283 · Mals #284 · Mals #285 · Mals #286 · Mals #287 · Mals #288 · Mals #289 · Mals #290 · Mals #291 · Mals #292 · Mals #293 · Mals #294 · Mals #295 · Mals #296 · Mals #297 · Mals #298 · Mals #299 · Mals #300 · Mals #301 · Mals #302 · Mals #303 · Mals #304 · Mals #305 · Mals #306 · Mals #307 · Mals #308 · Mals #309 · Mals #310 · Mals #311 · Mals #312 · Mals #313 · Mals #314 · Mals #315 · Mals #316 · Mals #317 · Mals #318 · Mals #319 · Mals #320 · Mals #321 · Mals #322 · Mals #323 · Mals #324 · Mals #325 · Mals #326 · Mals #327 · Mals #328 · Mals #329 · Mals #330 · Mals #331 · Mals #332 · Mals #333 · Mals #334 · Mals #335 · Mals #336 · Mals #337 · Mals #338 · Mals #339 · Mals #340 · Mals #341 · Mals #342 · Mals #343 · Mals #344 · Mals #345 · Mals #346 · Mals #347 · Mals #348 · Mals #349 · Mals #350 · Mals #351 · Mals #352 · Mals #353 · Mals #354 · Mals #355 · Mals #356 · Mals #357 · Mals #358 · Mals #359 · Mals #360 · Mals #361 · Mals #362 · Mals #363 · Mals #364 · Mals #365 · Mals #366 · Mals #367 · Mals #368 · Mals #369 · Mals #370 · Mals #371 · Mals #372 · Mals #373 · Mals #374 · Mals #375 · Mals #376 · Mals #377 · Mals #378 · Mals #379 · Mals #380 · Mals #381 · Mals #382 · Mals #383 · Mals #384 · Mals #385 · Mals #386 · Mals #387 · Mals #388 · Mals #389 · Mals #390 · Mals #391 · Mals #392 · Mals #393 · Mals #394 · Mals #395 · Mals #396 · Mals #397 · Mals #398 · Mals #399 · Mals #400 · Mals #401 · Mals #402 · Mals #403 · Mals #404 · Mals #405 · Mals #406 · Mals #407 · Mals #408 · Mals #409 · Mals #410 · Mals #411 · Mals #412 · Mals #413 · Mals #414 · Mals #415 · Mals #416 · Mals #417 · Mals #418 · Mals #419 · Mals #420 · Mals #421 · Mals #422 · Mals #423 · Mals #424 · Mals #425 · Mals #426 · Mals #427 · Mals #428 · Mals #429 · Mals #430 · Mals #431 · Mals #432 · Mals #433 · Mals #434 · Mals #435 · Mals #436 · Mals #437 · Mals #438 · Mals #439 · Mals #440 · Mals #441 · Mals #442 · Mals #443 · Mals #444 · Mals #445 · Mals #446 · Mals #447 · Mals #448 · Mals #449 · Mals #450 · Mals #451 · Mals #452 · Mals #453 · Mals #454 · Mals #455 · Mals #456 · Mals #457 · Mals #458 · Mals #459 · Mals #460 · Mals #461 · Mals #462 · Mals #463 · Mals #464 · Mals #465 · Mals #466 · Mals #467 · Mals #468 · Mals #469 · Mals #470 · Mals #471 · Mals #472 · Mals #473 · Mals #474 · Mals #475 · Mals #476 · Mals #477 · Mals #478 · Mals #479 · Mals #480 · Mals #481 · Mals #482 · Mals #483 · Mals #484 · Mals #485 · Mals #486 · Mals #487 · Mals #488 · Mals #489 · Mals #490 · Mals #491 · Mals #492 · Mals #493 · Mals #494 · Mals #495 · Mals #496 · Mals #497 · Mals #498 · Mals #499 · Mals #500 · Mals #501 · Mals #502 · Mals #503 · Mals #504 · Mals #505 · Mals #506 · Mals #507 · Mals #508 · Mals #509 · Mals #510 · Mals #511 · Mals #512 · Mals #513 · Mals #514 · Mals #515 · Mals #516 · Mals #517 · Mals #518 · Mals #519 · Mals #520 · Mals #521 · Mals #522 · Mals #523 · Mals #524 · Mals #525 · Mals #526 · Mals #527 · Mals #528 · Mals #529 · Mals #530 · Mals #531 · Mals #532 · Mals #533 · Mals #534 · Mals #535 · Mals #536 · Mals #537 · Mals #538 · Mals #539 · Mals #540 · Mals #541 · Mals #542 · Mals #543 · Mals #544 · Mals #545 · Mals #546 · Mals #547 · Mals #548 · Mals #549 · Mals #550 · Mals #551 · Mals #552 · Mals #553 · Mals #554 · Mals #555 · Mals #556 · Mals #557 · Mals #558 · Mals #559 · Mals #560 · Mals #561 · Mals #562 · Mals #563 · Mals #564 · Mals #565 · Mals #566 · Mals #567 · Mals #568 · Mals #569 · Mals #570 · Mals #571 · Mals #572 · Mals #573 · Mals #574 · Mals #575 · Mals #576 · Mals #577 · Mals #578 · Mals #579 · Mals #580 · Mals #581 · Mals #582 · Mals #583 · Mals #584 · Mals #585 · Mals #586 · Mals #587 · Mals #588 · Mals #589 · Mals #590 · Mals #591 · Mals #592 · Mals #593 · Mals #594 · Mals #595 · Mals #596 · Mals #597 · Mals #598 · Mals #599 · Mals #600 · Mals #601 · Mals #602 · Mals #603 · Mals #604 · Mals #605 · Mals #606 · Mals #607 · Mals #608 · Mals #609 · Mals #610 · Mals #611 · Mals #612 · Mals #613 · Mals #614 · Mals #615 · Mals #616 · Mals #617 · Mals #618 · Mals #619 · Mals #620 · Mals #621 · Mals #622 · Mals #623 · Mals #624 · Mals #625 · Mals #626 · Mals #627 · Mals #628 · Mals #629 · Mals #630 · Mals #631 · Mals #632 · Mals #633 · Mals #634 · Mals #635 · Mals #636 · Mals #637 · Mals #638 · Mals #639 · Mals #640 · Mals #641 · Mals #642 · Mals #643 · Mals #644 · Mals #645 · Mals #646 · Mals #647 · Mals #648 · Mals #649 · Mals #650 · Mals #651 · Mals #652 · Mals #653 · Mals #654 · Mals #655 · Mals #656 · Mals #657 · Mals #658 · Mals #659 · Mals #660 · Mals #661 · Mals #662 · Mals #663 · Mals #664 · Mals #665 · Mals #666 · Mals #667 · Mals #668 · Mals #669 · Mals #670 · Mals #671 · Mals #672 · Mals #673 · Mals #674 · Mals #675 · Mals #676 · Mals #677 · Mals #678 · Mals #679 · Mals #680 · Mals #681 · Mals #682 · Mals #683 · Mals #684 · Mals #685 · Mals #686 · Mals #687 · Mals #688 · Mals #689 · Mals #690 · Mals #691 · Mals #692 · Mals #693 · Mals #694 · Mals #695 · Mals #696 · Mals #697 · Mals #698 · Mals #699 · Mals #700 · Mals #701 · Mals #702 · Mals #703 · Mals #704 · Mals #705 · Mals #706 · Mals #707 · Mals #708 · Mals #709 · Mals #710 · Mals #711 · Mals #712 · Mals #713 · Mals #714 · Mals #715 · Mals #716 · Mals #717 · Mals #718 · Mals #719 · Mals #720 · Mals #721 · Mals #722 · Mals #723 · Mals #724 · Mals #725 · Mals #726 · Mals #727 · Mals #728 · Mals #729 · Mals #730 · Mals #731 · Mals #732 · Mals #733 · Mals #734 · Mals #735 · Mals #736 · Mals #737 · Mals #738 · Mals #739 · Mals #740 · Mals #741 · Mals #742 · Mals #743 · Mals #744 · Mals #745 · Mals #746 · Mals #747 · Mals #748 · Mals #749 · Mals #750 · Mals #751 · Mals #752 · Mals #753 · Mals #754 · Mals #755 · Mals #756 · Mals #757 · Mals #758 · Mals #759 · Mals #760 · Mals #761 · Mals #762 · Mals #763 · Mals #764 · Mals #765 · Mals #766 · Mals #767 · Mals #768 · Mals #769 · Mals #770 · Mals #771 · Mals #772 · Mals #773 · Mals #774 · Mals #775 · Mals #776 · Mals #777 · Mals #778 · Mals #779 · Mals #780 · Mals #781 · Mals #782 · Mals #783 · Mals #784 · Mals #785 · Mals #786 · Mals #787 · Mals #788 · Mals #789 · Mals #790 · Mals #791 · Mals #792 · Mals #793 · Mals #794 · Mals #795 · Mals #796 · Mals #797 · Mals #798 · Mals #799 · Mals #800 · Mals #801 · Mals #802 · Mals #803 · Mals #804 · Mals #805 · Mals #806 · Mals #807 · Mals #808 · Mals #809 · Mals #810 · Mals #811 · Mals #812 · Mals #813 · Mals #814 · Mals #815 · Mals #816 · Mals #817 · Mals #818 · Mals #819 · Mals #820 · Mals #821 · Mals #822 · Mals #823 · Mals #824 · Mals #825 · Mals #826 · Mals #827 · Mals #828 · Mals #829 · Mals #830 · Mals #831 · Mals #832 · Mals #833 · Mals #834 · Mals #835 · Mals #836 · Mals #837 · Mals #838 · Mals #839 · Mals #840 · Mals #841 · Mals #842 · Mals #843 · Mals #844 · Mals #845 · Mals #846 · Mals #847 · Mals #848 · Mals #849 · Mals #850 · Mals #851 · Mals #852 · Mals #853 · Mals #854 · Mals #855 · Mals #856 · Mals #857 · Mals #858 · Mals #859 · Mals #860 · Mals #861 · Mals #862 · Mals #863 · Mals #864 · Mals #865 · Mals #866 · Mals #867 · Mals #868 · Mals #869 · Mals #870 · Mals #871 · Mals #872 · Mals #873 · Mals #874 · Mals #875 · Mals #876 · Mals #877 · Mals #878 · Mals #879 · Mals #880 · Mals #881 · Mals #882 · Mals #883 · Mals #884 · Mals #885 · Mals #886 · Mals #887 · Mals #888 · Mals #889 · Mals #890 · Mals #891 · Mals #892 · Mals #893 · Mals #894 · Mals #895 · Mals #896 · Mals #897 · Mals #898 · Mals #899 · Mals #900 · Mals #901 · Mals #902 · Mals #903 · Mals #904 · Mals #905 · Mals #906 · Mals #907 · Mals #908 · Mals #909 · Mals #910 · Mals #911 · Mals #912 · Mals #913 · Mals #914 · Mals #915 · Mals #916 · Mals #917 · Mals #918 · Mals #919 · Mals #920 · Mals #921 · Mals #922 · Mals #923 · Mals #924 · Mals #925 · Mals #926 · Mals #927 · Mals #928 · Mals #929 · Mals #930 · Mals #931 · Mals #932 · Mals #933 · Mals #934 · Mals #935 · Mals #936 · Mals #937 · Mals #938 · Mals #939 · Mals #940 · Mals #941 · Mals #942 · Mals #943 · Mals #944 · Mals #945 · Mals #946 · Mals #947 · Mals #948 · Mals #949 · Mals #950 · Mals #951 · Mals #952 · Mals #953 · Mals #954 · Mals #955 · Mals #956 · Mals #957 · Mals #958 · Mals #959 · Mals #960 · Mals #961 · Mals #962 · Mals #963 · Mals #964 · Mals #965 · Mals #966 · Mals #967 · Mals #968 · Mals #969 · Mals #970 · Mals #971 · Mals #972 · Mals #973 · Mals #974 · Mals #975 · Mals #976 · Mals #977 · Mals #978 · Mals #979 · Mals #980 · Mals #981 · Mals #982 · Mals #983 · Mals #984 · Mals #985 · Mals #986 · Mals #987 · Mals #988 · Mals #989 · Mals #990 · Mals #991 · Mals #992 · Mals #993 · Mals #994 · Mals #995 · Mals #996 · Mals #997 · Mals #998 · Mals #999 · Mals #1000

Geology adapted from Newfoundland Department of Mines and Energy Open File Map 82-7.

Produced By: Black Pine Limited St. John's, NF (709) 730-4425

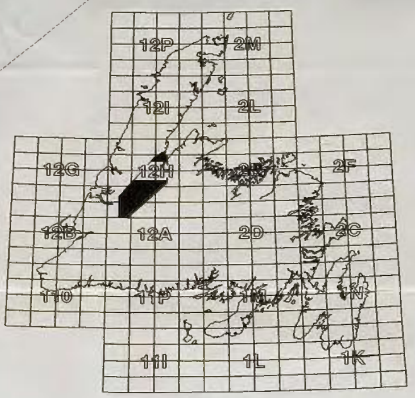

DEER LAKE BASIN GEOLOGY

PROJECT: JH–MSc	AREA: Deer Lake Basin, NF

GEOLOGY OF THE CARBONIFEROUS DEER LAKE BASIN

FIGURE	SUPERVISOR: DHC Wilton
NTS SHEET(S): Parts of 12A,H	DRAWN BY: BLACK PINE LTD. (23/12/97)
SCALE: 1:125,000	FILE: DER–COMP.DWG

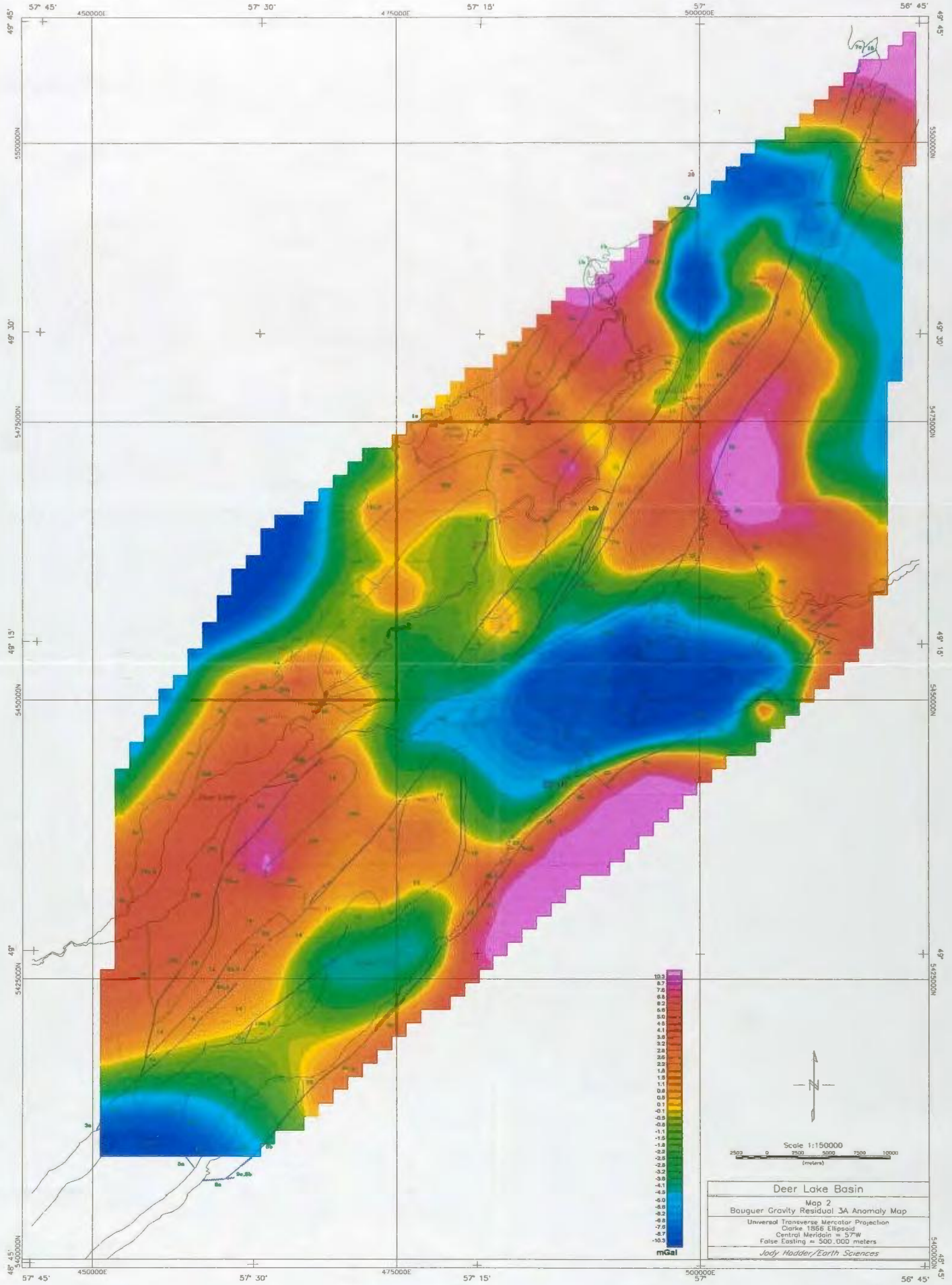
57° 45'
57° 30'
57° 15'
57°
56° 45'
49° 45'
49° 30'
49° 15'
49°
48° 45'
4500000E
4750000E
5000000E
5500000N
5475000N
5450000N
5425000N
5400000N
10.3
8.7
7.6
6.8
6.2
5.6
5.0
4.5
4.1
3.8
3.2
2.8
2.6
2.2
1.8
1.5
1.1
0.8
0.5
0.1
-0.1
-0.5
-0.6
-1.1
-1.5
-1.8
-2.2
-2.5
-2.8
-3.2
-3.6
-4.1
-4.5
-6.0
-6.8
-7.6
-8.7
-10.3
mGal
Scale 1:150000
2500 0 2500 5000 7500 10000
(meters)
Deer Lake Basin
Map 2
Bouguer Gravity Residual 3A Anomaly Map
Universal Transverse Mercator Projection
Clarke 1866 Ellipsoid
Central Meridain = 57°W
False Easting = 500,000 meters
Jody Hodder/Earth Sciences

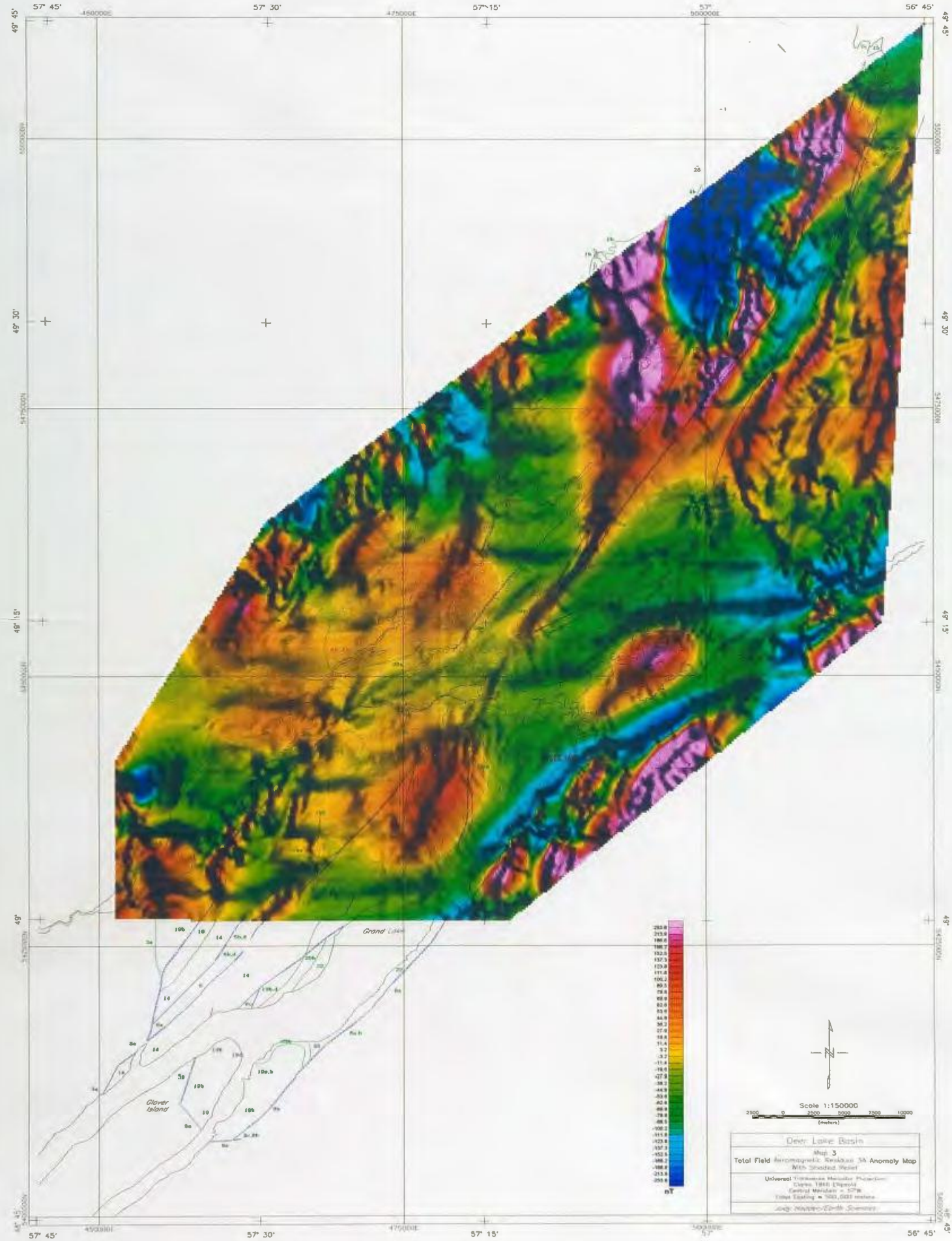
57° 45'
57° 30'
57° 15'
57°
56° 45'
49° 45'
49° 30'
49° 15'
49°
4500000E
4750000E
5000000E
5500000N
5475000N
5450000N
5425000N
5400000N
Grand Lake
Glover Island
nT
Scale 1:150000
2500 0 2500 5000 7500 10000
(meters)
Deer Lake Basin
Map 3
Total Field Aeromagnetic Residual 1st Anomaly Map
With Shaded Relief
Universal Transverse Mercator Projection
Clarke 1866 Ellipsoid
Central Meridian = 57°W
False Easting = 500,000 meters
Lambert Conformal Conic Projection

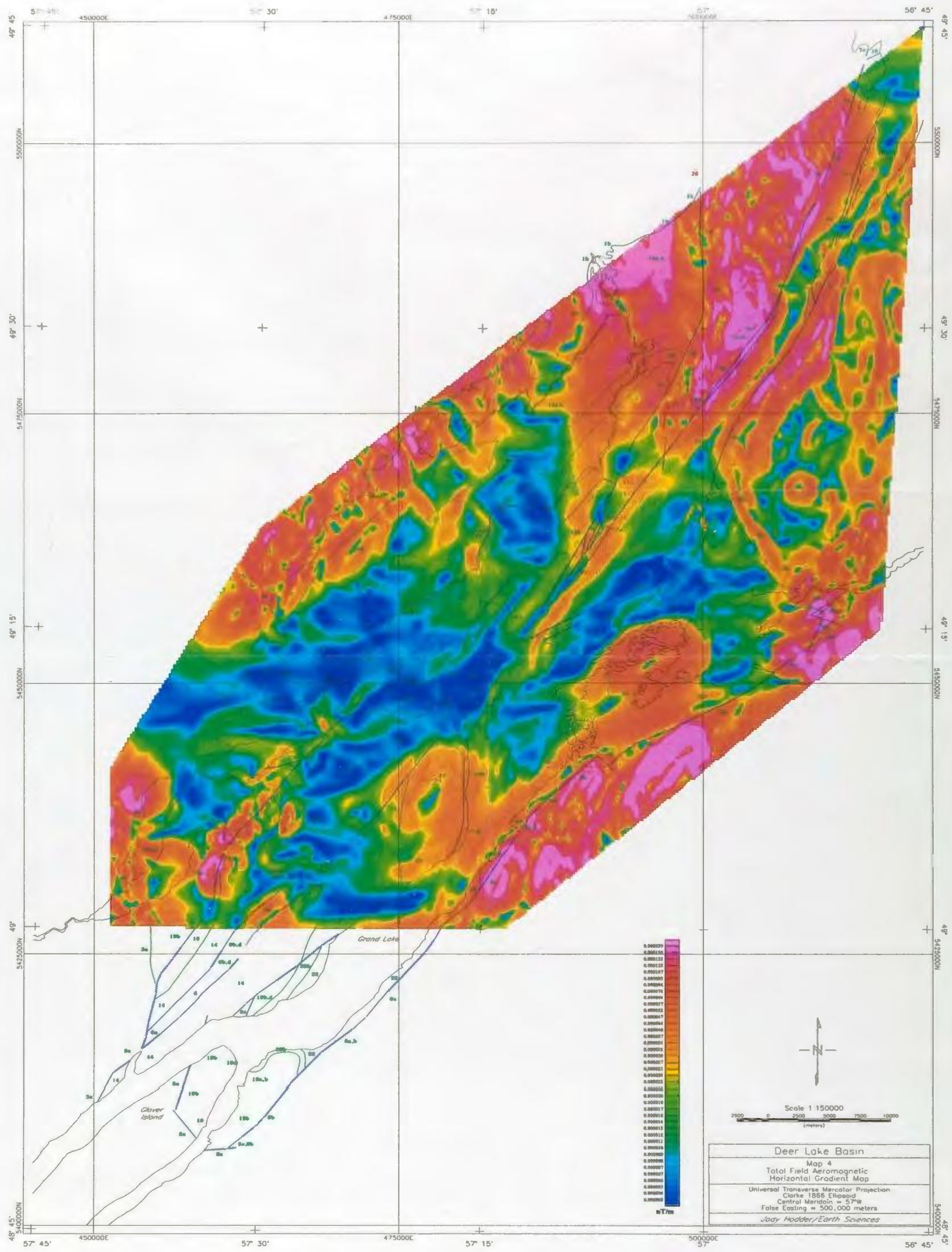
57° 45'
450000E
57° 30'
475000E
57° 15'
500000E
57°
56° 45'
49° 45'
49° 30'
49° 15'
49°
5500000N
5475000N
5450000N
5425000N
5400000N
Grand Lake
Glover Island
mT/m
N
Scale 1 150000
2500 0 2500 5000 7500 10000
(meters)
Deer Lake Basin
Map 4
Total Field Aeromagnetic
Horizontal Gradient Map
Universal Transverse Mercator Projection
Clarke 1866 Ellipsoid
Central Meridain = 57°W
False Easting = 500,000 meters
Jody Hodder/Earth Sciences